Improvement in Adhesion for the Epoxy-SiC System via Plasma and Silane Surface Modification Techniques

by

Elizabeth M.H. Neyman

Thesis submitted to the faculty of
Virginia Polytechnic Institute and State University
in partial fulfillment of the requirements for the degree of

MASTER OF SCIENCE

in Materials Science and Engineering

John G. Dillard, Chairman
B.J. Love
S. Corcoran

July 10, 2003
Blacksburg, Virginia

Keywords: Adhesion, Silicon Carbide, Epoxy, Silane, Plasma, Surface Modification, X-ray Photoelectron Spectroscopy, Coatings

Improvement in Adhesion for the Epoxy-SiC System via Plasma and Silane Surface Modification Techniques

Elizabeth M.H. Neyman

ABSTRACT

The adhesion durability of coatings and encapsulant materials utilized in electronic packaging is vital for device reliability in the microelectronics industry. Due to adverse operating conditions such as high moisture and high temperature environments, the adhesion between an adhesive and its substrate is typically compromised. This thesis addresses the advantages of employing plasma pretreatments and surface derivatization using silane coupling agents as surface modification techniques in an effort to enhance the adhesive bonding of epoxy to SiC coated Si wafers (SiC/Si). Durability was evaluated by immersing coated-Si samples in aqueous solutions at elevated temperature (60 °C) to simulate prolonged severe operating conditions.

Three surface modification approaches for the SiC/Si substrate to be discussed include: 1) a silane coupling agent treatment, which involves a reaction of either 3-aminopropyltriethoxysilane (APS) or 3-glycidoxypropyltrimethoxysilane (GPS) with the substrate, 2) an oxygen plasma pretreatment followed by a silane treatment, and 3) a water/oxygen plasma pretreatment followed by a silane treatment. Samples were immersed in aqueous solutions at various pH at 60 °C for extended periods of time. Adhesion durability of treated epoxy/SiC/Si systems was qualitatively evaluated by visual inspection for debonding, and quantitatively evaluated using a probe test to evaluate the critical strain energy release rate G_c. Additionally, X-ray photoelectron spectroscopy (XPS) surface characterization was carried out following the surface treatments and again after complete failure in the durability tests.

The durability tests illustrated that surface treatments involving an oxygen plasma pretreatment prior to silane derivatization resulted in significant improvement in adhesive performance. Furthermore, the results of XPS analysis suggested that the improved bonding was due to cleaning of the substrate surface, promotion of silane adsorption and the formation of a thicker oxide layer. The effectiveness of the surface modification methods in relationship to surface chemistry and adhesion for the epoxy/SiC/Si system is reported and discussed in this work.

DEDICATION

to

My parents, Le Thi Huong and Vu Duc Minh

ACKNOWLEDGEMENTS

I must, foremost, thank my advisor, Dr. John Dillard, for his patience, support and guidance. Although I was not a chemistry major, he was willing to take me under his wing and help me become the researcher that I am today. I have benefited much from his knowledge and wisdom, as well as his kindness and generosity.

Many thanks are owed to Dr. Sean Corcoran and Dr. Brian Love for participating on my committee, Dr. Kai-tak Wan and Dr. Zuo Sun for their work on the probe test, and Frank Cromer for his invaluable help on surface analytical instrumentation and data analysis. In addition, I would also like to acknowledge the Hewlett Packard Corporation for their financial support in making the project possible.

I would also like to thank my fellow colleagues, David Xu and Sumitra Subrahmanyan. David for his collaborative work on the project, and Sumitra for help making life in and out of the lab much more enjoyable.

Lastly, my deepest gratitude is owed to my family and friends, especially my parents who believed in me and supported me through the good and bad times. Also, I thank my husband, Patrick, for not only correcting the many grammar mistakes on my thesis but also for helping me keep focus. Finally, I'd like to thank my daughter, Julia, for bringing smiles to my face despite of life's chaotic moments.

CONTENTS

FIGURES

TABLES

1 INTRODUCTION

Epoxies are widely used in the microelectronics industry as coating and encapsulant materials to provide environmental protection as well as thermo-mechanical protection to integrated circuit (IC) devices. Several requirements exist for a coating/encapsulant material, including high modulus of elasticity, high glass transition temperature (T_g), low thermal expansion, low moisture absorption and good adhesion between the adherend and the polymeric material.[1] Epoxies have been most frequently used as packaging materials due to their excellent chemical and corrosion resistance, thermal insulation, electrical characteristics, physical properties, low shrinkage, excellent adhesion and reasonable material cost.[2] The role of the coating/encapsulant is critical in electronic assemblies since the material serves as an insulator as well as a protective coating against adverse operating conditions such as high temperature (50-200 °C[3]), humidity, chemical attack, current leakage and mechanical stress that ultimately result in IC failure. Delamination (total loss of adhesion) between substrate and epoxy is still a major concern for yield loss and device reliability, especially in high humidity and elevated thermal conditions.[4,5]

Surface pretreatment is extremely important in most adhesion systems. To achieve optimum adhesion durability, it is often necessary to modify the native substrate surface. Silane coupling agents significantly improve adhesion between inorganic oxides and polymer resins.[6] The coupling agent, usually an organofunctional alkyltrialkoxysilane, is a hybrid that contains both organic and inorganic functionalities, thus allowing it to act as a chemical bridge between two dissimilar materials. Although there is extensive documentation on the uses of organosilanes as adhesion promotors, the effectiveness of a coupling agent in a bonded system is highly specific and dependent on the substrate, polymer and silane deposition parameters.

Surface modification via plasma treatment is a non-solution surface pretreatment method for improving adhesion.[7] Plasma treatments are commonly used in semiconductor processing and offer an attractive means to alter surface characteristics because they combine the features of safety, cleanliness and cost effectiveness while enhancing adhesion performance. Plasma

treatments that utilize nonpolymerizing gases are capable of removing carbon-containing contaminants from the surface in addition to physically and chemically altering the surface of the adherend. Plasma treatment is an efficient means of incorporating desired chemical functionalities on the surface to promote interaction and adhesion with the selected adhesive.

In this study, silane and plasma surface modification processes are investigated for the improvement of adhesion of a model epoxy to silicon carbide-coated silicon wafers (SiC/Si). Silicon carbide is the coating of interest because it is extremely stable, is capable of withstanding high heat, has low thermal expansion and high resistance to acids and bases.[8] Silicon carbide is commonly used in high temperature, high speed, high power and radiation applications. 3-aminopropyltriethoxysilane (APS) and 3-glycidoxypropyltrimethoxysilane (GPS) were used to improve adhesion durability. Oxygen and water/oxygen plasma pretreatments prior to the deposition of either APS or GPS were investigated to further enhance adhesion performance. Three different surface modification methodologies were studied: (1) silane treatment of SiC/Si with APS or GPS, (2) O_2 plasma treatment of SiC/Si followed by silane treatment and (3) H_2O/O_2 plasma treatment of SiC/Si followed by silane treatment.

Two approaches were followed to evaluate adhesion durability. In the immersion test approach, as-received and surface-modified epoxy-SiC/Si specimens were immersed in aqueous solutions and qualitatively evaluated (i.e. blisters and debonding features) for adhesion performance. In the second approach, the probe test was used to quantify adhesion via the determination of the critical strain energy release rate, G_c, as a function of immersion time. In both studies, adhesive bonding was tested in an environment that simulated microelectronic system applications that involved the immersion of bonded specimens in four different aqueous solutions, referenced by their pH, at 60 °C. X-ray photoelectron spectroscopy (XPS) was extensively used to study the surfaces of modified substrates and to determine the failure mode of the bonded systems. The intent of this thesis is to provide an understanding of the relationship between surface preparation and epoxy adhesion while developing surface modification methods that will improve long term durability of the epoxy/SiC/Si system.

[1] M.B. Vincent and C.P. Wong, *Sold. Surf. Mount Technol.*, **1999**, *11*, 33.

[2] C.P. Wong, *Chip Scale Review*, **1998**, *2*, 30.

[3] W.G. Potter, *Epoxide Resins*, Iliffe: London, 1970, p. 91.

[4] J.V.C. van Vroonhoven, *J. Electron. Packag*., **1993**, *115*, 28.

[5] C.K. Gurumurthy, J. Jiao, L.G. Norris, C.Y. Hui and E.J. Kramer, *Appl. Fracture Mech. Electron. Packag*., **1997**, *222*, 41.

[6] E.P. Plueddemann, *Silane Coupling Agents*, Plenum Press: New York, 1991, Chapter 1.

[7] R.A. DiFelice, Ph.D. Thesis, Virginia Tech, May 2001, p. 2.

[8] C.A. Harper, *Electronic Assembly Fabrication*, McGraw-Hill: New York, 2002, p. 515.

2 LITERATURE REVIEW

2.1 ADHESION, ADHESIVES AND SEALANTS

Adhesives and sealants have greatly contributed to our everyday lives, and also to the advancement of modern technology. Adhesives can be found as close as the pressure sensitive adhesive tape sitting on a desk or in hi-tech aerospace and computer applications. The design and performance of an adhesive system depend on the structure and chemistry of bonding surfaces, desired thermo-mechanical properties of the adhesive, as well as environmental factors.

The study of adhesion is a multidisciplinary field involving areas such as chemistry, surface science, physics, materials science and mechanics. The word 'adhesion' stems from the Latin root adhaerere, meaning 'to stick to'.[1] Interestingly, Robert Boyle in 1661 was one of the earliest scientists to use the term in a scientific context.[2] The modeling of adhesion as two surfaces or bodies bonded to each other is generally straightforward. However, understanding why or how this phenomenon occurs is quite complex. According to ASTM[3], 'adhesion' is defined as "the state in which two surfaces are held together by interfacial forces which may consist of valence forces, interlocking action or both". By this definition, the establishment of adhesion relies on understanding the interface at the atomic and molecular levels. Although no concrete explanations for this phenomenon exist, there is strong evidence supporting four main theories of adhesion. The theories are mechanical interlocking, diffusion, adsorption and electrostatic. In most cases, a combination of these theories is used to model adhesion.

2.1.1 MECHANICAL INTERLOCKING THEORY

The mechanical interlocking theory proposes that an adhesive adheres to a substrate primarily by mechanically keying into the substrate's surface irregularities.[4] This theories states that improved adhesion is due to an increase in interfacial surface area.[5] Surface topography plays a crucial role in this theory, both on a macroscopic and microscopic scale. On a macroscopic scale, this theory is applicable in the adhesion of fibrous materials such as wood and leather. A common knowledge among carpenters is that roughening the wood prior to gluing, otherwise known as giving it more 'tooth', will result in a stronger joint. On a

microscopic scale, this concept can be described as a 'hook and eye' concept.[6] Packham *et al.*[7] demonstrated that the adhesion of a polymer to anodized aluminum was dependent on mechanical interlocking of the adhesive in the pores of the aluminum oxide.

2.1.2 DIFFUSION THEORY

The diffusion theory was originally proposed by the Russian scientist, Voyutskii[8]. This theory applies to adhesion in polymer-polymer systems and states that adhesion of two polymer surfaces is due the intermingling of polymer chains at a molecular level. For this intermingling to occur, the materials must be in close contact, polymer chains must be long and mobile to diffuse across the interface and surfaces must exhibit a high degree of compatibility.[4,6]

2.1.3 ADSORPTION THEORY

The adsorption theory is perhaps the most applicable and widely accepted theory. This theory asserts that adhesion is attributed to the intermolecular forces between atoms and molecules on the surface of two materials that are in intimate contact.[9] Under the umbrella of this theory, two adsorption distinctions have been made: chemisorption and physisorption.[10] The latter refers to the condition where a material is physically adsorbed, or held together by secondary forces, and no chemical bonds are involved. Secondary forces consist of London dispersion forces, dipole interactions (polar forces) and hydrogen bonding. Secondary interactions alone can result in strong adhesive strength provided that close intermolecular contact is present.[11] Chemisorption is due to primary bond formation, ionic or covalent, across the interface. Although difficult to achieve, this type of adhesion is the strongest, and thus most capable of load bearing.

2.1.4 ELECTROSTATIC THEORY

In 1957, Deryaguin *et al.*[12] proposed that adhesion might be attributed to electrostatic forces between interfaces. This theory is based on the presence of an electric double layer where two oppositely charged surfaces intermingle, resulting in a diffuse layer of ionic bonds. This theory accounts for the electrical discharges observed when a piece of pressure sensitive tape is quickly debonded from a rigid substrate by rapid peeling.

2.1.5 POLYMER – METAL ADHESION

The strong adhesion strength in polymer–metal systems is best explained by the adsorption theory.[4,13] Potter[13] suggested that hydroxyl groups in most epoxies are capable of forming hydrogen bonds with hydroxyl groups on metal oxides. The hydroxyl groups are formed as a result of the opening of the epoxide ring by the curing agent. By measuring the bond strengths of an anhydride-cured epoxy to aluminum, De Bruyne[14] found that the lap shear strength of the bonds was a function of the concentration of hydroxyl groups in the resin. Chou and Tang[15] studied the interfacial reactions between a polyimide and chromium. They suggested that improved adhesion was due to the formation of metal-oxygen-carbon complexes at the interface. Inagaki *et al.*[16] investigated the adhesion between a plasma-treated Kapton film and copper. They concluded that the enhanced adhesion was due to the bonds between the plasma-formed carboxyl groups and oxidized metal surface. All of the reported investigations provide strong evidence that polymer-metal adhesion is due to an adsorption mechanism.

2.2 EPOXY POLYMERS IN MICROELECTRONIC PACKAGING

In electronic packaging, epoxy resin systems are most commonly used as coatings, encapsulants and photoresist materials. In this section, the discussion of epoxy polymers will mainly be focused on coatings and encapsulant materials. In these cases, the epoxide serves as an insulator as well as a protective coating against adverse operating conditions such as high temperature (50-200 °C[17]), humidity, chemical attack, current leakage and mechanical stress.[18]

Epoxy resins are widely used in the electronics industry due to their versatility and advantageous properties. Epoxy resins can be cured by a variety of curing agents, thus allowing the system to be tailored with a wide range of desired properties.[19] The incorporation of filler and modifiers in the polymer system further allows versatility.[20] Low shrinkage (typically 1 %), fast cure kinetics and low coefficient of thermal expansion (CTE) all make the epoxy polymer a popular material in embedding applications.[21,22] Epoxies are also high in strength, resisting 12,000 – 14,000 psi in tension and have good thermal conductivity.[21] Thermal conductivity is an important property because the encapsulant material must be able to dissipate the thermal energy produced by the electronic components. Epoxy encapsulated and coated components may operate at temperatures as high as 125°C – 150°C, depending on the formulation of the system.[21]

Since epoxies are inherently polar and may be heated to obtain low viscosity, they are able to wet and adhere to many types of surfaces. Furthermore, epoxy resins have low permeability, with a typical water adsorption of 0.1% - 0.25%.[23] This is perhaps one of the most important aspects of an epoxy adhesive since it allows the polymer to shield delicate embedded circuitry from environmental moisture, solvent and ionic contaminants that attack the substrate, ultimately resulting in IC failure. Although epoxy resins can provide a versatile, inexpensive and practical means of providing the necessary barrier to preserve the integrity of microelectronic devices, delamination between substrate and encapsulant/coating is still a major concern for device yield and reliability for microelectronic manufacturing.[24,25]

2.3 SILICON CARBIDE (SiC)

Silicon carbide (SiC) is a wide-band-gap semiconductor that is commonly used in high-temperature, high-speed, power and radiation applications. This compound is extremely stable, having the capability to withstand temperatures of up to 1000°C without degradation. Furthermore, exceptionally high thermal conductivity, low CTE and resistance to acids and bases make SiC an attractive substrate. Silicon carbide may be formed by various processes including hot pressing, chemical vapor deposition (CVD) and casting. Since single crystalline SiC is quite expensive, a thin layer of SiC is often deposited by CVD onto a silicon (Si) substrate/wafer.[26]

To study the adhesion of epoxy on SiC, the surface chemistry of the substrate must be understood. It is well established that SiC is covered with a thin layer of oxide (SiO_2) that is terminated by silanol groups (Si-OH), thus rendering the surface hydrophilic.[27] Chemisorbed water molecules are often found on the surfaces of SiC since water molecules can readily interact with the surface silanol groups via hydrogen bonding. A schematic drawing of the surface of a hydrophilic SiC/Si wafer is given in Figure 2.1.

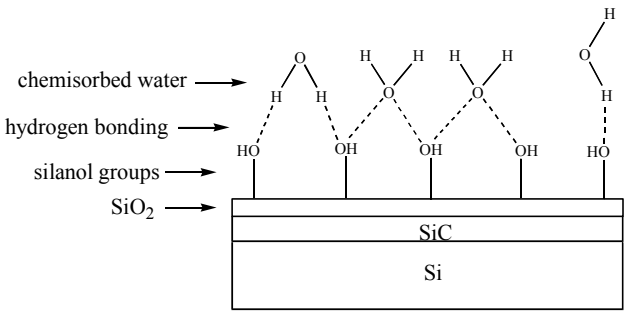

Figure 2.1 Schematic drawing of a hydrophilic SiC/Si wafer surface covered with a native oxide (SiO_2) and chemisorbed water molecules.

2.4 SILANE COUPLING AGENTS (SCA)

The term silane coupling agents was coined in the 1940s in reference to a category of organosilanes for enhancing adhesion and moisture resistance in glass fiber reinforced polymer composites.[28,29] Two major problems were encountered in the development of fiberglass-reinforced polymer composites: 1. the bond between the organic resin and inorganic fiber was easily hydrolyzed by water, and 2. stresses induced by thermal cycling across the fiber-resin interface resulted in bond failure due to thermal expansion coefficient mismatch.[29] The formation of glass-resin bonds did not yield the strength and stability necessary for desired performance, especially under hot-wet conditions. By applying a thin layer of coupling agent to the glass fibers, scientists were able to overcome these obstacles and fiberglass-reinforced plastic composites were developed into high performance materials.

Silane coupling agents are hybrid molecules that contain both inorganic and organic functionalities, thus allowing them to act as bridges between two dissimilar materials. Molecules defined as "coupling agents" are chemicals that promote adhesion between mineral phases and organic phases. Organofunctional alkyltrialkoxysilanes are most often used as coupling agents with a typical formula: $R\text{-}(CH_2)_n\text{-}Si(OR')_3$ where R′ is an alkyl group, R is a functional group and n = 0-3.[28] The alkoxy group $-Si(OR')_3$ is capable of undergoing hydrolysis, in turn interacting with an inorganic substrate (e.g. metal oxides or hydroxides) via hydrogen bonding while the organofunctional group, R (e.g. $-NH_2$), may be tailored to react with a specific adhesive. Silane coupling agents are commonly deposited utilizing a sol-gel reaction and may form monolayers or multilayers depending on sol-gel solutions and substrate. The application of

these materials increases adhesive bond strength and resistance to moisture by many means such as improving wettability, rheology and/or strengthening the interphase of the inorganic and organic boundary layers.[29] Although a considerable amount of work has been carried out on organosilanes as adhesion promotors, the theory and mechanism of coupling agents are still not well established.[30]

2.4.1 SOL-GEL PROCESSING

Sol-gel processing is a powerful method in material fabrication due to its many advantages such as low temperature solution processing with high purity, the precise control and tailoring of complex chemical composition and physical structure, control of pore structure and preparation of thin films and coatings with good optical quality.[31] Sol-gel technology has been applied to a wide range of processes from producing glass and ceramics to chemical and biological sensors. Perhaps sol-gel technology's most pronounced impact has been on the field of coatings. Thin sol-gel layers can be applied via spin coating[32], dipping[33] or impregnation[34]. Conductive coatings, passivation coatings, optical-control- and antireflective coatings[35,36,37], adhesion promoting coatings[29], just to name a few, all have used the sol-gel deposition technique to obtain homogeneous coatings.

Silane coupling agents are commonly applied via sol-gel processing which involves the generation of colloidal suspensions ("sol") that are subsequently converted to gels and then to solid materials.[38] A sol is defined as a dispersion of colloidal particles (1 nm – 1 μm) that are suspended via Brownian motion within a fluid matrix.[39] A gel is described as a "spanning cluster," or a solid network that entraps and immobilizes the remaining sol. Sol-gel layers are often applied using aqueous or alcoholic solutions containing precursors such as metal alkoxides, metal salts or silicon alkoxides.

2.4.2 SOL-GEL CHEMISTRY OF SILICATES

The sol-gel process involves a complex pattern of chemical reactions that proceed simultaneously. The properties of the sol-gel materials, e.g. density, thickness, porosity, surface functionality, strongly depend on the preparation method. By controlling the conditions of each processing stage, one can optimize the characteristics of the resulting material. A general silicon

alkoxide sol-gel process consists of five stages[31] listed below. The stages are listed separately, although in real systems, several of these steps may occur simultaneously.

1. Hydrolysis: $Si(OR)_4 + nH_2O \leftrightarrow Si(OR)_{4-n}(OH)_n + nROH$

2. Condensation: $X_3SiOH + HOSiX'_3 \leftrightarrow X_3Si\text{-}O\text{-}SiX'_3 + H_2O$ or
$X_3SiOR + HOSiX'_3 \leftrightarrow X_3Si\text{-}O\text{-}SiX'_3 + ROH$

3. Gelation: Formation of a solid network that entraps the remaining solution (sol).

4. Drying: The loss of water, alcohol or other volatile components, first as syneresis (expulsion of the liquid as the gel shrinks), then as evaporation of the liquid from the pores.

5. Densification: Thermal treatment leading to the collapse of the open structure and formation of a dense material.

The first step of the sol-gel process is the hydrolysis of the silicon alkoxide. Since hydrolysis of the silicon alkoxide precursor is often hindered due to steric constraints[40] of the substituents, its low reactivity towards hydrolysis is dependent on pH and reaction temperature rather than the amount of water. Usually, an acid or base catalyst is incorporated into the reaction to dramatically promote hydrolysis. The hydrophobicity of the precursor also influences the hydrolysis process. The hydrophobic nature of the alkoxy groups limits the solubility of the precursor in water. A co-solvent, such as alcohol, is often required to obtain miscibility. [31]

In real systems, hydrolysis reactions occur concurrently with condensation reactions. Condensation reactions can be either water condensation or alcohol condensation processes. As with hydrolysis, condensation reactions may be acid or base catalyzed. The overall reaction kinetics of hydrolysis and condensation are very complex. For example, for a system SiABCD, where A, B, C, and D may be OR, OH or OSi, and the system is only defined as $Si(OR)_x(OH)_y(OSi)_z$ with $x + y + z = 4$, even if the second z silicon species is ignored, this still gives 15 chemically different species related by 10 hydrolysis reactions, 55 water condensation reactions, and 100 alcohol condensation reactions. Even if the reverse reactions were ignored, 165 rate constants would have to be determined to characterize the overall reaction.[41]

As a result of hydrolysis and condensation, links are formed between silica sol particles. These links become so extensive that it becomes a three dimensional solid network that entraps

and entangles the left over sol particles. This process is known as gelation. At gelation, there is no discrete chemical change, only a sudden increase in viscosity. The gel is then dried at or near ambient temperature, often followed by a heat treatment for further drying and densification.

In the specific case of applying a coupling agent by a sol-gel reaction, a generic model is usually adopted to describe the deposition mechanism of the modified layer as shown in Figure 2.2. In the sol-gel reaction, the alkoxy groups of the organosilane undergo hydrolysis and polycondensation. The polycondensation reaction can be either alcohol condensation or water condensation, both of which usually commence before the hydrolysis is complete. The hydrolyzed and partially oligomerized silane molecules interact via hydrogen bonding with surface hydroxy groups that are present on silicon and most metal surfaces. A heat treatment is usually applied to eliminate water and promote covalent siloxane linkages[42,43] (Si-O-Si) between silane molecules and surface substrates. Although the simplistic model has provided a base to the understanding of the role of coupling agents, most scientists[44] agree that the mechanism by which the organosilanes bind to surfaces is much more complex since the effectiveness of each silane coupling agent varies from substrate to substrate.

2.4.3 SILANE SURFACE MODIFICATION

In the silane surface modification process, the morphology of the sol-gel layer is highly dependent on deposition variables including solvent, pH, reaction time, curing time and temperature, substrate and silane. Layer thickness, the modification density, the orientation of the surface molecules and the type of interaction of the modification layer with the surface substrate are all properties that are affected by deposition parameters.[45]

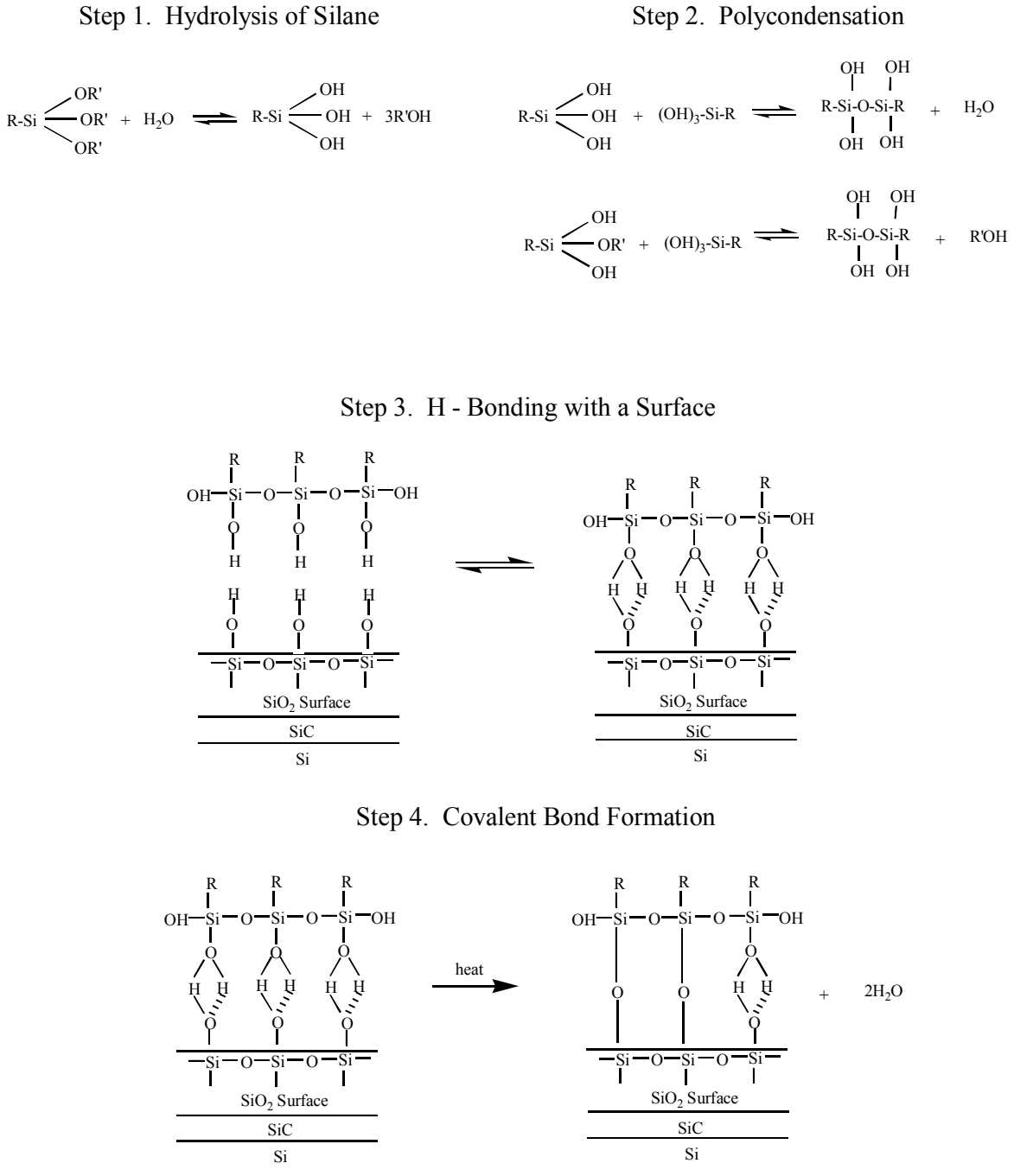

Figure 2.2 Silane deposition mechanism via a sol-gel reaction.

Kang *et al.*[46] used solid-state NMR to study the structures and dynamics of amino functional silanes adsorbed on Cab-O-Sil silica surfaces. The ^{29}Si NMR spectra of treated silica showed that the silane molecules were chemically bonded to the surface through siloxane bonds with surface silanol groups. The amount of coupling agent adsorbed increased with increased concentration of the treatment solution. This is consistent with an earlier study conducted by Ishida *et al.*[47] Spectra suggested monolayer coverage was obtained in solution concentrations of 2%, while multilayer coverage with evidence of a polysiloxane network was obtained using solutions above this concentration. Although Tripp *et al.*[48] has also demonstrated the formation of a polysiloxane network for some silane systems, other researchers[49,50] have found that siloxane films formed on glass substrates commonly exist as multiple layers instead of a monolayer. In polymer-metal systems, Plueddemann[29] concluded that monolayer coverage is rarely observed and multilayers <100Å are more commonly achieved in practice.

Okabayashi *et al.*[51] studied the behavior of 3-aminopropyltriethoxysilane (APS) on silica gel with diffuse reflectance infrared Fourier transform (DRIFT) spectra and provided evidence that the structure of APS was dependent on both the concentration used and the reaction time. At low concentrations (approximately 0.2-0.3 M), NH_3^+ groups were dominant on the silica surface; NH_2 groups were present where higher solution concentrations (approximately 0.6-0.7 M) were used. The author further suggested that the presence of NH_3^+ was indicative of a cyclic structure of APS. Ishida *et al.*[52] also proposed two structural models dependent on the degree of curing, which included a ring structure involving the protonated amine group and a free extended amine group. Plueddemann[29] proposed that APS could exist as a five- or six-membered ring or a linear structure depending on the pH of the solution. Esumi *et al.*[53] also found that the orientation of APS depended on solution pH. In alkaline solutions, APS adsorption was through the protonated amino group that generated a less stable interface, whereas in acidic conditions, the adsorption was through the hydrolyzed part of the molecule, thus allowing the formation of strong siloxane bonds. Chu *et al.*[54] claimed that at least four different APS nitrogen environments exist depending on the solvent employed (aqueous versus nonaqueous) and substrate.

In a study by De Haan *et al.*[55], covalent attachments of 3-aminopropyltriethoxysilane (APS) and 3-methacryloxypropyltrimethoxysilane (MPS) to silica powders were investigated using

FTIR and cross-polarization magic angle spinning (CP/MAS) NMR. It had been proposed in earlier studies[56,57] that covalent bonds between trifunctional silanes and substrates occur as mono-, bi- or tridentate linkages. De Haan *et al.*[55] provided evidence that the nature of the linkages was dependent on the solvent, coupling agent and heat treatment used in the application. The use of nonaqueous toluene solvent in APS deposition resulted in mainly mono- and bidentate linkages, whereas the use of water as the solvent yielded only bi- and tridentate linkages (no monodentate linkages) and definite crosslinking. Heating the gel to 200°C, in both cases resulted in an increase of tridentate bonding. In the case of dry toluene deposited MPS, mainly mono- and bidentate structures formed with only small quantities of tridentate and crosslinking structures, even upon heating. In a similar study, Caravajal *et al.*[58] found evidence that the amount of coverage and structure of silane using dry toluene were highly dependent on the availability of surface water.

Schrader *et al.*[59] and Johannson *et al.*[60] were the first to propose the presence of chemisorbed and physisorbed silane coupling agents on the surface of glass fibers. Using radio isotope-labeled APS, Schrader *et al.*[61] were able to quantify the amount of coupling agent in each layer. The physisorbed layer is defined as not interacting with the surface and may be easily removed by solvent washing. Schrader classified chemisorbed silane as two types, one that was removed by boiling water, and another that is a monolayer or less that cannot be removed by boiling water. Ishida *et al*[62] studied the structural differences of chemisorbed and physisorbed silanes.

Using grazing angle FTIR, Underhill *et al.*[63] studied the adsorption of 3-gycidoxy-propyltrimethoxysilane (GPS) in 1% aqueous solution on FPL-etched aluminum as affected by solution pH and hydrolysis time. Underhill[63] found that the amount adsorbed on the Al surface was not dependent of hydrolysis time or pH of solutions, but was dependent on the concentration of silane in solution. They proposed that the silane molecules actually do not interact with the Al but with adventitous carbon, and hence must permeate this layer to bind with aluminum. As a result, the deposition rate is highly dependent on pH if adsorption onto the surface was controlled by interaction of Si-OH and Al-OH entities. Although the extent of hydrolysis has little or no effect on the amount of silane adsorption, Underhill has shown that it has a significant effect on the adherence of the deposited silane film to the substrate. From FTIR spectra, the presence of chemisorbed and physisorbed silane was also observed.[63] Films deposited at a high pH tend to produce physisorbed silane.

Ondus *et al.*[64] showed that the nature of silane bonding is highly influenced by the substrate surface. In a FTIR study, Ordus *et al*[64] monitored the adsorption of APS on titanium, iron, aluminum 1100 and aluminum 2024 from a 1% APS aqueous solution. After a annealing at 110°C, an increase in the degree of polymerization was observed for the titanium, iron and aluminum 1100 samples. However, for films formed on aluminum 2024, spectra showed that the amine was oxidized to an imine with little or no extent of polymerization.

Although there is extensive literature on the reactions of silanes, and the structure and properties of silanes on surfaces, it is extremely difficult to draw firm conclusions about the general mechanisms for a specific system since almost every researcher has used a different combination of substrate, silane and application variables. No literature was found for silane coupling agents deposited on SiC or SiC/Si.

2.4.4 ADHESION PROMOTORS

Silane coupling agents have been utilized in many applications due to their ability to provide an interface with high stability between polymer and inorganic substrates, especially at high humidity and elevated temperatures. A good example of this is a study carried out by Ritter *et al.*[65,66] in which a double cleavage drilled compression test (DCDC) was used to evaluate the adhesion and reliability of epoxy/glass interfaces produced with APS. These interfaces represent a model system for the polymer/inorganic interfaces found in microelectronic packaging structures. Under compressive loading, crack growth results indicated that samples with silane coupling had a four-fold increase in resistance to moisture-assisted crack growth (95% relative humidity) compared to samples without silane.[65] Silane (APS) epoxy/glass (soda-lime) samples were also tested under cyclic loading at 95% relative humidity (RH).[66] Some samples were aged in distilled water at 70°C for 3 h, at 90°C for 3, 12 or 36 h, and at 94°C for 3, 10 or 34 h prior to testing. From fatigue crack growth evaluation, it was evident that accelerated aging did not decrease the resistance of the epoxy/glass interfaces and caused a modest increase in the resistance of the interface to cyclic fatigue. Samples that were aged at 98°C in water and subjected to cyclic loading resulted in cohesive failure and fractal crack growth. In addition, glass composition (soda-lime vs. fused silica) did not influence the silane bonding of epoxy to glass since the resistance of these interfaces to cyclic fatigue was similar.

Characterization of epoxy/glass systems with silane bonding, 3-aminopropyltriethoxysilane (APS) and octadecytrichlorosilane (OTS), was conducted by Woerdeman *et al.*[67] The strain energy release rate (G) and thermodynamic adhesion energy (W) were determined using the JKR (Johnson, Kendall and Roberts) method[68]. The data showed that at a given crack speed, the fracture energy of the epoxy/APS system was almost an order of magnitude higher than that of the epoxy/OTS system. The authors[67] attributed this to the gross chemical difference between the silanes, APS being polar with an amine functional group and OTS being nonpolar.

The topography of the APS system on glass, deposited by two different procedures, was studied using atomic force spectroscopy (AFM).[68] Scans showed that different silanation procedures yielded considerably different films with regards to surface topography, specifically surface roughness. AFM results also showed that silane films were not homogeneous but were deposited as patches. Dwight *et al.*[69] has also found this to be true. In a study by Darque-Ceretti *et al.*[70], the effectiveness of different coupling agents (tetraethoxysilane, aminosilane and vinylsilane) in the adhesion of silicone adhesive to oxide surfaces was evaluated using the single lap shear adhesion test. The average rupture shear stress and shear strain for the various silane treated specimens showed that the aminosilane and vinylsilane coupling agents gave the highest adhesion with cohesive fracture.

Alternative surface pretreatments to improve the durability of polymer/metal oxide bonds are widely sought to eliminate the use of toxic materials associated with organic primers and metal surface treatments.[71] In one study[72], a pretreatment method consists of grit-blasting the substrate, then boiling the substrate and lastly immersing it in a 1% 3-glycidoxytrimethoxysilane (GPS) solution. The pretreatment of aluminum alloys achieved notable improvements in bond durability with epoxy resins when compared with simple abrasion pretreatments. Using wedge style double cantilever beam specimens, samples were evaluated at 50°C and 95% RH for 1000 h. The "Grit-blast + Boil + Silane" pretreatment offered durability that was comparable or better than that achieved with the benchmark factory phosphoric acid anodization process. X-ray photoelectron spectroscopy (XPS) failure analysis provided evidence that the "Grit-blast + Boil + Silane" pretreatment resulted in failure predominantly in the epoxy, indicating that the pretreatment produced a sufficiently hydrolytically stable interfacial bond. Less durable treatments failed in the weakened oxide layer. Similar studies[73,74] have also suggested that GPS molecules improve the hydrolytic stability of the adhesive bond.

In the chip packaging industry, the proper adhesion of epoxy to the lead frame is important for device reliability. In a study by Song *et al.*[75], three different silane coupling agents were used to improve adhesion between epoxy resins and alloy 42 lead frames in high humidity conditions. The adhesion strength of specimens immersed in an 80°C water bath was measured by a 90° peel test. Peel strengths with the three different coupling agents (APS, GPS, N-β-(aminoethyl)-γ-aminopropyltrimethoxysilane (AAMS)) as a function of concentration showed that maximum adhesion strength was obtained at 4 wt% for APS and 0.5 wt% for AAMS and GPS. The highest initial adhesion strength, 200 N/m (compared with samples without silane, 45 N/m), was obtained with APS, but durability in a high humid environment was the best with AAMS. This is consistent with the result of Bonniau and Bunsell[76]. Moisture absorption tests[76] at 90°C/100% RH showed that silane treated samples resulted in slower moisture absorption and 4-8 wt% less water uptake.

Silane coupling agents have also been added to polymers to modify properties as well as increase adhesion. Wong *et al.*[77,78,79] have documented that the addition of a silane coupling agent to epoxy can enhance rheology, wetting and adhesion to various substrates. The study found that on average, unmodified epoxy adhesion strength to various substrates decreased 90% after immersion in boiling water whereas silane modified epoxy decreased 35% after the boiling water treatment. Epoxy functionalized silane had a maximum interfacial toughness enhancement (evaluated by die shear testing), whereas methacrylate functionalized silane had no significant effect on the interfacial toughness on various substrates. The viscosity of the polymer can also be decreased or increased depending on the silane used. Generally, thermal expansion and water adsorption were not affected by silane addition.

2.5 PLASMA TREATMENT

The application of plasma treatment in semiconductor device manufacturing has been invaluable to the advancement of microelectronic technology. Low pressure plasmas, also known as cold plasmas, nonequilibrium plasmas, and glow discharge processes, are incorporated in processing techniques such as sputtering[80], thin film deposition[81] (e.g. plasma enhanced chemical vapor deposition, plasma polymerization), ionitriding (used for surface hardening of

metals[82] and glasses[83]), dry cleaning[84], and plasma etching[85]. Plasmas may also be employed to chemically and physically alter an organic or inorganic surface to promote adhesion.[86] This discussion will primarily focus on the basic concepts of plasma, and surface modifications via non-polymer-forming plasma treatments.

2.5.1 PLASMA FUNDAMENTALS

A plasma is often defined as a partially ionized gas composed of atoms, ions, electrons, photons and neutral species all present in various states and energetic conditions.[87] Although a plasma consists of charged species, it is overall electrically neutral.[88] The plasma state is frequently referred to as the fourth state of matter, apart from solid, liquid, and gas states.[40,88]

Three essential items are needed to generate a plasma: (1) a reaction chamber, (2) a vacuum system with low pressure conditions (typically 1–10^{-3} Torr) to sustain the plasma state and (3) an energy source for ionization. Cold plasmas are usually generated electrically from an external energy source such as direct current (DC), radio frequency (RF) or microwave frequency (MW). The energy source generates an electric field in the reactor in which energy is transferred to free electrons. Excited electrons then collide with molecules and surfaces. Inelastic electron collisions with molecules produce neutral excitations, fragmentation into atoms and radicals (i.e. reactive species) and the formation of excited emitting species.[89, 90] Each electron carries an energy of 1-10 eV that is capable of breaking most covalent bonds.[91] Although the fraction of the gas that is ionized is low, typically 10^{-6} – 10^{-3} , reactive species (namely atoms, radicals and charged particles) are extremely reactive and can produce a variety of interactions with surfaces. Typical reactions that may occur in a plasma are given in Figure 2.3.

i)

Ionization:	$e + XY \rightarrow 2e + XY^+$
Attachment:	$e + XY \rightarrow XY^-$
Dissociation:	$e + XY \rightarrow e + X + Y$
Polar Dissociation:	$e + XY \rightarrow e + X^+ + Y^-$
Dissociative:	
- Ionization	$e + XY \rightarrow 2e + X + Y^+$
- Recombination	$e + XY^+ \rightarrow X + Y^*$
- Attachment	$e + XY \rightarrow X + Y^-$
Electron Impact Detachment:	$e + XY^- \rightarrow 2e + XY$

ii)

Charge Transfer	
- Resonant:	$X^+ + X \rightarrow X + X^+$
- Non resonant:	$X^+ + Y \rightarrow X + Y^+$
Recombination:	$X^+ + Y^- \rightarrow X\,Y$
Associative Detachment:	$X + Y^- \rightarrow XY + e$
Excitation Transfer:	$X + Y^* \rightarrow X^+ + Y + e$
	$\rightarrow XY^+ + e$
	$\rightarrow X^* + Y$

Figure 2.3 Representative types of reactions that occur in plasma: i) electron-molecules collisions, ii) heavy-particle collisions.

The main feature of a low pressure plasma is that reactive species are generated under "nonequilibrium" or "cold" conditions. Since electrons retain most of the energy gained from the electric field, thus not achieving thermodynamic equilibrium, gas molecules are rather "cold" with temperatures near ambient. This is an important feature in plasma processing since surface treatments may be carried out without producing thermal degradation.[89] Plasma treatments may be very complex involving a significant number of process variables in addition to the treatment time, temperature and atmosphere variables. Details of plasma composition are strongly influenced by power, the reactor design and gas composition.

2.5.2 INDUCTIVELY COUPLED PLASMA (ICP)

Inductively coupled plasma (ICP) is becoming one of the most important types of plasma reactors used in semiconductor processing.[84] A typical ICP reactor consists of a tubular vacuum

chamber, pumping unit, gas feeding system and gas controllers, pressure gage, a RF power supply (usually operating at 13.56 MHz) and a power transfer device. The major advantages of this type of generator are that no internal electrodes are needed (reducing plasma contamination), the plasma is easily sustained at a low pressure (< 50 mTorr) and has inherently high ionization efficiencies.[92] A radio frequency inductively coupled plasma is used in this research to modify substrates in an effort to promote adhesion.

2.5.3 PLASMA SURFACE MODIFICATION

The interaction between a plasma and a surface is not completely understood. As a solid surface undergoes plasma exposure, reactive species attack the surface physically by particle impact, transferring kinetic energy resulting in the heating of the surface and possibly removing atoms from structural sites. Plasma species also react chemically with the surface. Fundamentally, there are three classes of reactive species in the plasma state: atoms, radicals and charged particles.[93] Atoms are extremely reactive and can produce etching and chemical implantation interactions with surfaces. In an etching reaction, oxygen atoms produced in an oxygen plasma react with an organic material, such as carbon-containing contaminants or polymers, to produce volatile compounds such as CO_2 and H_2O. Oxygen atoms as well as oxygenated radicals and ions can implant into the surface, thus producing a surface with higher surface energy and wettability. Table 2.1 lists the plasma–surface interactions that are associated with the different types of reactive species.

Table 2.1 Plasma–surface interactions due to different fragments in a plasma.

Fragment	**Interaction**
atoms	etching
	chemical implantation
radicals	chemical implantation
	radical generation
charged particles	etching
	ion implantation

Surface activation by plasma treatment utilizing gases such as oxygen, hydrogen, helium, argon and nitrogen is perhaps one of the most efficient means of altering surface chemistry. Radicals and other activated species in the non-polymer-forming plasma can abstract hydrogen atoms from the surface, thus generating radicals on the solid surface resulting in a surface that is reactive or 'active'. Although this process is commonly referred to as 'activation', the term has also been used loosely to describe any surface modification process (not necessarily by means of radical formation) that leaves the surface more reactive.

The use of a plasma to activate silicon has been explored in low temperature direct bonding techniques of hydrophilic Si wafers that are used in fabrication of silicon-on-insulator (SOI) structures, and advanced microelectromechanical and optical devices. Suni *et al.*[94] studied the effects of plasma activation on the hydrophilic bonding of Si and SiO_2 (thermally grown on Si). Wafers were plasma treated in an argon, oxygen or nitrogen plasma and directly bonded with another wafer by annealing at various temperatures (100°C – 500°C). By applying the crack-opening method[95], the bonding energies of the bonded wafers (SiO_2 bonded to Si, also denoted as oxide/native oxide) were determined as a function of experimental parameters. Results showed that a 30-second plasma treatment yielded strong bonding for all plasma treated substrates. Bond energies of the plasma activated systems were approximately 2500 mJ/m^2 after annealing at 300°C, whereas the nontreated system only yielded a bond energy of <500 mJ/m^2. An experiment where the plasma treatment time was varied showed that a short plasma exposure of up to 30 seconds was more efficient than treatments of several minutes. Atomic force microscopy (AFM) measurements showed that surface roughness increased with extended plasma treatment. The authors[94] of this investigation suggested that plasma activation of Si and SiO_2 creates a surface structure that contains a high concentration of OH groups, thus resulting in high bond strengths.

Silicon direct bonding experiments utilizing activation methods were also conducted by Krauter *et al.*[96] In the experiments, three different activation procedures were investigated for Si and SiO_2 specimens: (1) chemical activation by hydrolyzed tetramethoxysilane (TMOS) (pH 10, 20 min., hydrolyzed in water), (2) exposure to an oxygen plasma (600 W, 1 Torr, 500 sccm, 5 min.) and (3) oxygen plasma followed by a TMOS treatment. In contrast to the large increase in bond strength reported for the pairing native oxide/native oxide after chemical activation by hydrolyzed TMOS[97] or after plasma activation[98], a significant bond strength was not attainable

for oxide/oxide bonding using any of the above three procedures. However, high bonding energies of about 1200 mJ/m^2 were achieved for oxide/native oxide bonding systems. The combination surface treatment of oxygen plasma followed by TMOS chemical activation resulted in the highest bonding energy, approximately 1400 mJ/m^2. The authors[96] claim that the TMOS method is able to increase the bonding energy by 20-50% by depositing Si-O species possessing a large number of reactive sites (presumably silanol groups), and that the oxygen plasma can also enhance bond strength at moderate temperatures by rendering specimens with highly hydrophilic surfaces. The authors[96], however, did not provide an explanation on how the combination of the two processes interact to yield the highest bond energy of the oxide/native oxide system.

Tong *et al.*[95] and Suni *et al.*[94] proposed that the disordered surface structure due to plasma treatment is responsible for the increased surface reactivity. Farrens *et al.*[98] suggested that Si-O-Si bond formation at the bonded interface is due to the plasma induced charging effect. Amirfeiz *et al.*[99] found no evidence to substantiate this hypothesis and instead suggested that the plasma treatment physically creates a porous surface structure that enhances the diffusivity of water molecules from the bonded interface resulting in high bonding of Si materials.

The effects of plasma treatment have been studied by various research groups. Reiche *et al.*[100] investigated the effects of oxygen plasma treatment on Si for dry etching processes used in microfabrication of advanced semiconductor devices. Variable angle spectroscopic ellipsometry (VASE) and high resolution transmission electron microscopy (HRTEM) evidence showed that exposure to an oxygen plasma (200 Pa, RF 600 W) resulted in the formation of a thin oxide layer (2 nm – 4 nm) in which the oxide layer thickness increased with exposure time up to 10 minutes. Infrared spectroscopic analysis showed Si-O-Si and Si-H_x (x = 1,2,3) vibration modes, all indicative of an oxide layer. Umezu *et al.*[101] showed that plasma-surface treatments of silicon wafers influenced surface roughness and surface defect density. It was shown that an argon plasma treatment resulted in no surface roughness but higher surface defect density, whereas hydrogen plasma treatment resulted in high surface roughness and low surface defect density. According to the authors[101], these events were due to argon reacting only physically with the Si surface via sputtering interactions, whereas hydrogen chemically reacts with the surface by diffusing into the sub-surface to break Si-O and Si-Si bonds. Similar results were reported by Weber *et al.*[102]

The surface modification process by plasma treatment has been incorporated into many diverse applications. In one study[103], a hydrogen plasma was used to clean Si wafers and to introduce hydrogen atoms into the surface to alter oxidation kinetics involved in forming thicker thermal oxide layers. In another study[104,105], oxygen, helium and air plasmas were used to improve the adhesion between an epoxy matrix and polymer fiber in the application of polymer fiber reinforced composites. It was found that the increase in adhesion was related to the increase in polarity of the modified surfaces. A plasma treatment was also used to improve the adhesion in metallized polymers that are commonly used in electronic devices, recording tapes and food packaging.[106] Compared to oxygen and ammonia plasmas, a helium plasma treatment was the most effective in increasing Kapton-Al adhesion. The authors[106] suggested that this might be attributed to the fact that the He plasma promotes crosslinking and active sites on the polymer surface.

In summary, although the plasma treatment is a cost effective and efficient method of altering surface chemical and physical properties, it is obvious that more research must be conducted to fully understand and optimize the surface modification effects induced by plasma treatments.

2.6 PROBE TEST

The probe test[107,108], developed by the Hewlett Packard Corporation, is a novel methodology for testing adhesion between a rigid polymeric thin-film and a rigid substrate. There are many techniques for evaluating thin-film adhesion; however, most are tensile in nature such as the standard peel tests[109,110] and blister tests[111,112]. These tests are not suitable for the epoxy thin film-wafer system under investigation since rigid thin-films are prone to fracture.

To compensate for the inflexibility of the films, the probe test measures adhesion in a compressive manner. Introduction of a conical shaped micro-probe within a film-substrate interface generates a debond and shear stress at the crack front as the debond propagates. As the probe is further inserted, a semi-circular crack (or debond) is generated at the probe tip. The profile and area of the debond are a direct function of the adhesion between the film and the substrate. Thus, from the dimension of the debond, thin-film adhesion can be evaluated and

quantified by the approximation[113] of the interfacial energy expressed via the critical strain energy release rate, G_c.

To determine the G_c for a given system, the semi-circular crack profile is approximated using Equation (1) given by Timoshenko[114] for the case of a symmetrical bending of circular plates with an applied external load at the center

$$w_0 = \frac{3Fa^2(1-v^2)}{2\pi Eh^3} \qquad \text{Eq. 2.1}$$

where w_o is the maximum deflection at the center, F is the external force, a is the crack radius, v is Poisson's ratio, E is the elastic modulus of the film and h is the film thickness. The critical strain energy release rate G_c for an elastic medium can be expressed as

$$G_c = -\frac{dU_E}{dA} \qquad \text{Eq. 2.2}$$

where G_c is the critical strain energy release rate, U_E is the elastic energy stored in an elastic medium and A is the crack area ($A = \pi a^2/2$). The elastic energy U_E can be written as

$$U_E = \int_0^{w_o} F dw \qquad \text{Eq. 2.3}$$

thus, resulting in the following equation for G_c

$$G_c = -\frac{d}{dA}\int_0^{w_o} F dw\,. \qquad \text{Eq. 2.4}$$

By rearranging Equation 2.1 and substituting F into Equation 2.4, G_c can then be expressed as

$$G_c = \frac{2Eh^3}{3(1-v^2)}\left(\frac{{w_o}^2}{a^4}\right). \qquad \text{Eq. 2.5}$$

Equation 2.5 was used to estimate all G_c values in this thesis.

2.7 ANALYTICAL TECHNIQUES

2.7.1 X-RAY PHOTOELECTRON SPECTROSCOPY (XPS)

X-ray photoelectron spectroscopy (XPS), also known as Electron Spectroscopy for Chemical Analysis (ESCA), is a powerful surface sensitive technique (approximately 50 Å) that allows the identification and quantification of atomic elements as well as information on the chemical state of the substituents at solid surfaces.[115] This technique utilizes an x-ray source, usually Mg K_α (1253.6 eV) or Al K_α (1486.6 eV), to ionize atoms of a solid resulting in the emission of photoelectrons.[116] A sample is placed in an ultrahigh vacuum environment and exposed to the x-ray beam. X-ray photons are absorbed by atoms resulting in the ionization and emission of core and valence electrons. In addition to the ejection of core electrons, Auger electrons are emitted as well.

The energy of a photon is given by the Einstein relation $E = h\nu$ where h is Plank's constant (6.62×10^{-34} J s) and ν is the frequency (Hz) of the radiation. The photoionization process is a result of the conservation of energy, and thus can be described by the equation $h\nu = KE + BE$ where KE is the kinetic energy of the photoelectron, $h\nu$ is the energy of the x-ray and BE is the binding energy or energy difference between the ionized and neutral atoms. The binding energy may also be taken as a direct measure of the energy required to emit an electron. Since binding energies are conventionally measured with respect to the Fermi-level of the solid rather than the vacuum level, a small correction, the work function Φ of the spectrometer, must be added to the equation yielding $h\nu = KE + BE + \Phi$.[116]

The photoelectrons and Auger electrons emitted from the sample are energy separated by an electron energy analyzer and detected by a position sensitive detector. A spectrum of the number of photoelectrons and Auger electrons as a function of BE is usually presented. Since each element has a characteristic BE associated with each core atomic orbital, detected signals (photopeaks) at particular energies indicate the presence of a specific element. Furthermore, the intensity of peaks is related to the concentration of the element, which allows the quantification of elements at the solid surface. Shifts in the BE provide information on oxidation states of the constituents. XPS is a well suited analytical technique for this research due to its ability to analyze substrate contamination, measure the elemental composition of modified and unmodified

surfaces, identify of chemical state of the surface (e.g. metal or oxide) and evaluate adhesion failure mechanisms.

2.7.2 AUGER ELECTRON SPECTROSCOPY (AES)

Auger electron spectroscopy (AES) is another surface sensitive analytical technique that provides information about the chemical composition of the surface of a solid. The major advantages of AES over other surface analysis techniques are its excellent spatial resolution (< 1 μm), high surface sensitivity (5 – 20Å), rapid data acquisition and elemental detection of elements of atomic number greater than helium. The Auger process starts with the excitation of the sample surface, most commonly by electron or hν bombardment. Under low vacuum conditions, the irradiation of the solid causes the ejection of an inner shell electron to form a vacancy that is filled by a second electron from a higher shell. To compensate for the energy change from this transition, either an x-ray is emitted or a third electron, otherwise known as the Auger electron, is emitted. The energies of the Auger electrons are measured by an electron spectrometer, and since the energy of the Auger electron is characteristic of the element from which it was emitted, elemental composition can be obtained. An Auger spectrum is a plot of electron signal intensity versus electron kinetic energy. Elemental quantification can also be obtained by AES since the intensities of peaks are proportional to elemental concentrations. In some cases, the chemical state of the surface atoms can also be determined from Auger electron energies and peak shapes.

AES is also commonly used for depth profiling. To analyze the samples in depth, Auger instruments incorporate ion beam sputtering to remove material from the sample surface. This process measures the elemental distribution as a function of depth into the sample. In this study, AES is used primarily for depth profiling.[117]

2.8 THESIS STATEMENT

This literature review has shown that silane coupling agents (SCAs) and plasma pretreatments are efficient means of surface modification processes for the improvement of adhesion. Although there is extensive documentation on the uses of SCAs and plasmas in adhesion promotion, the study of SiC as a substrate has not been published. The objective of this thesis is to demonstrate that a surface treatment combining both plasma treatment and SCA processes can enhance the adhesion in an epoxy/SiC/Si bonded system.

[1] C.T. Onions, The Oxford English Dictionary on English Etymology, Claredon Press: Oxford, 1966.

[2] J.A. Simpson and E.S.C. Weiner, *Oxford English Dictionary,* 2nd ed., Claredon Press: Oxford, 1989.

[3] "Standard Terminology of Adhesives," D 907, *Annual Book of ASTM Standards*, American Society for Testing and Materials.

[4] B. Ellis, *Chemistry and Technology of Epoxy Resins*, Blackie Academic & Professional: London, 1993, p. 207.

[5] A.J. Kinloch, *Adhesion and Adhesives, Science and Technology*, Chapman and Hill: New York, 1987, Chapter 1.

[6] D.E. Packham, *Handbook of Adhesion*, John Wiley and Sons: New York, 1992, p. 273.

[7] K. Bright, B.W. Malpas and D.E. Packham, *Nature,* **1969**, *223*, 1360.

[8] S.S. Voyutskii, *Autohesion and Adhesion of High Polymers*, Wiley: New York, 1963, p. 132.

[9] A.J. Kinloch, *Adhesion and Adhesives, Science and Technology*, Chapman and Hill: New York, 1987, Chapter 3.

[10] D.E. Packham, *Handbook of Adhesion*, John Wiley and Sons: New York, 1992, p. 39.

[11] A.J. Kinloch, *J. Mat. Sci.*, **1980**, *15*, 2141.

[12] B.V. Deryaguin and N.A. Krotova, *Proc. 2nd. Int. Congr. Surface Activity*, **1957**, *3*, 417.

[13] W.G. Potter, *Epoxide Resins*, Iliffe: London, 1970, p. 213.

[14] D.A. Debruyne, *J. Appl. Chem*., **1956**, *6*, 303.

[15] N.J. Chou and C.H. Tang, *J. Vac. Sci. Technol*., **1984**. *A2*, 751.

[16] N. Inagaki, S. Tasaka and K. Hibi, *J. Adhes. Sci. Technol.*, **1994**, *8*, 395.

[17] W.G. Potter, *Epoxide Resins*, Iliffe: London, 1970, p. 91.

[18] J.H. Lai, *Polymer for Electronic Applications*, CRC Press: Boca Raton, 1989.

[19] H. Lee and K. Neville, *Handbook of Epoxy Resins*, McGraw-Hill: New York, 1967, Chapter 2.

[20] B. Ellis, *Chemistry and Technology of Epoxy Resins*, Blackie Academic & Professional: London, 1993, Chapter 4.

[21] D.P. Seraphim, R. Lasky and C.Y. Li, *Principles of Electronic Packaging*, McGraw-Hill: New York, 1989, p. 336.

[22] C.A. Harper, *Handbook of Electronic Packaging*, McGraw-Hill: New York, 1968, Chapter 7.

[23] J.W. Lee, in *Epoxy Resins: Chemistry and Technology*, C.A. May (Ed.), CRC Press: Boca Raton, 1988, p. 110.

[24] J.C.W. van Vroonhoven, *J. Elec. Pack*., **1993**, *115*, 28.

[25] C.K. Gurumurthy, J. Jiao, L.G. Norris, C.Y. Hui and E.J. Kramer, *Application of Fracture Mechanics in Electronic Packaging*, ASME, AMD-Vol.222/EEP-Vol.201997, p. 41.

[26] C.A. Harper, *Electronic Assembly Fabrication*, McGraw-Hill: New York, 2002, p. 515.

[27] W. Monch, *Semiconductor Surfaces and Interfaces*, Springer: Berlin, 2001, p. 186.

[28] W.D. Bascom, *Engineered Materials Handbook Vol. 3: Adhesives and Sealants*, ASM International: USA, 1990, p. 254.

[29] E.P. Plueddemann, *Silane Coupling Agents*, Plenum Press: New York, 1991, Chapter 1.

[30] R.P. Digby and S.J. Shaw, *J. Adhes. Adhes*., **1998**, *18*, 261.

[31] J.D. Wright and N. Sommerdijk, *Sol-Gel Materials: Chemistry and Applications*, Taylor and Francis: London, 2001, Chapter 6.

[32] S. Sakka and K. Kamiya, *J. Non-Cryst. Solids*, **1982**, *48*, 31.

[33] H. Dislich and P. Hinz*, J. Non-Cryst. Solids*, **1982**, *48*, 11.

[34] D.E. Clark, *Science of Ceramic Processing*, Wiley: New York, 1986, p. 237.

[35] R.B. Pettit, C.S. Ashley and C.J. Brinker, *Sol-Gel Technology for Thin Films, Fibers, Preforms, Electronics, and Specialty Shapes*, L.C. Klein (Ed.), Noyes: Park Ridge, 1988, p. 80.

[36] R.B. Pettit and C.J. Brinker, *Solar Energy Mat*., **1986**, *14*, 269.

[37] R. Badheka, N.J. Bazin, P.A. Sermon, M.S.W. Vong and J.G. Leadley, *Sol-Gel Processing of Advanced Materials*, L.C. Klein, E.J.A. Pope, S. Sakka, J.L. Woolfrey (Eds.), American Ceramic Society: Westerville, 1988, p. 235.

[38] C.J. Brinker and G.W. Sherer, *Sol-Gel Science: The Physical and Chemistry of Sol-Gel Processing*, Academic Press: London, 1990, Chapter 1.

[39] D.J. Shaw, *Colloid and Surface Chemistry*, Butterworth: Oxford, 1992, Chapter 1.

[40] K.J. McNeil, J.A. DiCapri, D.A. Walsh and R.F. Pratt, *J. Am. Chem. Soc*., **1980**, *102*, 1859.

[41] R.A. Assink and B.D. Kay, *J. Non-Cryst. Solids,* **1988**, *99*, 359.

[42] S.J. Davis and J.F. Watts, *Int. J. Adhes.*, **1993**, *16*, 5.

[43] J. Fang, B.J. Flynn, Y.L. Leung, P.C. Wong, K.A.R. Mitchell and T. Foster, *J. Mater. Sci. Letter*, **1997**, *16*, 1675.

[44] L.D. White and C.P Tripp, *J. Colloid Interface Sci.*, **2000**, *232*, 400.

[45] P. Van Der Voort and E.F. Vansant, *J. Liq. Chrom. Rel. Technol*., **1996**, *19*, 2723.

[46] H.J. Kang and F. Blum, *J. Am. Chem. Soc.*, **1991**, *95*, 9391.

[47] H. Ishida and J. Koenig, *J. Colloid Interface Sci.*, **1978**, *64*, 555.

[48] C.P. Tripp and M.L. Hair, *Langmuir*, **1991**, *8*, 1120.

[49] K.W. Allen, *J. Adhes. Sci. Technol.*, **1992**, *6*, 23.

[50] E.K. Drown, H. Al Moussawi and L.T. Drzal, *J. Adhes. Sci. Technol.*, **1991**, *5*, 865.

[51] H. Okabayashi, I. Shimizu, E. Shimizu, E. Nishio and C.J. O'Connor, *Colloid Polym. Sci*., **1997**, *275*, 744.

[52] C.H. Chiang, H. Ishida and J.L. Koenig, *J. Colloid Interface Sci*., **1980**, *74*, 396.

[53] K. Esumi and K. Meguro, *Bull. Chem. Soc. Jpn*., **1983**, *56*, 331.

[54] C.W. Chu, D.P. Kirby and P.D. Murphy, *J. Adh. Sci. Technol.*, **1993**, *7*, 417.

[55] J.W. De Haan, H.M. Van Den Bogaert, J.J. Ponjee and L.J.M. Van De Ven, *J. Colloid Interface Sci.*, **1986**, *110*, 591.

[56] D.W. Sindorf and G.E. Maciel, *J. Amer. Chem. Soc*., **1983**, *105*, 3767.

[57] E.J.R. Sudholter, R. Huis, G.R. Hays and N.C.M. Alma, *J. Colloid Interface Sci*., **1985**, *103*, 554.

[58] G.S. Caravajal, D.E. Leydon, G.R. Quinting and G.E. Maciel, *Anal. Chem*., **1988**, *60*, 1776.

[59] M.E. Schrader, I. Lemer, F.J. D'Oria and L. Deutsh, *Soc. Plas. Ind*., **1967**, *22*, Sec.13-A.

[60] O.K. Johannson, F.O. Stark and R. Barney, AFML-TRI-65-303, Part 1, 1965.

[61] M.E. Schrader, *J. Adhes*., **1970**, *2*, 202.

[62] S.R. Culler, H. Ishida and J.L. Koenig, *J. Colloid Interface Sci*., **1985**, *106*, 334.

[63] P.R. Underhill, G. Goring and D.L. DuQuesnay, *Int. J. Adhes. Adhes.*, **1998**, *18*, 307.

[64] D.J. Ondrus and F.J. Boerio, *J. Colloid Interface Sci*., **1988**, *124*, 349.

[65] J.E. Ritter, J.R. Fox, D.I. Hutko and T.J. Lardner, *J. Mater. Sci.*, **1998**, *33*, 4581.

[66] J.E. Ritter and A. Huseinovic, *J. Elec. Pack*., **2001**, *123*, 401.

[67] D.L. Woerdeman, N. Amouroux, V. Ponsinet, G. Janeau, H. Hervet, and L. Leger, *Compos.: Part A*, **1999**, *30*, 95.

[68] K.L. Johnson, K. Kendall and A.D. Roberts, *Poc. Roy. Soc. London A*, **1971**, *324*, 301.

[69] D.W. Dwight, F.M. Fowes, D.A. Cole, M.J. Kulp, P.J. Sabat, L.Jr. Salvati and T.C. Huang, *Acid-Base Interactions: Relevance to Adhesion Science and Technology*, K.L. Mittal and H.R. Anderson (Eds.), Utrecht: Netherlands, 1991, p. 243.

[70] E. Darque-Ceretti and M. Aucouturier, *J. Colloid Interface Sci*., **1997**, *4*, 243.

[71] R.A. Pike, *Int. Conf. Adh.* (Adhesion '90), **1990**, 11/1.

[72] A.N. Rider and D.R. Arnott, *Int. J. Adhes. Adhes*., **2000**, *20*, 209.

[73] A.N. Rider and D.R. Arnott, *Surf. Interface Anal*., **1996**, *24*, 583.

[74] D.R. Arnott, A.R. Wilson, A.N. Rider, L.T. Lambrianidis and N.G. Farr, *Appl. Surf. Sci.*, **1993**, *70*, 109.

[75] S.M. Song and C.E. Park, *Pan Pacific Microelectron. Symp*., Proc. Technical Prog., Sur. Mount Technol. Assoc., **1988**, 441.

[76] P. Bonniau and A.R. Bunsell, *J. Composite Mater*., **1981**, *15*, 272.

[77] M.B. Vincent and C.P. Wong, *Sold. Surf. Mount Technol.*, **1999**, *11*, 33.

[78] Q. Yao, J. Qu, J. Wu and C.P. Wong, *IEEE Trans. Electon. Packag. Manuf.*, **1999**, *22*, 264.

[79] S. Luo and C.P. Wong, *IEEE Trans. Comp. Packag. Technol*., **2001**, *24*, 38.

[80] L.Maissel, Application of Sputtering to the Deposition of Films in *Handbook of Thin Film Technology*, L.I. Maissel and R. Glang (Eds.), McGraw-Hill: New York, 1970, Chapters 1-3.

[81] J.R. Hollahan and R.S. Rosler, Plasma Deposition of Inorganic Films in *Thin Film Processes*, J.L. Vossen and W. Kerns (Eds.), Academic: New York, 1978, Chpater 1-5.

[82] J.W. Coburn and H.F. Winters, *J. Vac. Sci. Technol.*, **1979**, *16*, 371.

[83] X. Zhou, R.A. Condrate and P.F. Johnson, *Mat. Res. Soc. Symp. Proc*., **1990**, *190*, 119.

[84] W.N.G. Hitchon, *Plasma Processes for Semiconductor Fabrication*, Cambridge Univ. Press: Cambridge, 1999, Chapter 5.

[85] E. Kay, J. Coburn and A. Dilks, *Top. Curr. Chem.*, **1980**, *94*, 1.

[86] A. Grill, *Cold Plasma in Materials Fabrication*, IEEE Press: NJ, 1994, Chapter 1.

[87] H.K. Yusuda, *Plasma Polymerization*, Academic Press: Orlando, 1985, Chapter 2.

[88] W.E. Mlynko, S.R. Cain, F.D. Egitto and F. Emmi, Plasma Processing in *Principles in Electronic Processing*, D.P. Seraphim, R. Lasky, C.Y. Li (Eds.), McGraw-Hill: New York, 1989, Chapter 14.

[89] R. d'Agostino, *Plasma Deposition, Treatment, and Etching of Polymers*, Academic Press: Boston, 1990, Chapter 1.

[90] M. Capiteli, R. Celiberto, G. Capriati, C. Gorse and S. Longo, Non-equilibrium Plasma Modeling in *Plasma Technology, Fundamentals and Applications*, M. Capiteli and C. Gorse (Eds.), Plenum Press: New York, p. 59.

[91] L.D. Nielsen, Ph.D. Thesis, Univeristy of Wisconsin-Madison, December 1995, Chapter 2.

[92] H. Suhr, Application of Non-equilibrium Plasmas to Organic Chemistry in *Techniques and Applications of Plasma Chemistry Polymers*, J.R. Hollahan and A.T. Bell (Eds.), John Wiley and Sons: New York, 1974, p. 23.

[93] R. d'Agostino, Plasma Surface Interactions in *Plasma Processing of Semiconductors*, P.F. Williams (Ed.), Klewer Academic: Boston, 1996, p. 221.

[94] T. Suni, K. Henttinen, I. Suni and J. Makinen, *J. Electrochem. Soc*., **2002**, *149*, G348.

[95] Q.Y. Tong and U. Gosele, *Semiconductor Wafer Bonding*, An Electrochemical Society Monograph, John Wiley and Sons: New York, 1999, Chapter 2-3.

[96] G. Krauter, A. Schumacher and U. Gosele, *Sensors and Actuators A*, **1998**, *70*, 271.

[97] J. Steinkirchner, T. Martini, M. Reiche, G. Kastner and U. Goesle, *Adv. Mater.*, **1995**, *7*, 662.

[98] S.N. Farrens, J.R. Dekker, J.K. Smith and B.E. Roberds, *J. Electrochem. Soc*., **1996**, *142*, 3949.

[99] P. Amirfeiz, S. Bengtsson, M. Bergh, E. Zanghellini and L. Borjesson, *J. Electrochem. Soc.*, **2000**, *147*, 2693.

[100] M. Reiche, M. Weigand and U. Goele, *Microchim. Acta*, **2000**, *133*, 35.

[101] I. Umezu, K. Kohono, K. Aoki, Y. Kohama, A. Sugimura and M. Inada, *Vac.*, **2002**, *66*, 453.

[102] C. Weber, *Physica B*, **1991**, *170*, 201.

[103] A. Szekeres, A. Paneva and S. Alexandova, *Vac*., **2001**, *61*, 263.

[104] J.R. Hall, C.A.L. Westerdahl, M.J. Bodnar and D.W. Levi, *J. Appl. Polym. Sci*., **1972**, *16*, 1465.

[105] C.A.L. Westerdahl, J.R. Hall, E.C. Schramm and D.W. Levi, *J. Colloid Interface Sci.*, **1974**, *47*, 610.

[106] R. Lamendola, E. Matarrese, M. Creatore, P. Favia and R. d'Agostino, *Mat. Res. Symp. Proc*., **1999**, *544*, 269.

[107] C. Scott, K.T. Wan and D. Dillard, *Proceedings of the 25th Annual Meeting of The Adhesion Society and The Second World Congress on Adhesion and Related Phenomena*, Orlando, FL, 2002, p. 139.

[108] D. Xu, K.T. Wan and J.G. Dillard, *Proceedings of the 26th Annual Meeting of The Adhesion Society and The Second World Congress on Adhesion and Related Phenomena*, Myrtle Beach, NC, 2003, p. 420.

[109] K. Kendall, *J. Phys. D*., **1975**, *8,* 1449.

[110] A.N. Gent and S. Kaang, *J. Appl. Polym. Sci*., **1986**, *32*, 4689.

[111] H. Dannenberg, *J. Appl. Polym. Sci.*, **1961**, *5*, 125.

[112] K.T. Wan, *J. Adhesion*, **1999**, *70*, 209.

[113] K.T. Wan, Z. Sun, C. Scott, D. Dillard and D. Xu, Personal Communication, 2003.

[114] S.P. Timoshenko and S. Woinosky-Krieger, *Theory of Plates and Shells*, 2nd ed., McGraw-Hill: New York, 1959, Chapter 3.

[115] H.M. Tong and L. Nguyen, *New Characterization Techniques for Polymer Films*, Wiley and Sons: New York, 1990, Chapter 11.

[116] W.M. Riggs and M.J. Parker, Surface Analysis by X-Ray Photoelectron Spectroscopy in *Methods of Surface Analysis*, A.W. Czanderna (Ed.), Elsevier: New York, 1989, Chapter 4.

[117] A. Joshi, L.E. Davis and P.W. Palmberg, Auger Electron Spectroscopy in *Methods of Surface Analysis*, A.W. Czanderna (Ed.), Elsevier: New York, 1989, Chapter 5.

3 EXPERIMENTAL

3.1 MATERIALS

3.1.1 ADHESIVE

A model epoxy consisting of a bis-phenol F diglycidyl ether (Figure 3.1) was used in all experiments. The bisphenol-F resin (Epon 862) was obtained from Shell Chemical Corporation, and cured with 4-methyl-2-phenylimidizole (provided by Aldrich). In addition, 1,4-butanediol (Aldrich, 99+ % purity) was incorporated into the model epoxy to increase the solubility of the curing agent. The epoxy was prepared by stirring the resin with 10 parts per hundred (phr) of 1,4-butanediol at 70 °C for approximately 5 minutes until a clear mixture was obtained. Then, 3 phr of 4-methyl-2-phenylimidizole was added to the mixture and heated at 70 °C for approximately 20 minutes. Care was taken to make sure that the curing agent was completely dissolved to obtain a homogeneous mixture. The epoxy was then degassed using a vacuum line. The adhesive was allowed to degas at room temperature for 30 minutes, then it was degassed in an ice water bath for 15 minutes followed by degassing in a hot water bath at 60°C for another 15 minutes. Proper removal of gas was crucial to obtain uniform adhesive films without bubbles. The epoxy was then deposited on a SiC/Si substrate either by spin casting or by the Teflon sandwich method (see Section 3.5.2). The epoxy was thermally cured at 130 °C for 1 hour in air. The structures of the epoxy adhesive components are shown in Figure 3.1.

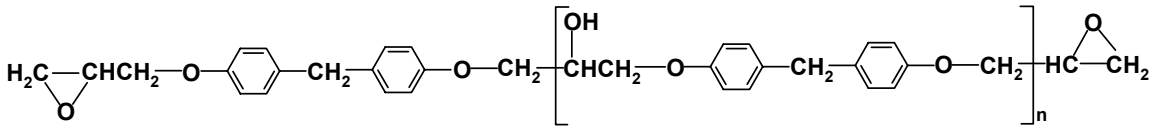

(a)

HO-CH_2-CH_2-CH_2-CH_2-OH

(b) 3 phr

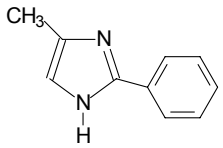

(c) 10 phr

Figure 3.1 Model epoxy composition: (a) bis-phenol F diglycidyl ether (Epon 862), (b) 1,4-butanediol and (c) 4-methyl-2-phenylimidizole .

3.1.2 SUBSTRATE

Silicon wafers coated with SiC (denoted as SiC/Si) were obtained from Hewlett Packard Corporation. The SiC layer was deposited by chemical vapor deposition (CVD). Wafers were cut into 12 mm x 12 mm (½" x ½") samples by first scribing the wafer using a diamond-tip scriber and then fracturing the specimen using pliers. The thickness of the wafers was approximately 66 μm. Substrates were surface modified with plasma and/or silane agents, and subsequently coated with the model epoxy adhesive.

3.1.3 SILANE COUPLING AGENTS

SiC/Si wafers were chemically modified using one of the two silane coupling agents: 3-aminopropyltriethoxysilane (APS) or 3-glycidoxypropyltrimethoxysilane (GPS). Silane coupling agents (SCAs), obtained from Aldrich with purities of 99% and 98%, respectively, were applied using a sol-gel reaction that involved ethanol as a solvent and hydrochloric acid (HCl) as a catalyst. The structures of the SCAs are shown in Figure 3.2. See Section 3.4 for further reaction details.

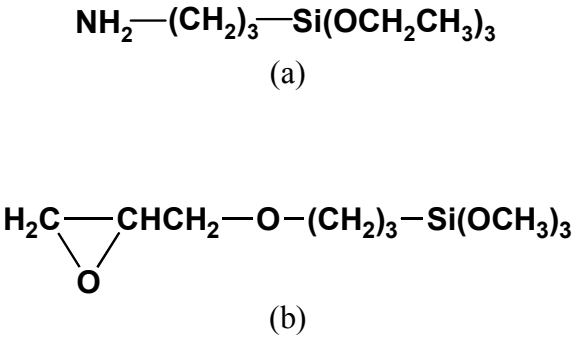

Figure 3.2 Structures for the silane coupling agents: (a) 3-amino-propyltriethoxysilane (APS) and (b) 3-glycidoxypropyltrimethoxysilane (GPS).

3.2 PLASMA REACTOR

A custom built 27.12 MHz RF plasma reactor was used for all plasma treatments.[1] A Pyrex glass tubular vessel with dimensions of approximately 75 cm x 10.5 cm served as the reactor chamber. The chamber had inlets for multiple gas introduction. Gas flows were monitored by mass flow controllers (Brooks Instruments Model 5850 and Model 5851). Vacuum was achieved by a turbo pump backed by a rotary pump. The pumps were connected to one end of the plasma chamber. On the other end of the chamber was a Hastings-Raydist thermocouple gauge and a 2-turn induction coil. The gauge measured chamber pressure while the induction coil delivered up to 5 kW of power from a 27.12 MHz inductively coupled power source (Plasma Power, Inc). An RF tuner was used to tune the coils to match the source resistance. Samples were placed at the bottom of the chamber, approximately 9 cm (3.5 inches) downstream from the coil. A schematic and a picture of the reactor are illustrated in Figure 3.3 and Figure 3.4, respectively.

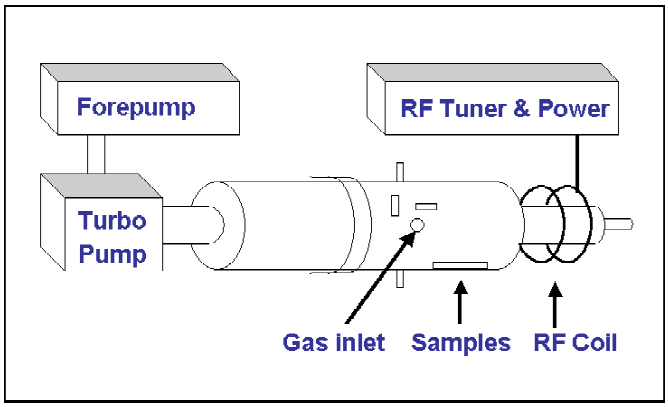

Figure 3.3 A schematic of the plasma reactor.[1]

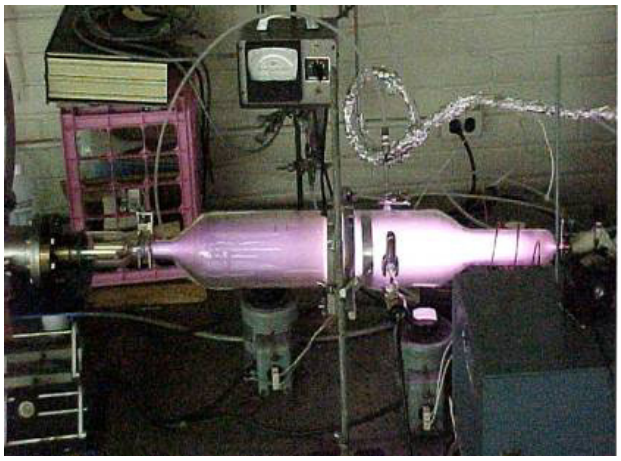

Figure 3.4 Picture of the RF plasma reactor.[1]

3.3 PLASMA TREATMENTS

Plasma pretreatments using oxygen and water/oxygen as the reactant gases were carried out at 50 W with a flow rate of 20 sccm. The plasma input power and gas flow rate were adapted from a DOE (Design of Experiment) model previously carried out.[2]

3.3.1 OXYGEN PLASMA

Substrates were placed in the reactor chamber, and the system was evacuated to a pressure of approximately 5-6 mTorr. Oxygen was introduced at a flow rate of 20 sccm and the gas was allowed to pass through the chamber for 2 minutes. The plasma was then ignited with an input power of 50 W, and the induction coil was tuned to match the source impedance to reduce the reflected power. After the desired time of plasma treatment (2, 5, 15 or 30 minutes), the samples were then purged with O_2 gas for 10 minutes to stabilize any reactive radicals or species that might be on the surface. Plasma treated samples were subsequently treated with silane coupling agents as described in Section 3.4.

3.3.2 WATER / OXYGEN PLASMA TREATMENT

The H_2O/O_2 plasma treatment is similar to the O_2 plasma treatment except that water was also introduced into the chamber by bubbling O_2 gas through H_2O at room temperature. The bubbler containing deionized water was placed in a Dewar to ensure temperature stabilization. The chamber was evacuated to 5-6 mTorr. A 10-minute O_2 plasma pretreatment as described in the previous section was first carried out as a cleaning procedure to remove any carbonaceous contaminants, then the wafers were subsequently surface modified with the H_2O/O_2 plasma treatment. For the H_2O/O_2 plasma treatment, O_2 was bubbled though water at a flow rate of 20 sccm. A needle valve was used to regulate the flow of H_2O/O_2 and to maintain the chamber pressure at 25 mTorr. The H_2O/O_2 gas was introduced into the chamber for 2 minutes. The plasma was ignited and substrates were exposed to the H_2O/O_2 plasma (50 W) for either 10 or 20 minutes.

Following the H_2O/O_2 treatment, the chamber was purged with O_2 gas (dry) for 10 minutes to stabilize any reactive species on the substrate surface. Plasma treated samples were subsequently treated with silane coupling agents as described in Section 3.4.

3.4 SILANE TREATMENT

As-received and plasma-treated SiC/Si samples were immersed in 5% (v/v) 0.1 M HCl in 100 mL of 100% ethanol for 15 minutes to promote the formation of hydroxyl groups on the surface of the substrate. A sol-gel reaction was then initiated by adding a solution consisting of 5% (v/v) 0.1 M HCl and 5% (v/v) silane coupling agent (APS or GPS) in 100 mL of 100% ethanol, ultimately resulting in a sol-gel solution that was 0.12 M in silane coupling agent. After samples were allowed to react in the sol-gel solution for 30 minutes, they were rinsed in ethanol and allowed to air dry at room temperature. The samples were then placed in an oven and heated for 30 minutes at 120 °C.

3-aminopropyltriethoxysilane (APS) and 3-glycidoxypropyltrimethoxysilane (GPS) were selected based on their reactivity with epoxy resins. The glycidylfunctional silane was an obvious choice since the adhesive used in this investigation was a glycidylfunctional epoxy resin, which means that the coupling agent should have a reactivity comparable to that of the epoxy resin. The aminofunctional silane was chosen based on the fact that amine groups react with epoxy groups via addition reactions by nucleophilic substitution.[3]

3.5 SAMPLE PREPARATION

3.5.1 IMMERSION TEST SAMPLES

Surface modified SiC/Si substrates were cleaved into 12 mm x 12 mm (approximately ½“ x ½“) samples and were spun-cast with the model epoxy to form a film approximately 10-40 μm thick. Drops of epoxy were placed on the substrate while a heating lamp warmed the epoxy and substrate to approximately 80 – 100 °C. The heating of the epoxy lowers the polymer viscosity, resulting in improved flowing and wetting. The sample was then spun at 2000 rpm for approximately 30 seconds. This procedure was often repeated several times to achieve the proper coverage or to obtain the desired adhesive thickness. The specimen was then left under the heat lamp for approximately 2 minutes to allow the epoxy to harden, and was subsequently placed in an oven at 130 °C in air for 1 hour to cure the epoxy adhesive. Due to the limited geometry of the sample, polymer buildup at the edges was common.

For treated samples where poor wettability of the surface was encountered, the epoxy was cast by sandwiching the epoxy/SiC/Si between two Teflon plates. Shims were placed between the plates to control film thickness. Via this procedure, a film of approximately 150 μm was obtained.

3.5.2 PROBE TEST SAMPLES

Samples were prepared by casting 70 μm thick epoxy films on 20 mm x 20 mm treated SiC/Si samples. A typical sample was prepared by first placing an 70 μm thick Teflon template on the sample. The epoxy was then placed on the SiC/Si wafer. Subsequently, the epoxy/template/SiC/Si samples were sandwiched and clamped between two Teflon plates and placed in an oven at 130 °C for 1 hour to cure. The dimensions of the Teflon plates were approximately 25 mm x 12 mm x 6 mm (1" x ½" x ¼"). A schematic of the Teflon sandwich arrangement is shown in Figure 3.5.

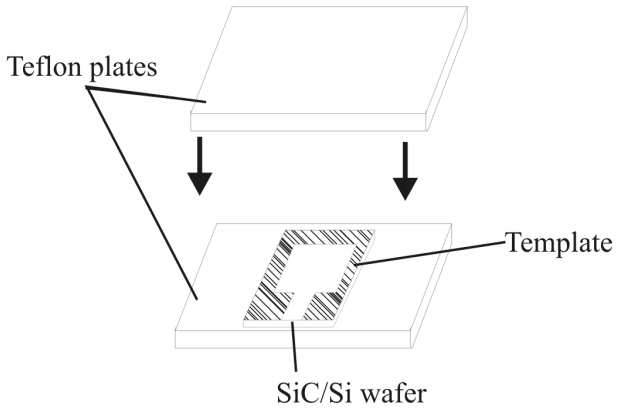

Figure 3.5 Diagram of the Teflon sandwich arrangement.

3.5.3 EDGE PROTECTION TREATMENT

After the samples were coated, they were immersed in a solution consisting of 5% (v/v) 0.1 M HCl and 5% (v/v) silane coupling agent in 100% ethanol for 30 minutes. The specimens were subsequently rinsed with ethanol, allowed to air dry and were heated for 30 minutes at 120 °C in air. The purpose of this treatment is to protect the edges of the film. The edge is an area where the interface is exposed, and therefore most vulnerable to water and solvent attack. Samples were edge treated with the same coupling agent that was used in silane treatment. Samples that were not silane treated were edge treated with APS. All samples were edge treated unless otherwise noted.

3.6 IMMERSION TEST

Specimens were immersed separately in four different aqueous solutions at 60 °C and periodically examined for evidence of debonding. The samples were visually examined as a function of time and debonding occurrences were recorded. The time to initial debond is defined as the first pronounced appearance of blister formation, solution leech-in, or film lifting from the surface, corners, or edges, as illustrated in Figure 3.6. The immersion test was carried out twice to ensure reproducibility. The pHs of the different aqueous solutions were 4.2, 6.7, 7.7 and 8.2. The solutions will be referenced by their pH value for identification.

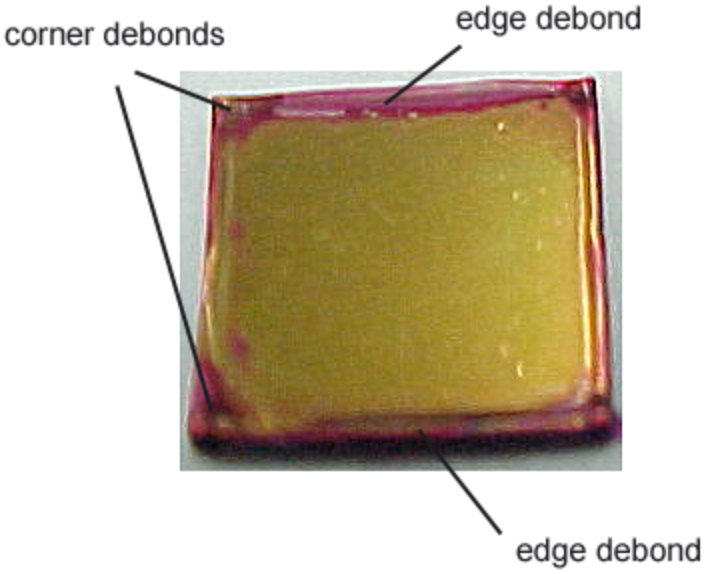

(a)

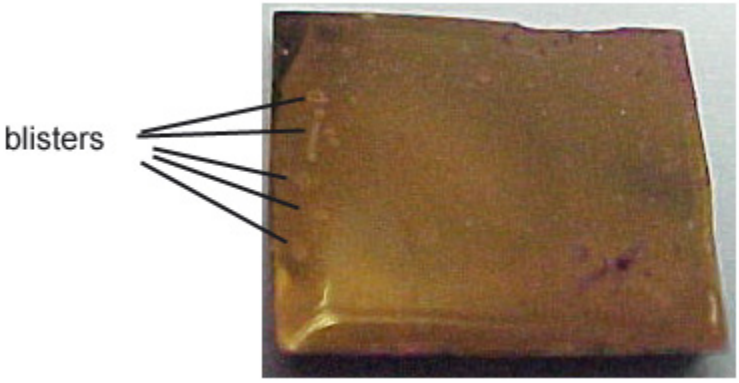

(b)

Figure 3.6 Examples of specimens showing initial debond failure: (a) lifting and solution leech-in at corners and edges, and (b) blister formation.

3.7 PROBE TEST

Specimens were immersed separately in three different aqueous solutions (pH 6.7 and pH 8.2 solutions, and deionized water) at 60 °C for 0, 1, 7, 14, 21, or 28 days. The samples were then removed from the solution, blotted lightly with a Kim-wipe tissue to remove excess solution and subsequently probed to test adhesion. Three probe runs were performed for each sample.

A schematic diagram of the probe test apparatus is shown in Figure 3.7. A tungsten probe with a tip radius of 10 μm was inserted at an edge of the adhesive film/substrate interface. The probe apparatus consisted of a Nikon UM-2 Measurescope microscope, a digital measuring stage and a Karl Suss micromanipulator that allowed the user to manipulate the probe along the Cartesian axes. A green filter with a wavelength of 414.5 nm was used to enhance the appearance of the debonded area. A digital camera was attached to the viewing lenses to photograph debonding events. All measurements were made with the probe angle of 25° relative to the plane of the substrate.

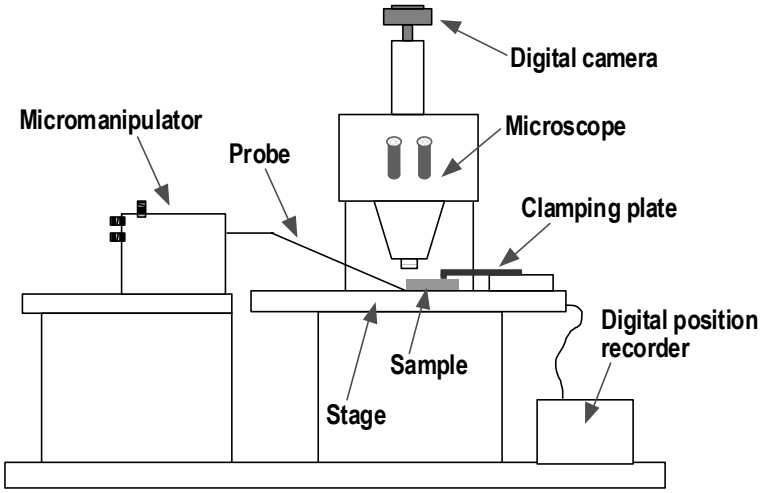

Figure 3.7 Schematic diagram of the probe test apparatus.[4]

As the probe was inserted into the interface, a semi-ellipsoidal delamination occurred as shown in Figure 3.8. To calculate the critical strain energy release rate G_c, the dimensions of the delamination, r_1 and r_2, at a probe penetration distance of 0.250 mm were recorded. Since Equation 2.5

$$G_c = \frac{2Eh^3}{3(1-v^2)}\left(\frac{{w_o}^2}{a^4}\right) \qquad \text{Eq. 2.5}$$

a = crack radius
w_0 = maximum film deflection
E = elastic modulus of the film
h = film thickness
v = Poisson's ratio

is based on a semi-circular crack and not a semi-elliptical crack, $a = \sqrt{r_1 \cdot r_2}$ was used to calculate the crack length a. The maximum defection of the film w_0 was determined by measuring the maximum vertical separation distance of the film from the substrate at the point of probe intrusion. All G_c values were determined for a probe penetration distance of 0.250 mm. Table 3.1 list the values used to calculate G_c.

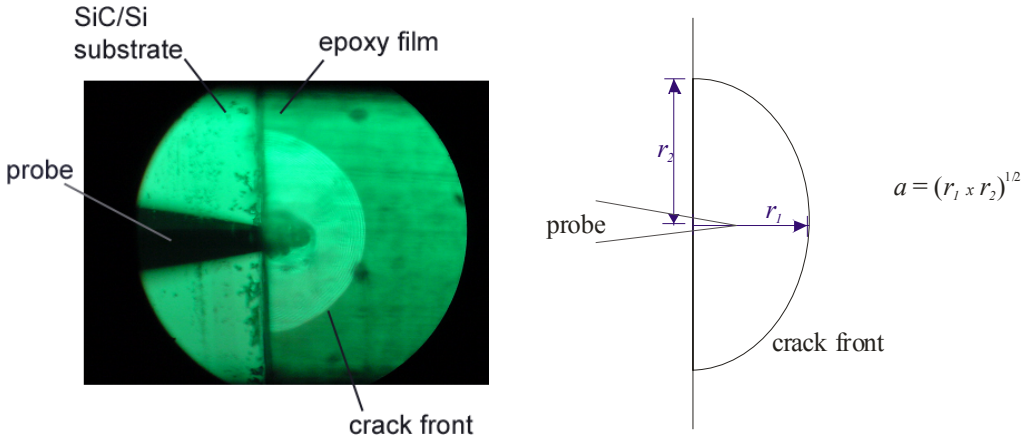

Figure 3.8 A picture and schematic drawing of a debonding event.

Table 3.1 Values used to calculate the critical strain energy release rate G_c.

w_0	116.6 μm
E	2.5 GPa[5]
v	0.33[6]
h	80 μm

3.8 SURFACE ANALYSIS

3.8.1 X-RAY PHOTOELECTRON SPECTROSCOPY (XPS)

A Perkin-Elmer Model 5400 XPS equipped with an Mg K_α x-ray source (hv = 1253.6 eV) was used to characterize all surfaces. The x-ray source was operated at 300 W. All spectra were taken from a spot size of 1 mm x 3 mm and a take off angle of 45°. X-ray satellite photopeaks were subtracted from all spectra and all peak assignments were referenced to the C-C/C-H carbon peak at 285.0 eV[7]. Analytical analyses of C 1s, Si 2p and N 1s photopeaks were carried

out by curve fitting the peaks using a Gaussian function. The photopeak assignments used for curve-fitting are based on literature values and are given in Table 3.2.

Consideration of chemical stoichiometry and full width at half maximum (FWHM) for curve-fit photopeaks was also used in the curve-fitting criteria. Assuming that the FWHM for SiC is approximately equivalent to the FWHM for elemental Si, the FWHM for SiO_2 from a thermally oxidized (TOX) Si wafer, determined as 1.7 eV[8], was used to curve-fit the Si 2p photopeaks (Si-C, SiO_2, Si-OR). For C and N photopeaks, the FWHMs for APS deposited on a Si TOX wafer were used as fitting parameters. The FWHM values for C and N were 1.8 eV and 2.0 eV, respectively.[8] Although the FWHM values were selected as reference standards, in some cases, the FWHM was varied by ± 0.2 eV to obtain the best curve-fit.

Table 3.2 XPS peak assignments for C 1s, O 1s, Si 2p and N 1s photopeaks.[7,9, 10, 11]

Peak Positions (eV)	Assignments
C-Si	283.1-283.6[10]
CH/CC	285.0[7]
C-O	286.3 – 286.7[9]
C=O	287.8 – 288.2[9]
O=C-O	289.2[9]
O-C	533.1 – 533.3[9]
O=C	531.6-532.1[9]
O-Si	532.4 – 533.0[9]
Si-C	100.4 – 100.7[10]
Si-O-Si	102.3 – 102.7[11]
Si-O_2 (SiC)	102.4 – 102.8[10]
Si-O_2 (silica, Si)	103.2 – 103.5[9]
-N-H_2	399.7 - 400.0[11]
-N-H_3^+	401.4 – 401.6[11]

3.8.2 AUGER ELECTRON SPECTROSCOPY (AES)

Depth profile studies were performed with a Perkin Elmer PHI 610 Scanning Auger Microprobe. The electron beam was operated at 3000 V at a current of 0.05 μA. Sputtering was achieved using a 4 kV argon ion beam. The ion beam current was 5 μA. Sputter rates were either 2.5 Å/min or 50 Å/min depending on estimated film thickness. The sputter rate was calibrated using a known oxide thickness of a Ta_2O_5 on Ta.

[1] R.A. DiFelice, Ph.D. Thesis, Virginia Tech, May 2001, p. 51.

[2] R.A. DiFelice, Ph.D. Thesis, Virginia Tech, May 2001, Chapter 5.

[3] B. Ellis, *Chemistry and Technology of Epoxy Resins*, Blackie Academic & Professional: London, 1993, p. 12.

[4] D. Xu, K.T. Wan and J.G. Dillard, *Proceedings of the 26th Annual Meeting of The Adhesion Society and The Second World Congress on Adhesion and Related Phenomena*, Myrtle Beach, NC, 2003, p. 420.

[5] W.G. Potter, *Epoxide Resins*, Iliffe: London, 1970, p. 99.

[6] B. Ellis, *Chemistry and Technologies of Epoxy Resins*, Blackie Academic and Professional: London, 1993, p. 105.

[7] D. Briggs, Applications of XPS in Polymer Technology in *Practical Surface Analysis by Auger and X-ray photoelectron spectroscopy*, D. Briggs and M.P.Seah (Eds.), John Wiley and Sons: New York, 1985, p. 359.

[8] D. Xu, Personal Communication; June, 13, 2003.

[9] C.D. Wagner, W.M. Riggs, L.E. Davis, J.F. Moulder and G.E. Muilenburg, *Handbook of X-Ray Photoelectron Spectroscopy,* Perkin Elmer: Eden Prairie, 1979, Appendix 3.

[10] R.C. Lee, C.R. Aita and N.C. Tran, *J. Vac. Sci. Technology*, **1991**, *A9*, 368.

[11] E.T. Vandenberg, L.B. Bertilsson, B.L. Kasjsa Uvdal, R. Erlandsson, H. Elwing and I. Lungstrom, *J. Colloid Interface. Sci.*, **1991**, *147*, 103.

4 SURFACE CHARACTERIZATION AND ADHESION

4.1 INTRODUCTION

The system of interest in this investigation is a thin film epoxy bonded to SiC that has been deposited on a Si wafer (SiC/Si). In this chapter, the first part of the discussion focuses on the as-received SiC/Si and model epoxy system. Detailed characterization of the unmodified materials and the unmodified bonded system serves as a reference and a basis of comparison for surface-modified systems. The second part of the chapter discusses surface treatments. In this study, three different surface modification approaches were investigated with the objective of improving the adhesion of the model epoxy to the SiC/Si wafer: 1. silane treatment of SiC/Si with APS or GPS, 2. O_2 plasma pretreatment of SiC/Si followed by silane treatment, and 3. H_2O/O_2 plasma pretreatment of SiC/Si followed by silane treatment. In both non-modified and modified systems, surface sensitive analysis techniques, XPS and/or AES, were utilized to obtain chemical information on the adhesive and substrate. Adhesion of the model epoxy bonded to SiC/Si was tested in four different aqueous solutions (referenced by their pHs) at 60 °C. Adhesive durability (time to debond) was evaluated using the immersion test (Section 3.6), and quantitatively measured using the probe test (Section 3.7) via the determination of the critical strain release energy rate, G_c. Failure analysis using XPS will also be discussed as related to adhesive bond durability.

4.2 XPS AND AES ANALYSES FOR NON-SURFACE MODIFIED MATERIALS

4.2.1 SIC/SI WAFERS

SiC/Si wafers were rinsed with acetone and blown dry with nitrogen gas just prior to XPS characterization. Carbon, oxygen, silicon and fluorine were detected in the wide-scan spectrum of the as-received SiC/Si wafer. Table 4.1 lists the elemental surface composition for the SiC/Si substrate. The curve-fit photopeaks for C 1s are shown in Figure 4.1 and peak assignments are

given in Table 4.2. The C 1s spectrum was resolved into four Gaussian peaks labeled C_{I-IV}. Peak C_I at a binding energy (BE) of 283.4 eV was attributed to carbide carbon in SiC while peak C_{II} at 285.0 eV was assigned to adventitious carbon (C-H/C-C). Peaks C_{III} (286.4 eV) and C_{IV} (288.9 eV) were also attributed to adventitous C in the form of C-O and $C=O_x$ (x=1), respectively. Peak C_{IV} is likely a composite peak consisting of C=O and O=C-O components. To check the carbon to oxygen stoichiometry, the absolute $Si-O_2$ content was calculated to be 6.6% (total % Si (Table 4.1) multiplied by the percent of $Si-O_2$ peak area (Table 4.3), 34.2% x 0.192 = 6.6%). Since there are two oxygen atoms for one silicon atom in SiO_2, 13.2% (6.6% x 2) was subtracted from the total oxygen content (17.8%), leaving 4.6% to account for the O-C and O_x=C contributions. The total contribution of O-C and O_x=C content in the O 1s spectrum is in agreement with that for the total contribution of O-C and O_x=C in the C 1s spectrum (4.6% and 5.2%, respectively). All carbon peak assignments with regard to binding energies were consistent with reported values for sputter deposited SiC[1] (C-Si at 283.1-283.6 eV; CH/CC at 285.0 eV; C-O at 286.5-286.7 eV; and C=O at 288.7-289.2 eV). The origin of fluorine is unknown. It is suspected that fluorine is present from wafer cleaning by the supplier. Nevertheless, the fluorine content was reproducible on all as-received wafer samples.

Table 4.1 XPS analysis for the as-received SiC/Si substrate (atomic %).

Sample	% C	% O	% Si	% F
SiC/Si	45.8	17.8	34.2	2.2

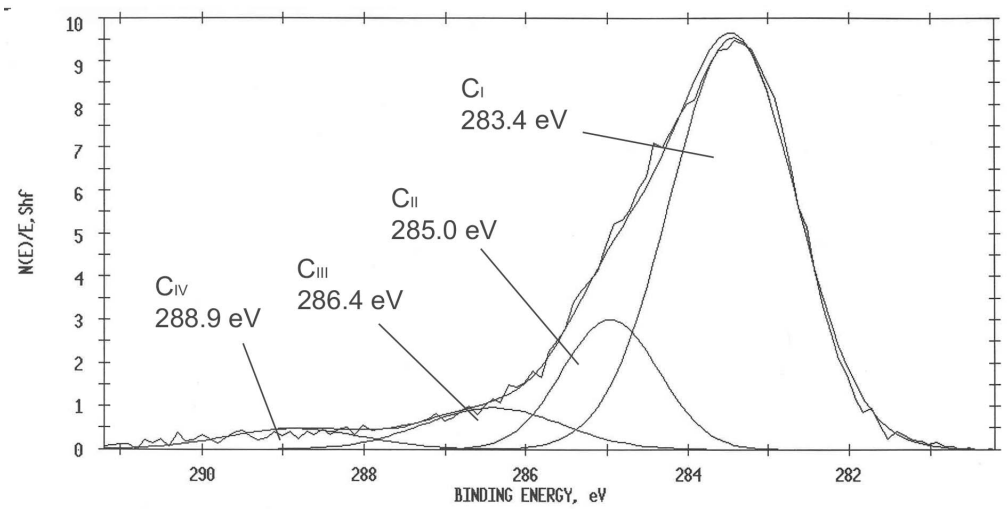

Figure 4.1 Curve-fit C 1s photopeaks for the as-received SiC/Si wafer.

Table 4.2 Peak assignments for the curve-fit C 1s photopeak for SiC/Si wafer.

Peak No.	Peak Position (eV)	% Area	Assignment
C_I	283.4	72.3	C-Si
C_{II}	285.0	16.4	C-H/C-C
C_{III}	286.4	7.9	C-O
C_{IV}	288.9	3.4	$C=O_x$

Table 4.3 Peak assignments for the curve-fit Si 2p photopeak for as-received SiC/Si wafer.

Peak No.	Peak Position (eV)	% Area	Assignment
Si_I	100.4	80.8	Si-C
Si_{II}	102.4	19.2	$Si-O_2$

The O 1s and Si 2p spectra are shown in Figure 4.2 with peak assignments in Table 4.3. Although a small percentage (~5%) of O-C and O_x=C is present, the O 1s spectrum (Figure 4.2a) primarily consists of a single, symmetric peak at BE of 532.3 eV which is in agreement with that that reported for O at the surface of SiC samples.[1] The Si 2p spectrum was curve-fit into two Gaussian peaks labeled as Si_I and Si_{II} (Figure 4.2b). Peak Si_I at 100.4 eV is attributed to Si bonded to C and peak Si_{II} at 102.4 eV is attributed to Si bonded to O from SiO_2. Both binding energy values are consistent with reported values[1]. Although the BE for SiO_2 for silica is at 103.3 eV, the BE for SiO_2 associated with SiC has been reported[1] as 102.4 – 102.8 eV by several authors. The presence of an oxidized surface is consistent with Rahaman's[2] proposed model of SiC powder involving an outer layer of adventitous carbon in the form of hydrocarbons and an intermediate layer of SiO_2 that overlays bulk SiC. Assuming that the model applies to the SiC films in this study, the thickness x of the oxide layer can be estimated using the following relationship[3]:

$$\frac{SiC}{SiO_2} = \left[\frac{\rho_{Si,c}}{\rho_{Si,o}}\right]\left[\frac{\exp(-x/\lambda_c)}{1-\exp(-x/\lambda_o)}\right] \qquad \text{Eq. 4.1}$$

where SiC and SiO_2 are the areas of the Si 2p peaks Si_I and $Si_{II,}$ respectively, $\rho_{Si,c}$ and $\rho_{Si,o}$ are the atomic densities of Si in the silicon carbide and silicon oxide, and λ_c and λ_o are the escape depths of the photoelectrons perpendicular to the sample surface in the carbide and oxide. Using the molecular weight and density of 60 g/mol and 2.2 g/cm^3 for SiC, 40 g/mol and 3.2 g/cm^3 for amorphous SiO_2, $\rho_{(Si,c)}/\rho_{(Si,o)}$ = 2.18, and λ_o = 1.9 nm and λ_c = 1.6 nm (all values were taken from Ref. 7), the thickness of the air oxidized layer was estimated to be 0.72 ± 0.07 nm.

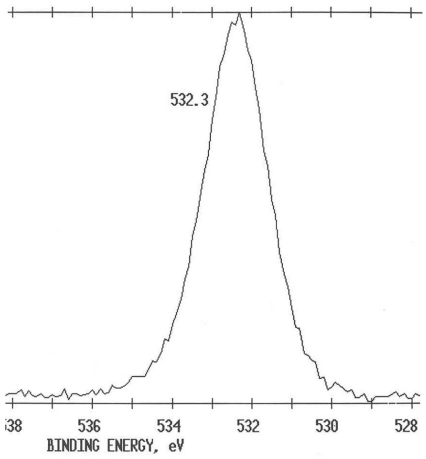

(a)

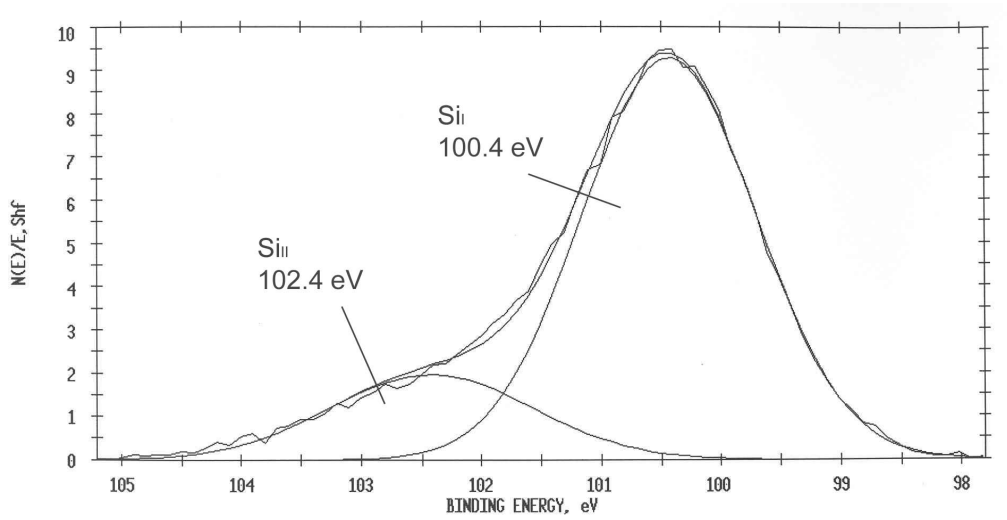

(b)

Figure 4.2 Photopeaks for as-received SiC/Si wafer: (a) O 1s and (b) Si 2p.

The Si to C atom ratio (Si_{SiC}/C_{SiC}) associated with SiC was calculated from the area ratio of the Si 2p peak I to the C 1s peak I divided by their respective sensitivity factors[4], 0.30 for C 1s and 0.34 for Si 2p. From three XPS runs, the resultant atom ratio Si_{SiC}/C_{SiC} was 1.1 ± 0.08 which is slightly higher than the theoretical Si_{SiC}/C_{SiC} value of 1.0. The experimental ratio indicates there is a slight excess of silicon atoms relative to carbon atoms on the surface. Deviation from the theoretical Si_{SiC}/C_{SiC} ratio of unity is dependent on the film deposition process and deposition parameters.[1]

Depth profiling using AES was carried out on acetone-cleaned SiC/Si samples. Figure 4.3 shows an AES depth profile for as-received SiC/Si (50 Å/min sputter rate). The plot shows that the composition was ~60% Si and ~40% C between the sputter depths of 100 Å and 1200 Å. This layer is the SiC layer. At 1300 Å, the Si content increased to almost 100% indicating that the SiC layer had been sputtered away revealing the Si substrate. Thus, the SiC is approximately 120 – 130 nm thick. A slower sputter rate of 2.5 Å/min was used to depth profile the oxide layer as shown in Figure 4.4. The thickness of the oxide layer was determined as the depth where the O line intersected the Si line in the % atomic vs. depth plot. The depth profile showed an oxide layer of approximately 0.8 nm, which is in agreement with the XPS approximation of 0.72 ± 0.07 nm from Eq. 4.1.

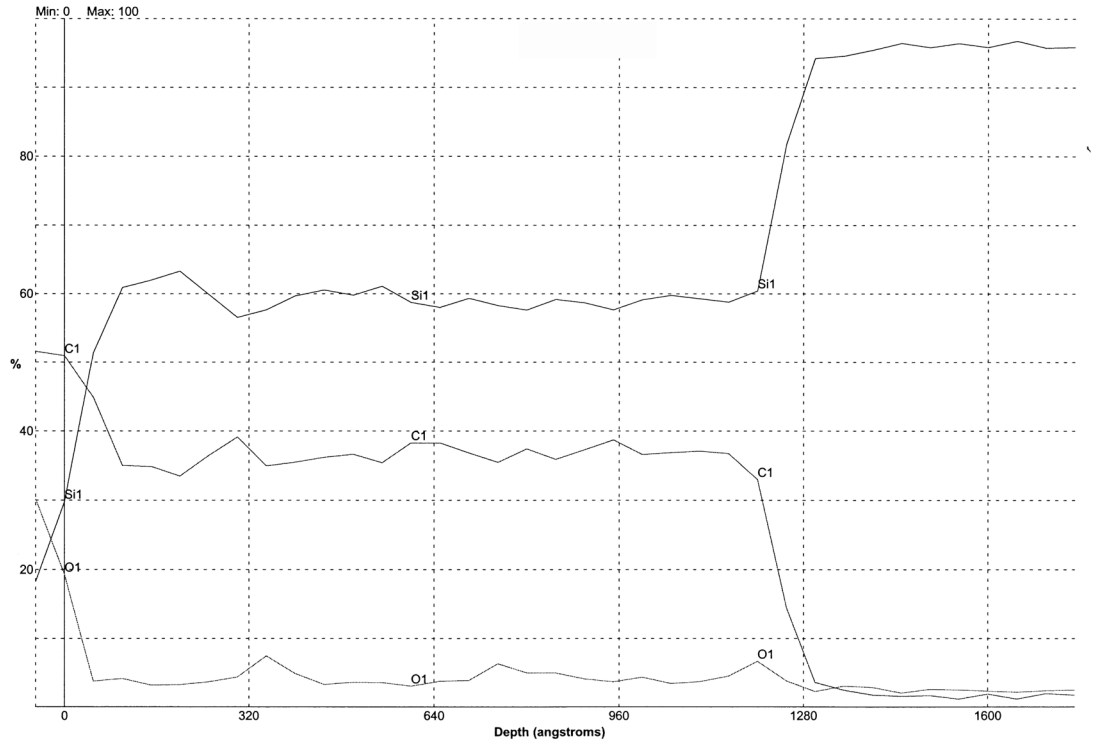

Figure 4.3 AES depth profile of SiC/Si wafer (50 Å/min).

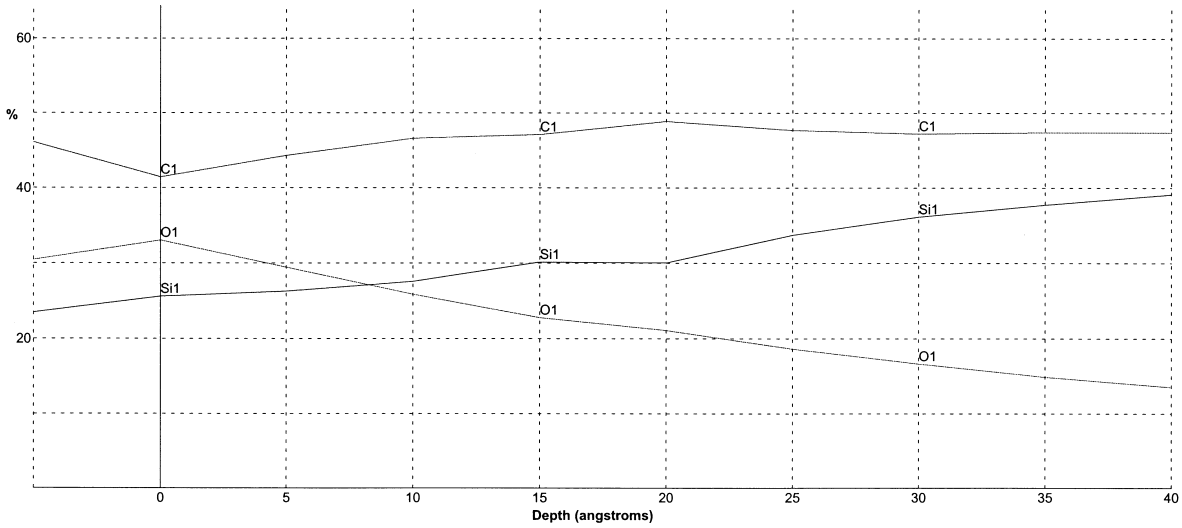

Figure 4.4 AES depth profile of the oxide (SiO_2) layer on a SiC/Si surface (2.5 Å/min).

4.2.2 EPOXY ADHESIVE

The model epoxy adhesive was deposited onto a SiC/Si wafer and cured as described in Section 3.5.1. The surface of the air side of the epoxy film was characterized via XPS. The XPS peak assignments and curve-fit for the C 1s photopeaks are shown in Table 4.4 and in Figure 4.5, respectively. The C 1s photopeak of the cured adhesive showed primarily two peaks: peak I at 285.0 eV due to C-H/C-C and peak II at 286.6 eV due to C-O. The second peak at 286.6 eV is characteristic of the epoxy groups in the resin, and thus is useful in determining failure modes. A single, fairly symmetrical photopeak at 533.1 eV shown in Figure 4.6 is attributed to the O component of C-O in the epoxy. The model epoxy surface is chemically composed of 81.5% C and 18.5% O (Table 4.5). Since no nitrogen was detected, it was assumed that the nitrogen incorporated from the imidazole curing agent exists in the bulk epoxy and not at the film surface.

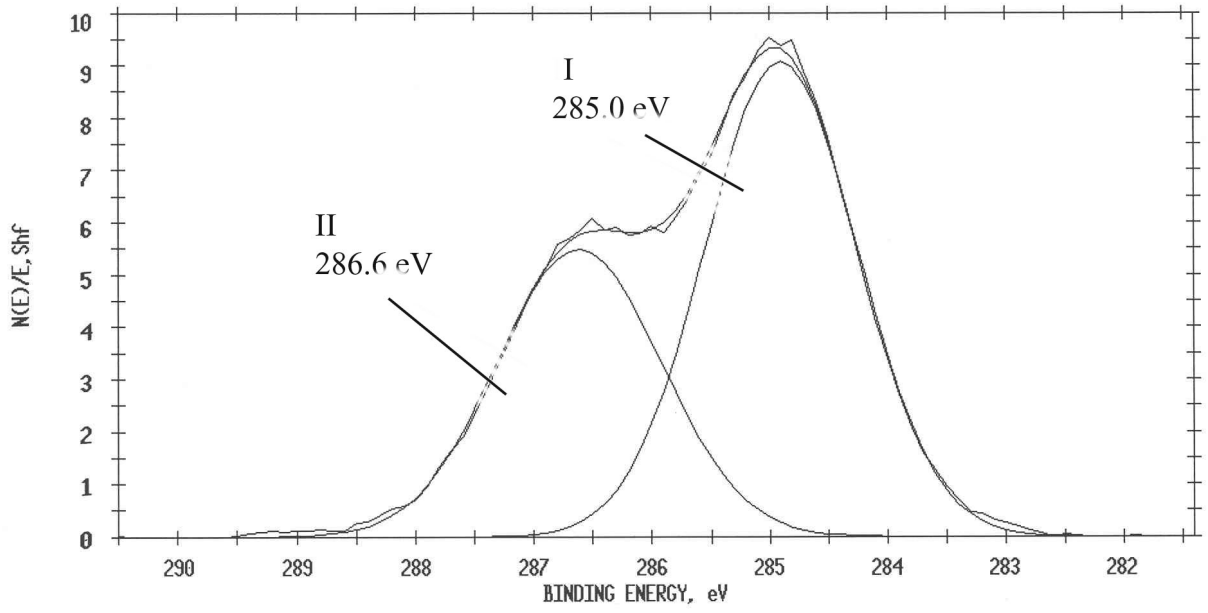

Figure 4.5 Curve-fit C 1s photopeaks for the model epoxy.

Table 4.4 Peak assignments for the curve-fit C 1s photopeak for the model epoxy.

Peak No.	Peak Position (eV)	% Area	Assignment
I	285.0	60.8	C-H/C-C
II	286.6	39.2	C-O

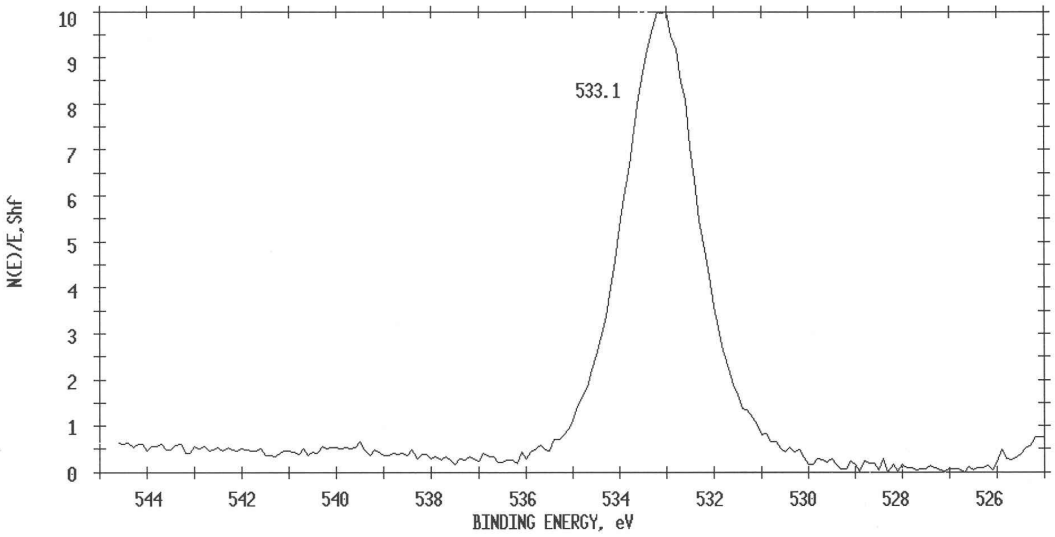

Figure 4.6 O 1s photopeak for the model epoxy.

Table 4.5 Elemental composition for the model epoxy (atomic %).

Sample	% C	% O	% N
epoxy	81.5	18.5	< 0.1

4.3 ADHESION DURABILITY FOR THE NON-SURFACE MODIFIED SYSTEMS

The performance of the model epoxy/SiC/Si bonded system was evaluated using the immersion test and probe test as described previously. In the immersion test, samples were immersed in four different aqueous solutions identified by their pH (pH 4.2, pH 6.7, pH 7.7, pH 8.2) and visually checked for debonding. For the probe test, samples were immersed in the pH 6.7 and pH 8.2 solutions, and in deionized water at pH 6.3 for comparison. In both tests, samples were tested in the solutions or in water at 60 °C.

Immersion test results showed that adhesion durability was quite poor in the epoxy/SiC/Si system (non-treated system) as shown in the adhesion durability data in Figure 4.7. The bar graph represents the time to debond; the number of days until failure was observed for the samples immersed in the different solutions at 60 °C. Time to initial debond is defined as the time of the first pronounced appearance of blister formation, ink leech-in, or film lifting from the surface, corners or edges; while time to complete debond, or complete failure, is defined as the time where 100% delamination of the adhesive film from the substrate had occurred. The adhesion performance of as-received samples treated with the edge protection (EP) treatment was compared with those without treatment. Samples without EP resulted in initial failure within 3-8 days, whereas initial failure occurred in up to 20 days for samples with the EP treatment. From immersion test observations, it was also noted that samples that were edge treated showed a longer time for complete failure than non-edge protected samples. Specimens without EP treatment resulted in complete debonding within 2-5 days of the observed initial debond. Edge protected samples did not reach complete failure until 12-15 days after the initial debond. Since all samples failed within 30 days, it is uncertain whether pH affects adhesion, especially since the solutions contain other components that may also influence debond behavior. Nevertheless, even with EP treatment, the adhesion durability of epoxy bonded to the non-surface treated SiC/Si substrate is poor.

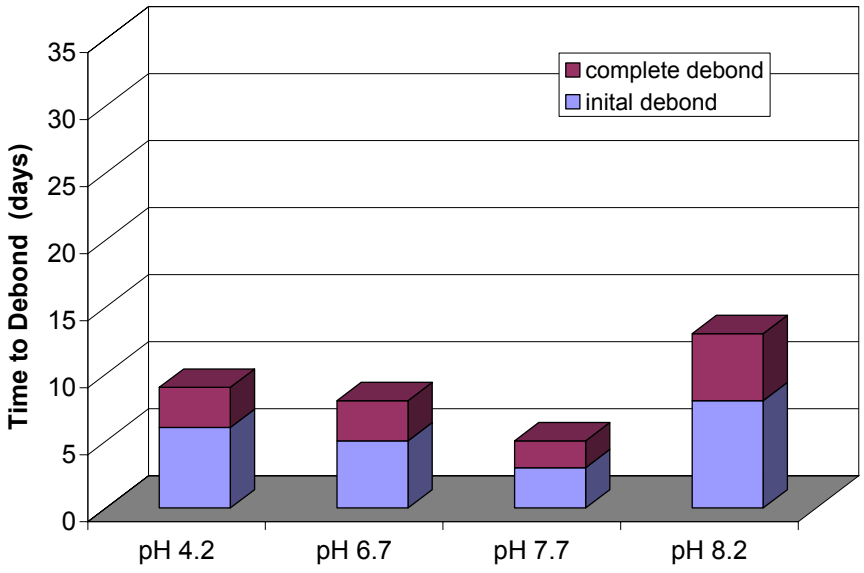

(a)

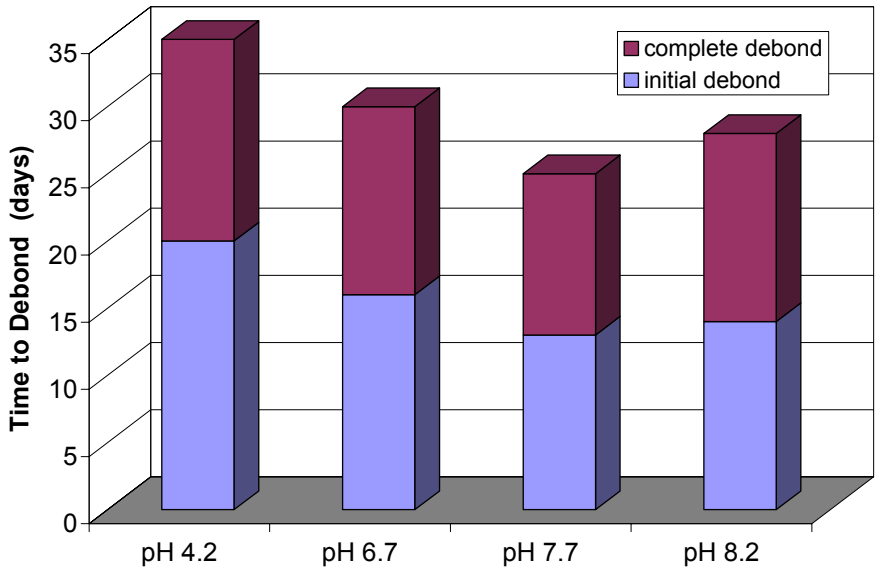

(b)

Figure 4.7 Adhesion durability data for epoxy/SiC/Si samples (no surface treatment) tested in various aqueous solutions at 60 °C: (a) no edge protection (EP) treatment, (b) edge protection treatment.

The poor adhesion performance is further supported by probe test results summarized in Table 4.6. The G_c for the bonded system measured on a dry specimen (no immersion) was ~141 J/m^2. After 24 hrs of immersion in the solutions, G_c dropped to 30-60 J/m^2, and decreased to 2-5 J/m^2 following 14 days of immersion. After 21 days of immersion, all samples failed either by debonding of the epoxy film at the sample edges (which prevented testing of the samples) or complete delamination.

Table 4.6 Critical strain energy release rate, G_c , as a function of time for specimens tested in pH 6.7 and pH 8.2 solutions, and deionized water (pH 6.3). Values are an average of 3 runs per sample.

Immersion Time (days)	pH 6.7 G_c (J/m^2)	pH 8.2 G_c (J/m^2)	H_2O (pH 6.3) G_c (J/m^2)
0 (dry)	141 ± 29		
1	58 ± 3	65 ± 8	34 ± 4
7	5 ± 3	10 ± 4	5 ± 1
14	2 ± 1	5 ± 1	3 ± 2
21	fail	fail	fail

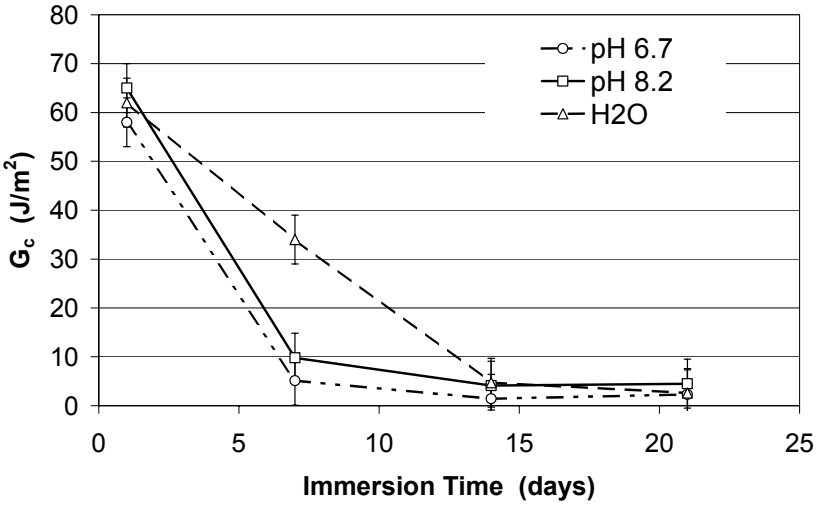

Figure 4.8 Critical strain energy release rate G_c as a function of time for epoxy/SiC/Si specimens tested in pH 6.7 and pH 8.2 solutions, and deionized water (pH 6.3).

4.4 DETERMINATION OF FAILURE MODE FOR NON-SURFACE MODIFIED SYSTEMS

XPS analysis of failed sample surfaces (epoxy film and SiC/Si substrate) was carried out to determine the failure mode. After complete failure of a sample, where 100% delamination occurred, the film and substrate were rinsed with deionized water, gently blotted with a Kim-wipe tissue to remove excess solution/water, and placed in a petri dish (failed side up) and air dried for at least 8 hours. Failed surfaces were then analyzed using XPS. All samples analyzed to determine failure mode were taken from the immersion test experiments.

Failure analysis was performed for samples immersed in aqueous solutions at pH 4.2, pH 6.7, pH 7.7 and pH 8.2. For the sample tested in the pH 6.7 solution, the C 1s spectrum (Figure 4.9a) of the failed substrate surface, compared to the as-received SiC/Si wafer (Figure 4.1), showed a decrease in atomic percent from 32.7% to 15.7% for the C-Si photopeak, an increase from 16.4% to 47.4% for C-H/C-C and an increase from 7.9% to 14.4% for C-O. The increase in C-H/C-C and C-O is indicative of epoxy on the failed substrate surface. The absolute concentrations of carbon and silicon species are listed in Table 4.7. In the Si 2p spectrum for the failed substrate shown in Figure 4.9b, the Si-C photopeak and the oxide photopeak are evident indicating that the oxide layer was still present. These results suggest that failure occurred within the oxide/epoxy interfacial region.

In the C 1s spectrum for the failed adhesive surface (Figure 4.10a), the photopeaks and atomic percentages for C-H/C-H and C-O (Table 4.7) were equivalent to the results for the as-prepared adhesive. Si 2p spectrum (Figure 4.10b) and elemental analysis showed 3.3% SiO_2 on the failed adhesive side, indicating that some of the oxide from the substrate was transferred onto the adhesive layer. These analyses indicate that failure occurred along the adhesive/oxide interface. An illustration of the proposed mode of failure is shown in Figure 4.11.

Adhesive/oxide failure in the interfacial domain was found for all samples tested regardless of the immersion solution pH. The data for samples tested in other pH solutions are listed in Tables 4.8 - 4.10. Failure in the interfacial region could be explained by the fact that a weak oxide layer is easily hydrolyzed by water. In addition, it is known that secondary bonds between the epoxy and siliceous substrates can be easily displaced by water molecules[5,6,7]; this displacement occurs even in absence of stress.[5] The very low G_c values (Figure 4.8) are

undoubtedly related to the ease with which secondary bonds between the epoxy and the substrate (SiO_2) can be broken.

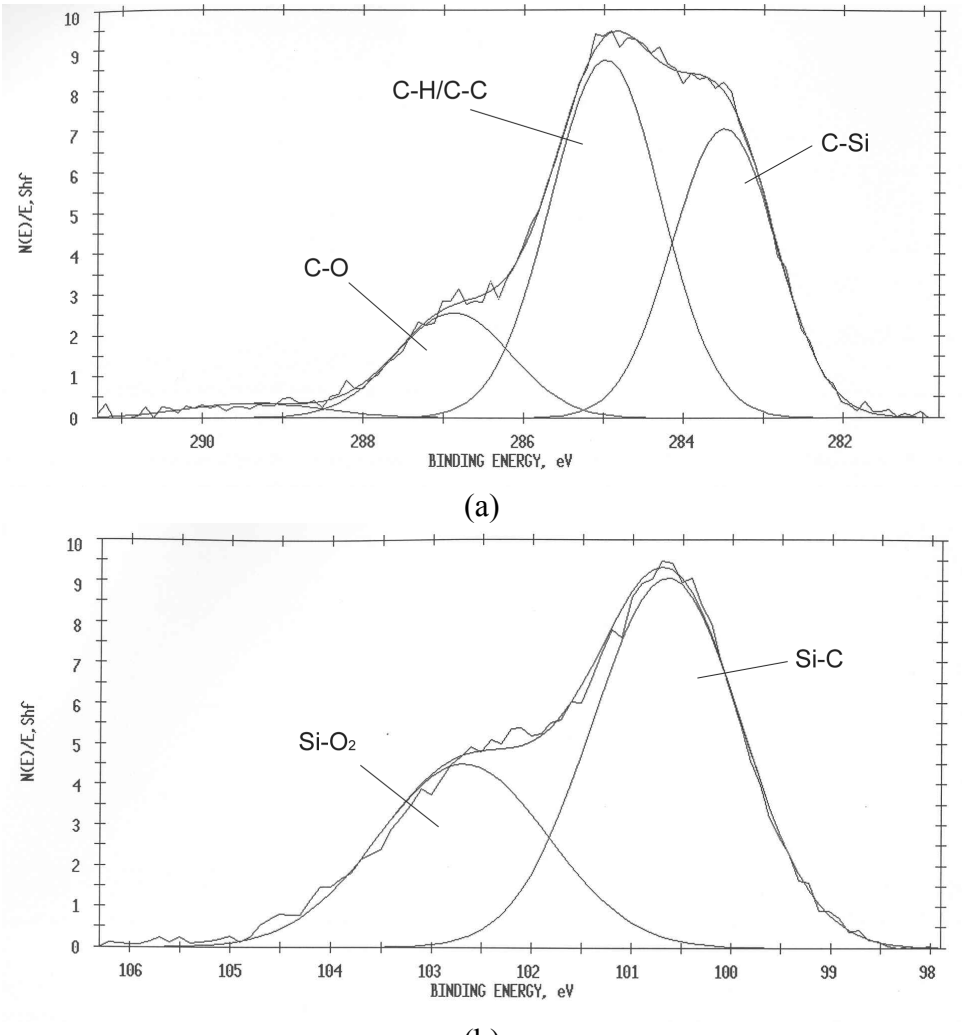

Figure 4.9 Curve-fit photopeaks for a failed substrate side (pH 6.7 solution): (a) C 1s and (b) Si 2p.

Table 4.7 Absolute percentages for C 1s and Si 2p curve-fit species for control and failed epoxy/SiC/Si (pH 6.7 solution).

Surface	% C-Si	% C-H/C-C	% C-O	% Si-C	% Si-O_2
substrate control	32.7	7.8	3.6	27.5	6.7
adhesive control	<0.1	49.5	31.9	<0.1	<0.1
substrate failed side	15.7	20.8	6.3	18.6	10.4
adhesive failed side	<0.1	46.5	27.3	<0.1	3.3

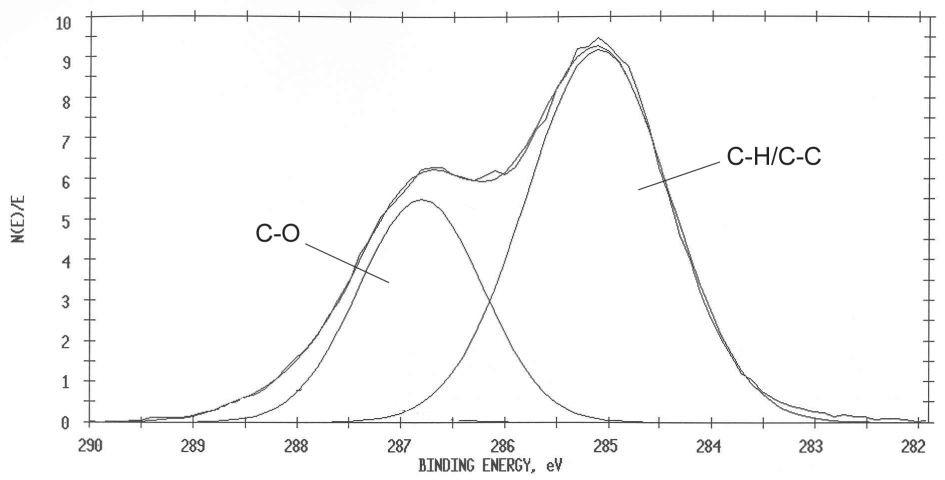

(a)

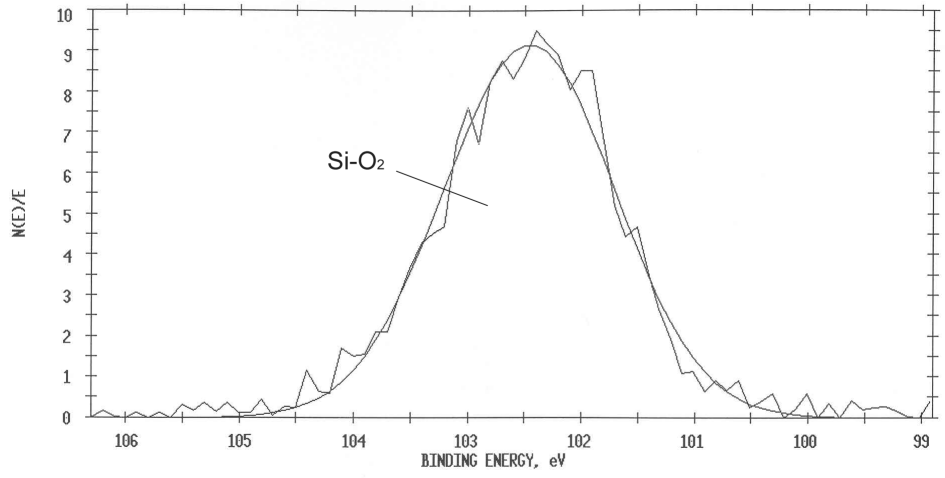

(b)

Figure 4.10 Curve-fit photopeaks for failed adhesive side (pH 6.7 solution): (a) C 1s, and (b) Si 2p.

Table 4.8 Absolute percentages for C 1s and Si 2p curve-fit species for control and failed epoxy/SiC/Si (pH 4.2 solution).

Surface	% C-Si	% C-H/C-C	% C-O	% Si-C	% Si-O_2
substrate control	32.7	7.8	3.6	27.5	6.7
adhesive control	<0.1	49.5	31.9	<0.1	<0.1
substrate failed side	25.7	14.2	4.9	26.2	7.2
adhesive failed side	<0.1	48.2	29.9	<0.1	1.8

Table 4.9 Absolute percentages for C 1s and Si 2p curve-fit species for control and failed epoxy/SiC/Si (pH 7.7 solution).

Surface	% C-Si	% C-H/C-C	% C-O	% Si-C	% Si-O_2
substrate control	32.7	7.8	3.6	27.5	6.7
adhesive control	<0.1	49.5	31.9	<0.1	<0.1
substrate failed side	14.2	22.2	6.9	17.2	9.6
adhesive failed side	<0.1	53.3	31.2	<0.1	5.2

Table 4.10 Absolute percentages for C 1s and Si 2p curve-fit species for control and failed epoxy/SiC/Si (pH 8.2 solution).

Surface	% C-Si	% C-H/C-C	% C-O	% Si-C	% Si-O_2
substrate control	32.7	7.8	3.6	27.5	6.7
adhesive control	<0.1	49.5	31.9	<0.1	<0.1
substrate failed side	28.5	10.9	4.0	29.6	4.4
adhesive failed side	<0.1	46.5	27.3	<0.1	0.8

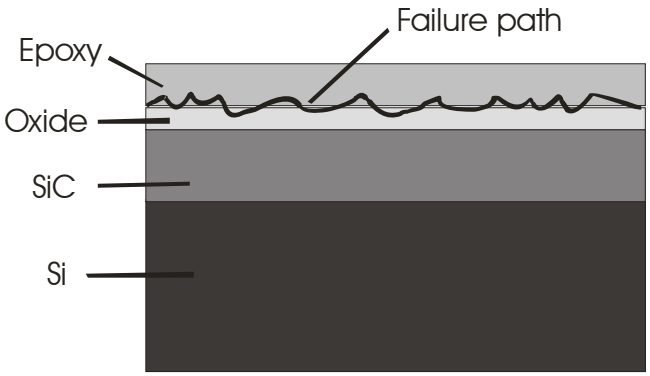

Figure 4.11 Proposed failure mode for non-surface modified epoxy/SiC/Si bonded system. (not drawn to scale)

4.5 XPS ANALYSIS OF TREATED SURFACES

4.5.1 SILANE TREATMENT

The properties of silane coupling agents are highly dependent on the application parameters, the organofunctional silane and the substrate surface. XPS analysis of an APS derivatized substrate (denoted as as-received/APS) showed 49.3% C, 22.5% O, 25.9% Si, 1.3% N and 1.0% F, see Table 4.11. Although only 1.3% nitrogen was detected, the presence of nitrogen is an indication that APS was adsorbed onto the surface. The C 1s spectrum also indicated the presence of APS. Compared to the as-received substrate, the curve-fit C 1s spectrum for as-received/APS in Figure 4.12 shows a large increase in the C-H/C-C peak intensity as represented by its C-H/C-C to C-Si peak area ratio of 1.5:1.0. The corresponding C-H/C-C to C-Si ratio for the as-received surface was 0.2. The absolute concentrations (C percentage multiplied by percent area, 49.3% x 0.48 = 23.7%) of C-H/C-C for as-received/APS and as-received surfaces were 23.7% and 7.8%, respectively. These data provided further evidence of silane adsorption

since the increase in C-H/C-C is due to presence of the alkyl chains of the silane. The N to CH/CC ratio was 1:12, which is not in agreement with the theoretical ratio of 1:3. Although the number of CH/CC is four times the theoretical number, the ratio of N to Si-O-Si is in agreement (within 10%) to the theoretical ratio of 1:1. It is uncertain why the N to CH/CC ratio is so high, it is reasonable that the excess C-H/C-C may be due to ubiquituous hydrocarbon contamination from the atmosphere.

In the curve-fit Si 2p spectrum (Figure 4.13a, Table 4.13), two primary peaks were detected. The photopeaks at 100.0 eV and 102.1 eV were assigned as Si-C and Si-O_x, respectively. A slight increase in peak intensity for the 102.1 eV photopeak was observed compared to the respective as-received peak (Figure 4.13b). The absolute concentration for this peak increased from 6.7% to 9.5%. The FWHM (full width at half maximum) was 12.5% greater than the FWHM for the as-received peak. This indicates that one or more other species are likely present within the photopeak. Since it is widely accepted that SCAs form Si-O-Si linkages with siliceous oxides[8,9], the increase in peak intensity and broadening of the peak are attributed to Si-O-Si bonding species, which have been reported[10] in the binding energy range 102.3 eV – 102.7 eV. The peak at 102.1 eV is therefore assigned as a SiO_x composite peak composed of SiO_2 and Si-O-Si components. Recall that the BE (binding energy) for SiO_2 on SiC is 102.4 eV. All of the XPS data support the adsorption of APS on the SiC/Si surface.

Table 4.11 XPS elemental composition (atomic %) for as-received/APS treated SiC/Si. Fluorine likely originated from the supplier's cleaning process.

Sample	% C	% O	% Si	%N	% F
as-received/APS	49.3	22.5	25.9	1.3	1.0

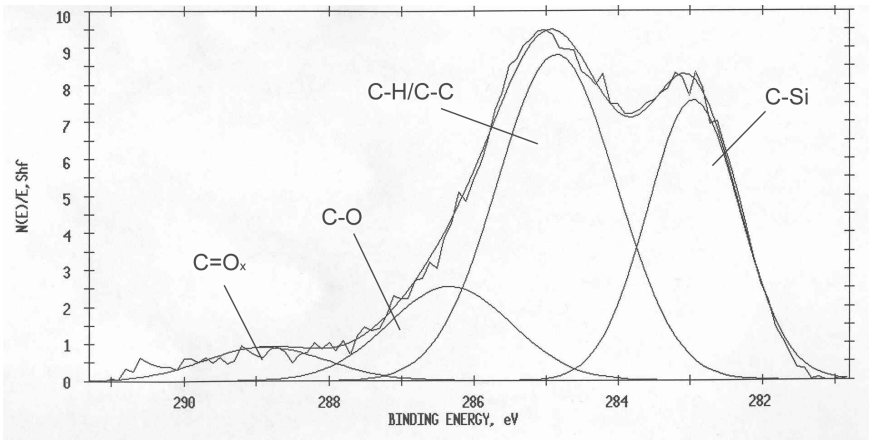

(a)

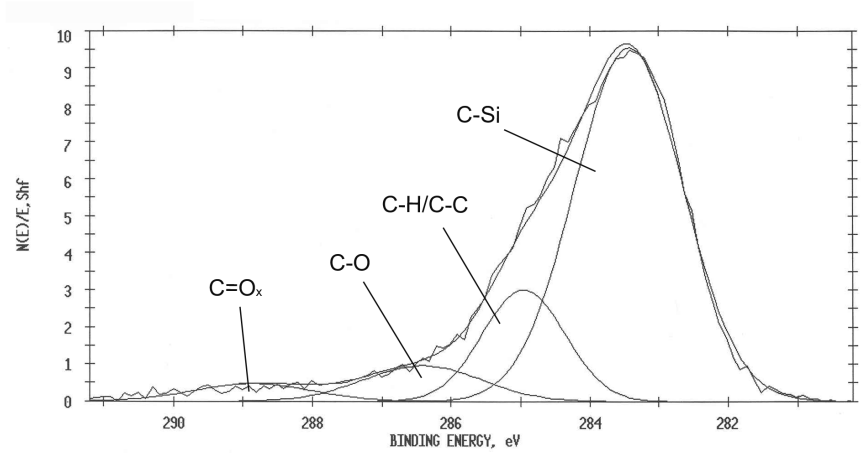

(b)

Figure 4.12 Curve-fit C 1s photopeaks for: (a) as-received/APS treated SiC/Si, and (b) as-received SiC/Si.

Table 4.12 Peak assignments for the curve-fit C 1s photopeak for as-received/APS treated SiC/Si.

Peak Position (eV)	% Area	Assignment
282.9	32.7	C-Si
285.0	48.0	C-H/C-C
286.3	14.3	C-O
288.8	5.0	$C=O_x$

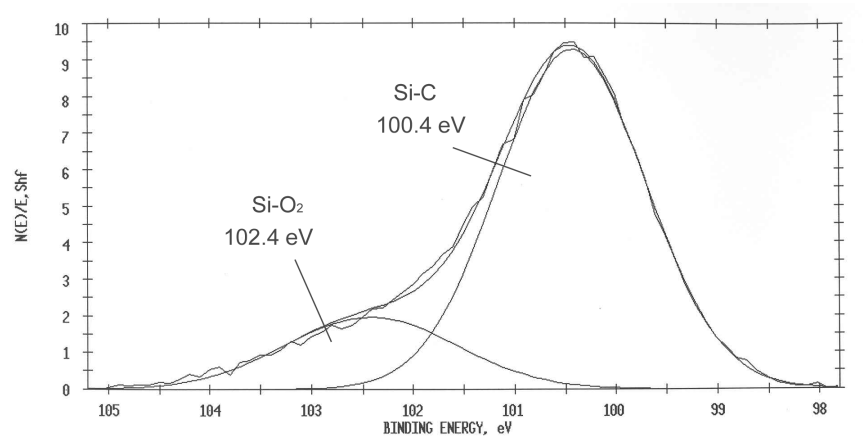

(a)

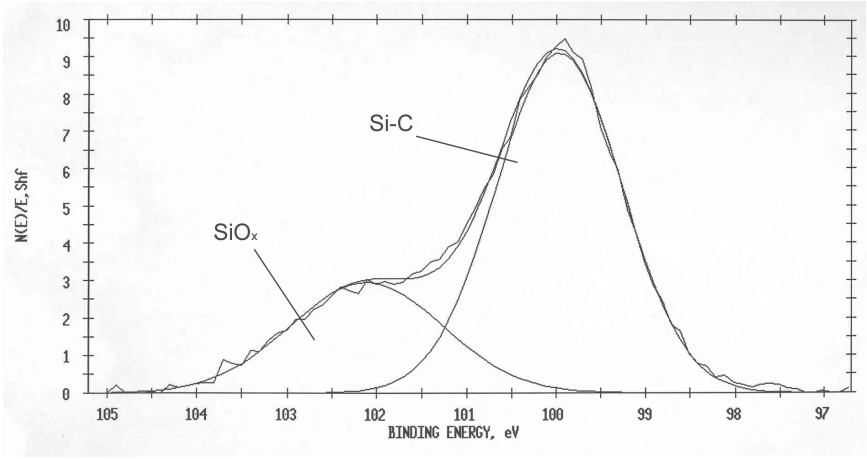

(b)

Figure 4.13 Curve-fit Si 2p photopeaks for: (a) as-received SiC/Si, (b) as-received/APS treated SiC/Si.

Table 4.13 Peak assignments for the curve-fit Si 2p photopeak for as-received/APS treated SiC/Si.

Peak Position (eV)	% Area	Assignment
100.0	71.9	Si-C
102.1	28.1	Si-O_x (Si-O-Si, Si-O_2)

The orientation of the APS on the surface is extremely important for the effectiveness of the silane as a coupling agent. APS exists in several different conformations depending on the deposition conditions and chemical nature of the substrate surface. Vandenber *et al.*[10] deposited APS onto gold, which has no oxide, and found that the amines quickly reacted with the atmosphere to form a bicarbonate salt, which was converted to an imine after heating. On aluminum oxide and silicon oxide, the amines: 1. hydrogen-bonded to the metal surface, or 2. abstracted protons from the metal surface to form protonated amines or 3. existed as neutral amines. Both IR and XPS showed a mixture of protonated and neutral amine groups when APS was deposited on aluminum or silicon. According to the literature[10,11], protonated and hydrogen bonded APS amines are oriented close to the silicon surface where they are believed to participate in electrostatic and hydrogen bonding with silicon oxide, while APS molecules with neutral amine groups are oriented away from the surface allowing the free amine to react with the intended polymer resin. A simple schematic of the possible conformations of APS is shown in Figure 4.14.

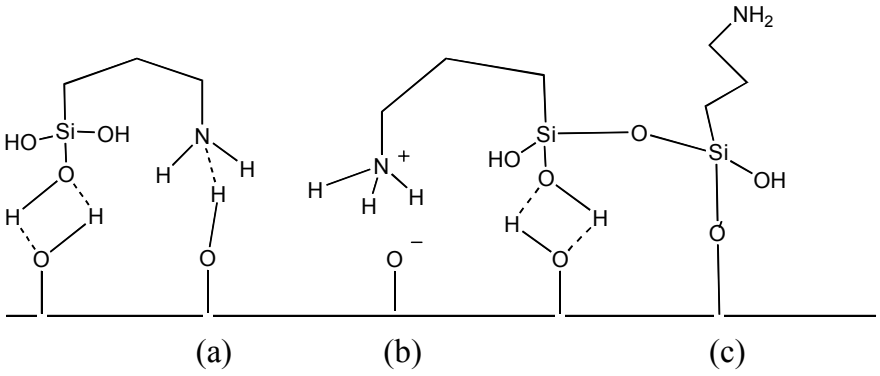

Figure 4.14 Schematic representation of possible APS structural conformations: (a) amine hydrogen-bonded, (b) amine protonated and (c) free amine.[10]

In this study, the deposition of APS resulted in two resolvable N 1s photopeaks as shown in the curve-fit spectrum in Figure 4.15. The lower energy nitrogen peak at 399.8 eV is attributed to the free amine and the higher energy peak at 401.7 eV is due to the protonated amine.[12,13] In Table 4.14, the peak assignments and the relative peak area percentages are listed. According to the curve-fit results, approximately 70 % of the nitrogen was neutral amine. The presence of the free amine APS functionality is highly desired due to its availability to react and 'couple' with the polymer adhesive.

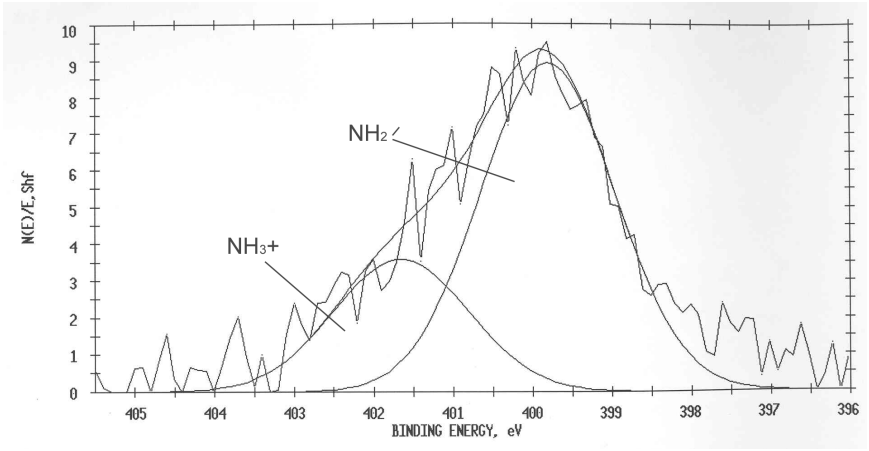

Figure 4.15 Curve-fit N 1s photopeaks for as-received/APS treated SiC/Si.

Table 4.14 Peak assignments for the curve-fit N 1s photopeak for as-received/APS treated SiC/Si.

Peak Position (eV)	% Area	Assignment
399.8	71.3	$N\text{-}H_2$
401.7	28.7	$N\text{-}H_3^+$

For the GPS surface-modified substrate (denoted as as-received/GPS), the results in Table 4.15 show that the atomic percentages of elements on a GPS treated surface were essentially equivalent (within 2%) to the composition for the as-received surface. With the exception of the C 1s photopeaks, the spectra for all the elements were essentially equivalent to those for the as-received substrate. In Figure 4.16, the C 1s spectrum of a GPS derivatized surface is compared to the spectrum for an as-received surface. To measure GPS adsorption, the C-H/C-C photopeak, characteristic of the alkyl chains, and C-O photopeaks, characteristic of the epoxy groups, were used as a measure of GPS adsorption. For the C-H/C-C and C-O photopeaks, a more intense C-H/C-C peak intensity and slight increase in C-O intensity relative to the respective as-received photopeaks were observed. The C-H/C-C and C-O absolute concentrations increased from 7.8% to 13.4% and 3.6% to 5.0%, respectively. Although the ratio of C-O to CH/CC, 1:3, disagreed with the theoretical ratio of 2:1, the increase in concentration of both species suggests that a small amount of GPS was adsorbed on the substrate surface. It is unknown why the experimental ratio does not agree with the theoretical ratio.

Table 4.15 Elemental composition (atomic %) for as-received/GPS treated SiC/Si. Fluorine originated from supplier's cleaning process.

Sample	% C	% O	% Si	% F
as-received/GPS	47.1	15.5	35.6	1.8

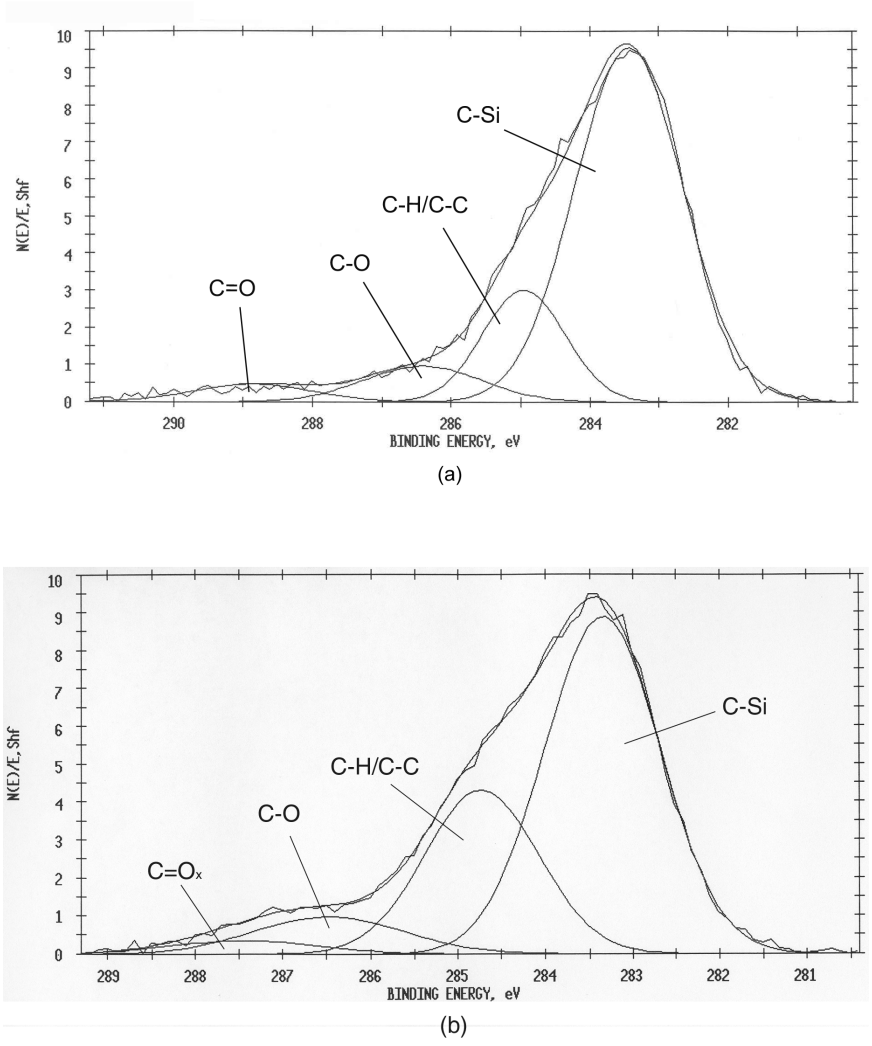

Figure 4.16 C1s spectra for: (a) as-received SiC/Si and (b) as-received/GPS treated SiC/Si.

4.5.2 OXYGEN PLASMA ACTIVATION AND SILANE TREATMENT

4.5.2.1 OXYGEN PLASMA PRETREATMENT

Substrates were pretreated in an O_2 plasma for 2, 5, 15 and 30 minutes. XPS elemental analysis (Table 4.16) shows that the C content decreased from ~ 46% to ~19%, O increased from ~18% to ~50%, Si % was relatively unchanged and F decreased to <0.1%. The increase in oxygen content suggests the formation of a thicker oxide layer attributed to SiO_2 formation on the silicon carbide surface. The increase in treatment time resulted in an increase in the Si-O_2 to Si-C (SiO_2/SiC) peak area ratio, indicating that the increase in oxide thickness is a function of treatment time. The oxide thicknesses of the pretreated samples were determined using Equation 4.1 from Section 4.2.1. Equation 4.1 was applied to obtain a graph of oxide thickness (x) versus SiO_2/SiC as shown in Figure 4.17. The graph shows that with a 2-minute plasma pretreatment, the oxide layer grew from 0.7 nm to 2.2 nm. With a 30 minute pretreatment, the oxide layer increased to 2.7 nm.

In Figure 4.18, the Si 2p and O 1s spectra for plasma treated SiC/Si are compared to the as-received spectra. Due to the oxidation of the SiC surface, an increase in BE for Si-O_2 from 102.4 eV to 103.3 – 103.7 eV, a decrease in BE for Si-C from 100.4 eV to 99.7 eV – 100.0 eV and an increase in oxygen BE from 532.3 eV to 533.0 eV were observed. The BE for the plasma-formed SiO_2 is consistent with literature values[14] for Si-O_2 on silica and Si-O_2 on silicon. The shifts in binding energies for oxygen, silicon dioxide and silicon species have also been observed in the O_2 plasma treatment of silicon substrates.[15] In all plasma treated cases, the Si to C ratio (Si/C) was in agreement (within 10%) with the ratio value of 1.1 for as-received SiC (see Section 4.2.1).

Table 4.16 Elemental analysis (atomic %) for O_2 plasma treated SiC/Si at various treatment times.

Sample	C%	O%	Si%	F%	SiO_2/SiC
As-received	45.8	17.8	34.2	3.2	0.23
2 min O_2 plasma	20.8	49.6	29.7	<0.1	1.2
5 min O_2 plasma	19.2	50.6	30.2	<0.1	1.4
15 min O_2 plasma	18.6	51.4	30.1	<0.1	1.6
30 min O_2 plasma	16.5	53.6	29.9	<0.1	1.9

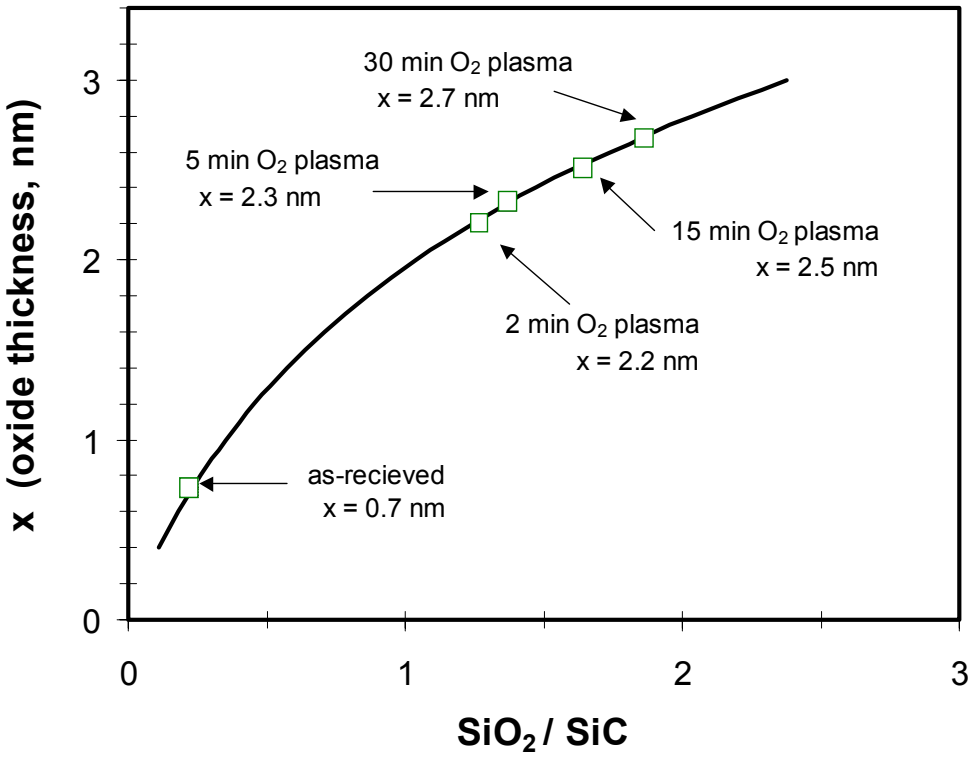

Figure 4.17 Oxide thickness as a function of SiO_2/SiC relative peak intensities.

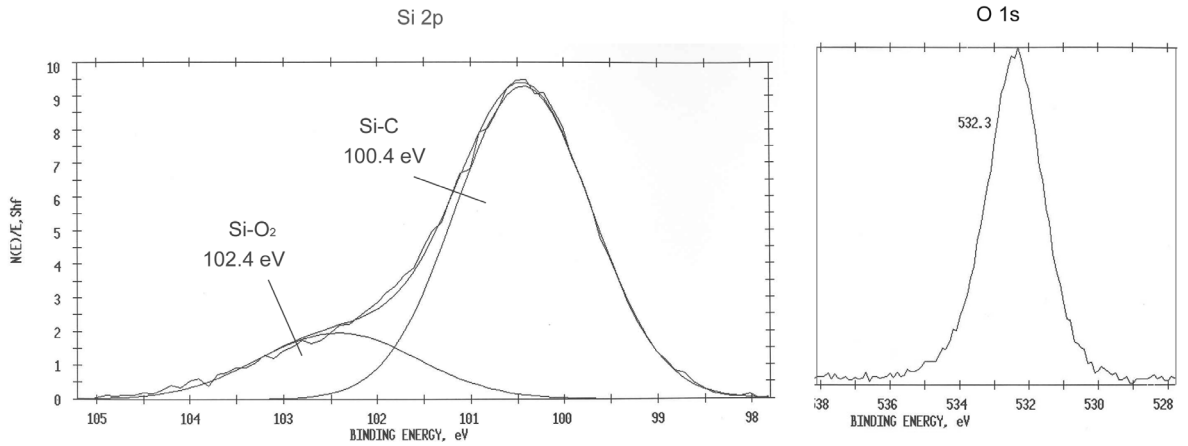

(a)

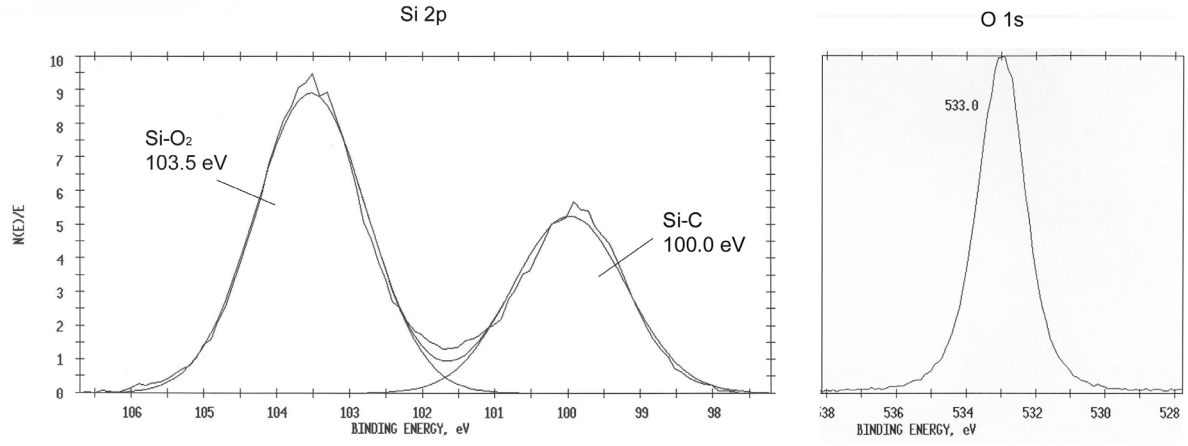

(b)

Figure 4.18 Si 2p and O 1s spectra for: (a) as-received SiC/Si and (b) a typical O_2 plasma-treated surface (15-minute oxygen plasma).

Analysis of the C 1s spectrum for a typical O_2 plasma-treated SiC/Si substrate (Figure 4.19) showed that the absolute percentage of C-H/C-C (~8%) was approximately equivalent to that for the as-received surface. Since it is well known that oxygen plasmas are routinely used to remove carbon-containing contaminants from surfaces, the amount of C-H/C-C detected on the plasma-modified surfaces did not reflect this cleaning process since one would expect a decrease in C-H/C-C content. However, the decrease in fluorine content to <0.1% and the increase in SiO_2 suggest that a cleaning effect and oxidation took place. Thus, it is believed that etching, removal of contaminants and oxidation occurred. The presence of C-H/C-C components may have been due to a re-adsorption of adventitous carbon from the atmosphere and/or from the plasma-induced conversion of carbon from SiC to hydrocarbon. The overall decrease in carbon percentage from ~46 % to ~19 % may be explained by the presence of the thicker plasma-formed oxide layer in addition to the removal of hydrocarbons by the O_2 plasma. In the as-received C 1s spectrum, the majority (72%) of the carbon content was attributed to C-Si. In the plasma-modified specimens, the dominant carbon species were both C-Si (42%) and C-H/C-C (42%). Since the XPS sampling depth is approximately 50 Å, a thicker oxide layer lying on top of the SiC surface would reduce the quantity of SiC detected, resulting in a decreased percentage of C-Si species and an overall decreased carbon content. A proposed simplified schematic representation of the sampling depths for as-received and plasma-modified surfaces is shown in Figure 4.20.

One concern regarding the pretreatment was the etching/oxidation effect of the O_2 plasma that may ablate/oxidize SiC to compromise the overall electronic performance. An AES depth profile was carried out to determine the SiC thickness after plasma treatment. The thickness of the SiC layer for the as-received SiC/Si wafer was approximately 120–130 nm. The SiC coating thicknesses after 10-, 20- and 30-minute O_2 plasma treatments were approximately 110, 100 and 90 nm, respectively, thus giving rise to an etching rate of approximately 10 nm per minute.

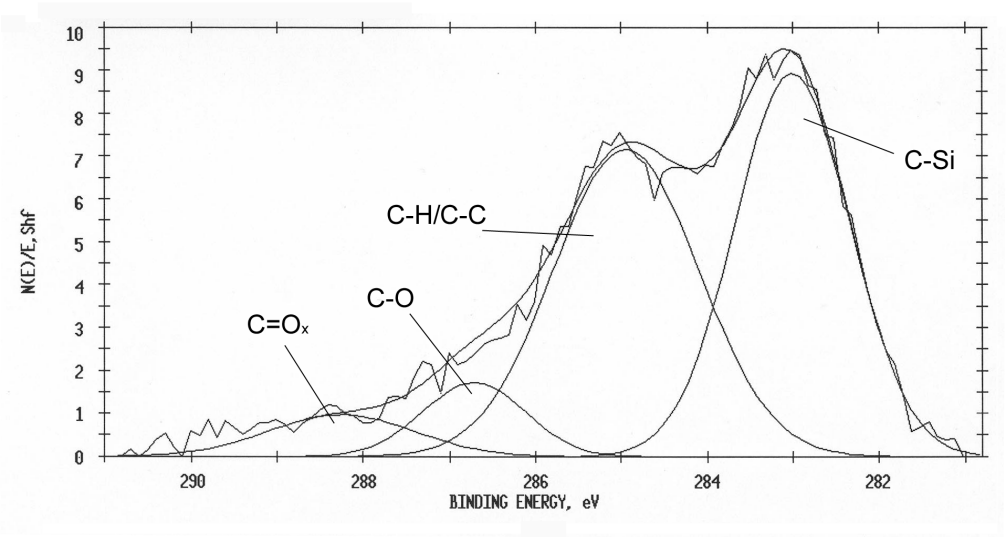

Figure 4.19 Curve-fit C 1s spectrum for a typical plasma pretreated SiC/Si surface (15-minute plasma treatment).

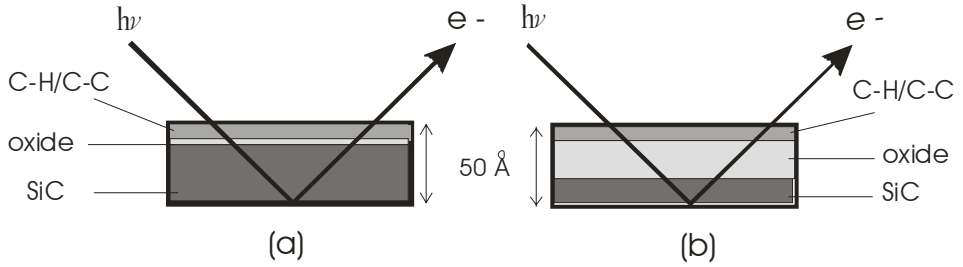

Figure 4.20 A proposed schematic representation of the XPS sampling depth for: (a) as-received surface, and (b) plasma-modified surface.

4.5.2.2 SILANE TREATMENT

After samples were pretreated with the O_2 plasma, they were further treated with either APS or GPS. In Figure 4.21, the curve-fit C 1s spectra for a typical O_2- plasma modified surface (as-prepared) and for a typical O_2-plasma/APS surface are compared. A large increase in the C-H/C-C photopeak relative to the C-Si peak was observed for the plasma/APS sample compared to the as-prepared sample. The C-H/C-C to C-Si ratios for the as- prepared and the O_2- plasma/APS were 0.9 and 4.2, respectively. The absolute concentration of C-C/C-H increased from 8.4% (as-prepared) to 24.8% (plasma/APS). These results indicate that APS was successfully deposited on the plasma-modified surface. In comparison with the silane treated samples without plasma pretreatment (as-received/silane), plasma/silane treated samples yielded a 2-3 fold increase in silane adsorption. The increase in APS adsorption is indicated also by the increase in atomic percentage of nitrogen, from 1.3% for the non-plasma/APS sample to 3-4% for plasma/APS sample (Table 4.17). For the plasma/APS specimens, the N:CH ratio was 1:4 which is close to the theoretical ratio of 1:3 for APS.

For plasma/GPS samples, the presence of GPS was evident as indicated by the relative intensities of the C-H/C-C and C-O photopeaks. A comparison of typical C 1s spectra for a plasma-modified surface and a plasma/GPS surface are shown in Figure 4.22. Using the C-H/C-C and C-O photopeaks as a measure of GPS adsorption, the plasma/GPS spectra from the various plasma pretreatment times showed an absolute increase in C-H/C-C from ~8% to ~15%, and an increase in C-O from ~1% to 4-5%. XPS data indicate that the amount of silane adsorption for the plasma modified samples may be greater than for the non-plasma/GPS samples by up to a factor of 2-3, as suggested by the absolute concentration of C-O attributed to GPS, 1.4% and ~3-4% for non-plasma/GPS and plasma/GPS, respectively. The C-O to C-C ratio (1:3) was not in agreement with the theoretical ratio for GPS (2:1). The disagreement in ratios cannot be accounted for.

The different plasma pretreatment times did not affect silane adsorption behavior. As listed in Table 4.17, the surface composition of the samples with varying pretreatment times was fairly consistent. For APS, the free amine to protonated amine ratios were also consistent at a value of 2.5, which is equivalent to the value for non-plasma/silane samples. The agreement in amine ratio suggests that the plasma treatment time did not affect the structural conformation of APS.

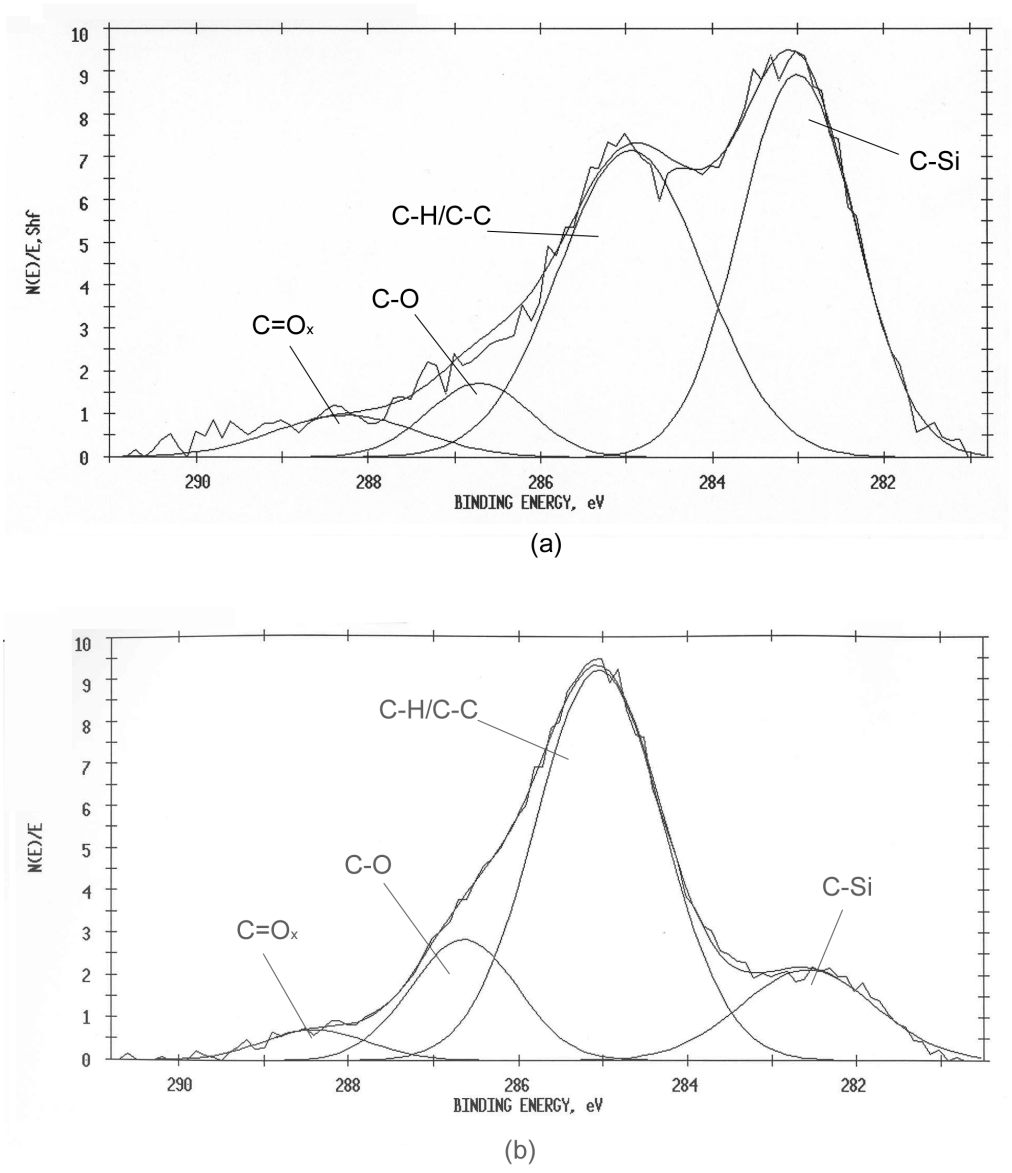

Figure 4.21 Curve-fit C 1s spectra for: (a) 15-minute O_2 plasma treated SiC/Si, and (b) 15-minute O_2 plasma/APS treated SiC/Si.

Table 4.17 XPS elemental analysis (atomic %) for SiC/Si substrates etched with O_2 plasma at various etch times and subsequently silane treated with GPS or APS.

Sample	C%	O%	Si%	N%
2 min O_2 plasma/ APS	36.7	38.0	21.7	3.6
5 min O_2 plasma/ APS	35.7	39.2	21.3	3.7
15 min O_2 plasma/ APS	38.1	38.1	20.5	3.4
30 min O_2 plasma/ APS	34.9	39.6	22.0	3.5
2 min O_2 plasma/ GPS	29.2	43.8	27.1	<0.1
5 min O_2 plasma/ GPS	28.7	44.8	26.5	<0.1
15 min O_2 plasma/ GPS	30.2	43.8	26.0	<0.1
30 min O_2 plasma/ GPS	26.1	47.2	26.7	<0.1

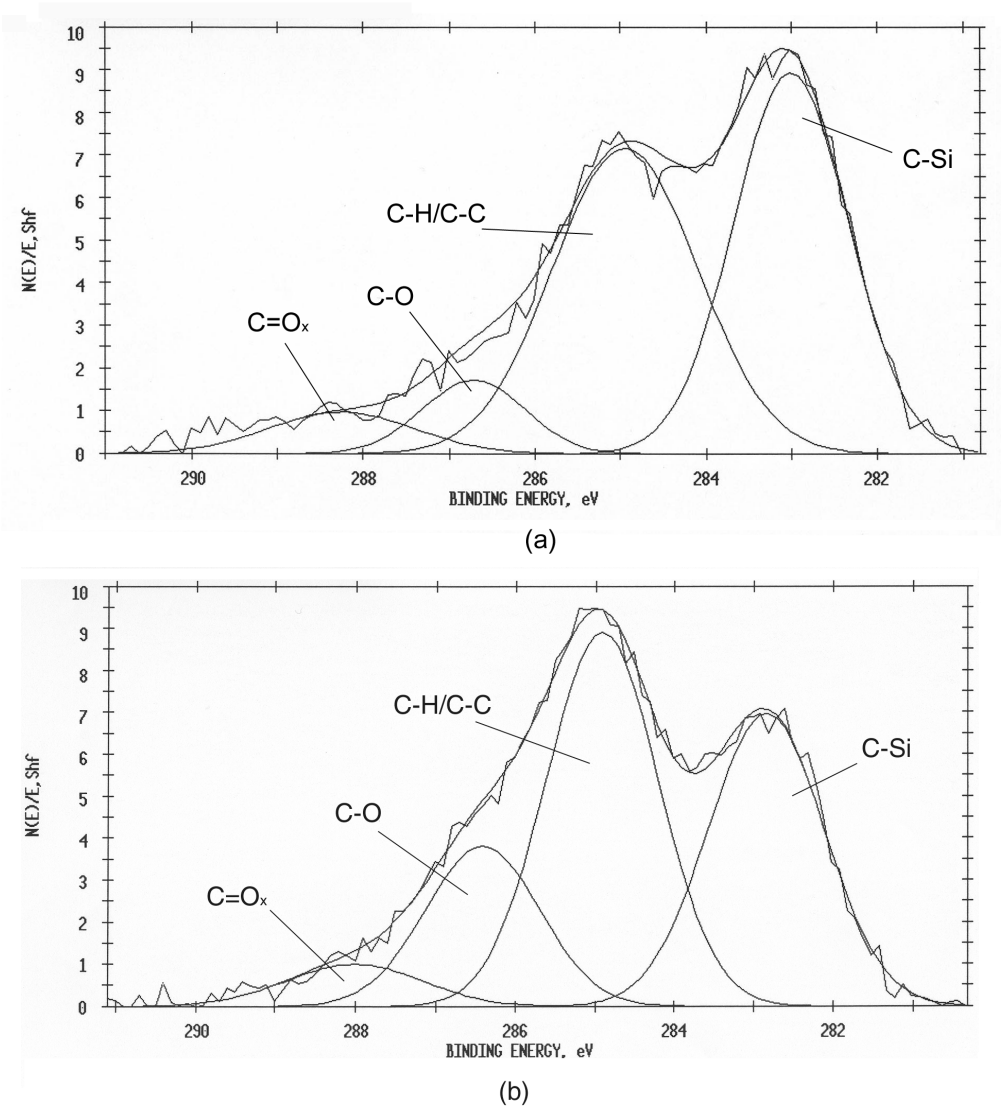

Figure 4.22 C 1s spectra for: (a) 15-minute O_2 plasma treated SiC/Si, and (b) 15-minute O_2 plasma/GPS treated SiC/Si.

4.5.3 WATER / OXYGEN PLASMA ACTIVATION AND SILANE TREATMENT

A water/oxygen plasma (H_2O/O_2) was utilized in an attempt to incorporate hydroxyl groups on the surface of the substrate. A 10-minute O_2 plasma treatment was first carried out on the SiC/Si wafers to remove carbonaceous contamination, and was subsequently followed by the H_2O/O_2 plasma treatment. The H_2O/O_2 plasma-modified specimens were then treated with either APS or GPS.

The XPS spectra of H_2O/O_2 plasma treated substrates showed essentially equivalent surface chemistry as surfaces treated in an O_2 plasma (Figure 4.23 and Table 4.18). XPS data for samples after treatment with silane also showed that approximately the same amount of silane was present on the H_2O/O_2- and O_2- plasma treated substrates. The H_2O/O_2 plasma treatment time was increased from 10 minutes to 20 minutes; however, the surface chemistry remained the same. Although the C-H/C-C photopeak in the C1s spectrum for the 20-minute H_2O/O_2 plasma surface appears less intense than the respective peak for the 10-minute H_2O/O_2 plasma, the resultant absolute percentages for the two peaks showed that they were in fact equivalent (6.5% and 6.7%, respectively). In short, the H_2O/O_2 plasma pretreatment did not seem to affect the surface chemistry or silane adsorption compared to the O_2 plasma pretreatment.

Table 4.18 XPS surface composition of SiC/Si substrates pretreated with H_2O/O_2 plasma or O_2 plasma, and subsequently treated with GPS and APS silane coupling agents

Sample	% C	% O	% Si	%N
10 min O_2 plasma	17.5	52.3	30.2	<0.1
10 min H_2O plasma	18.3	52.3	29.4	<0.1
20 min H_2O plasma	16.3	53.2	30.5	<0.1
10 min O_2 plasma / GPS	25.3	46.8	27.9	<0.1
10 min H_2O plasma /GPS	21.1	50.2	28.7	<0.1
20 min H_2O plasma /GPS	24.3	48.2	27.5	<0.1
10 min O_2 plasma / APS	31.5	40.8	25.6	2.1
10 min H_2O plasma / APS	34.3	38.3	24.7	2.7
20 min H_2O plasma / APS	36.9	37.0	23.5	2.6

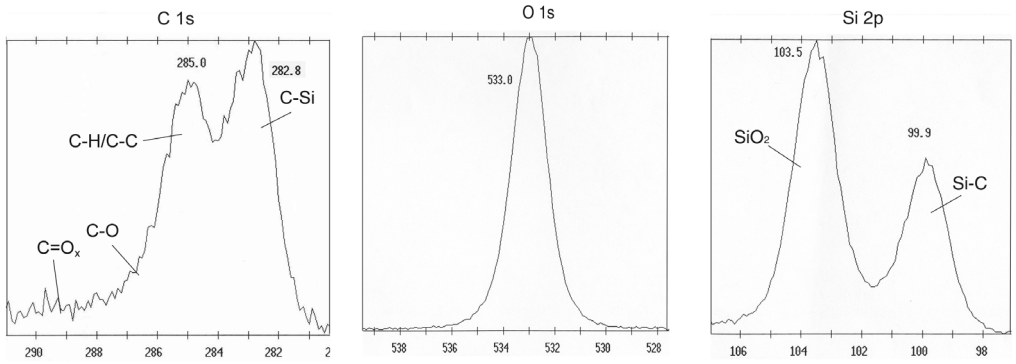

(a) 10 O_2 plasma

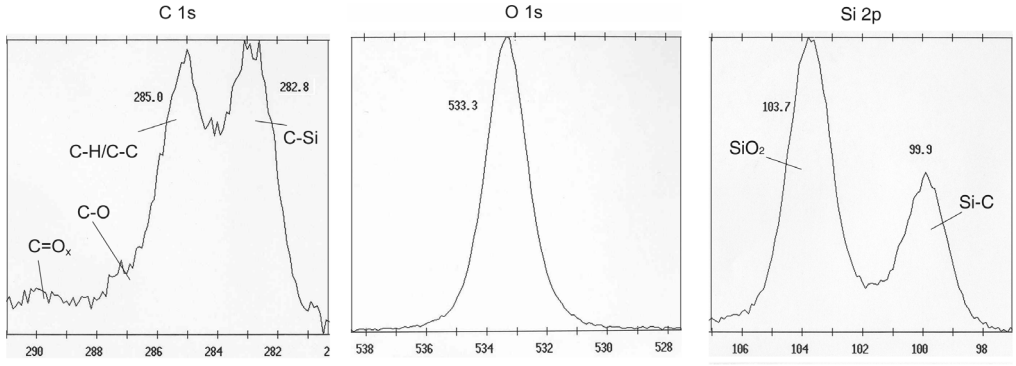

(b) 10 H_2O/O_2 plasma

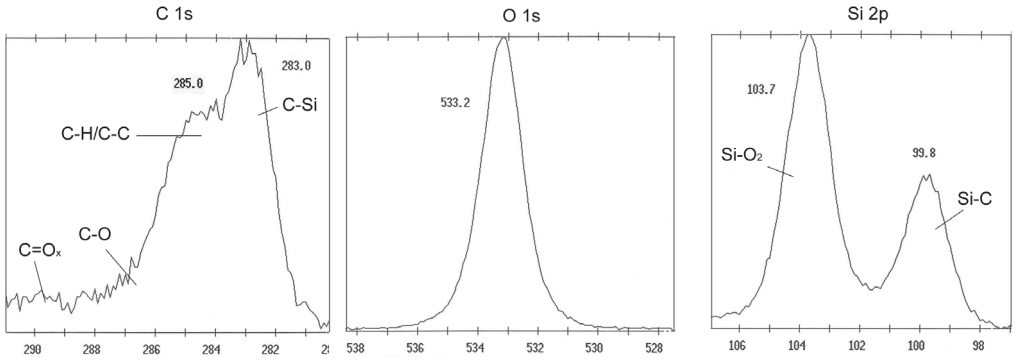

(c) 20 H_2O/O_2 plasma

Figure 4.23 C 1s, O 1s and Si 2p spectra for: (a) 10-minute O_2 plasma, (b) 10-minute H_2O/O_2 plasma, and (c) 20-minute H_2O/O_2 plasma treatment of SiC/Si.

4.6 ADHESION DURABILITY INFLUENCED BY SURFACE MODIFICATION

4.6.1 IMMERSION STUDIES

Durability tests for epoxy coated, surface treated SiC/Si samples immersed in pH 4.2, 6.7, 7.7 and 8.2 solutions showed that the various surface treatments enhanced adhesion of the epoxy adhesive to modified SiC/Si. In Figure 4.24, a bar graph of initial failure time for the as-received, GPS, APS, 2min.O_2 plasma/GPS and 2min.O_2 plasma/APS samples are shown. In the as-received system, initial debonding occurred in less than 20 days. Surfaces modified with GPS or APS on as-received samples showed initial debonding at approximately 90 days of immersion. The adhesion durability was further enhanced for samples that had been oxygen plasma/silane treated. With just a 2-minute O_2 plasma pretreatment, initial debonding occurred at approximately 200 days for the GPS samples and approximately 350 days for the APS samples.

Adhesion performance was further improved by increasing the O_2 plasma pretreatment time. The adhesion durability data measured in terms of initial debond time for plasma/silane samples are shown in Figure 4.25. For both GPS and APS samples, the 2- and 5-minute O_2 plasma treatments yielded about the same durability, whereas the samples receiving plasma treatment times of 15 and 30 minutes, exhibited an increase in durability. In general, the APS treated samples outperformed the GPS treated samples. For a 15-minute O_2 plasma treatment time, all GPS samples exhibited initial failure at approximately 350 days whereas some APS samples did not show any failure for immersion tests lasting up to 500+ days. The 30-minute plasma/APS sample exhibited the best performance with no sign of initial failure following 500+ days of immersion. Since the immersion tests ended at 500 days, the lifetimes of the epoxy-SiC/Si samples are unknown.

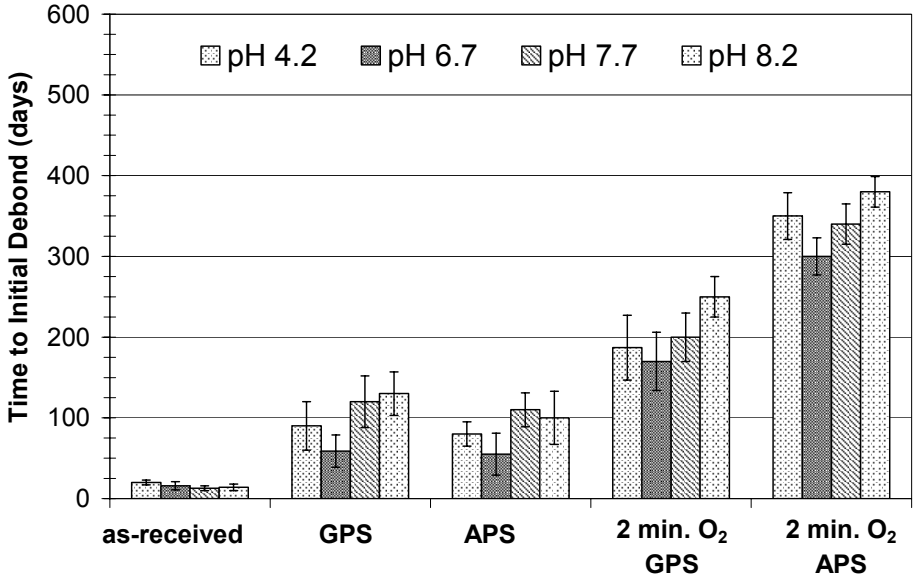

Figure 4.24 Adhesion durability: time to initial debond data for as-received and treated epoxy/SiC/Si samples tested in various solutions at 60°C.

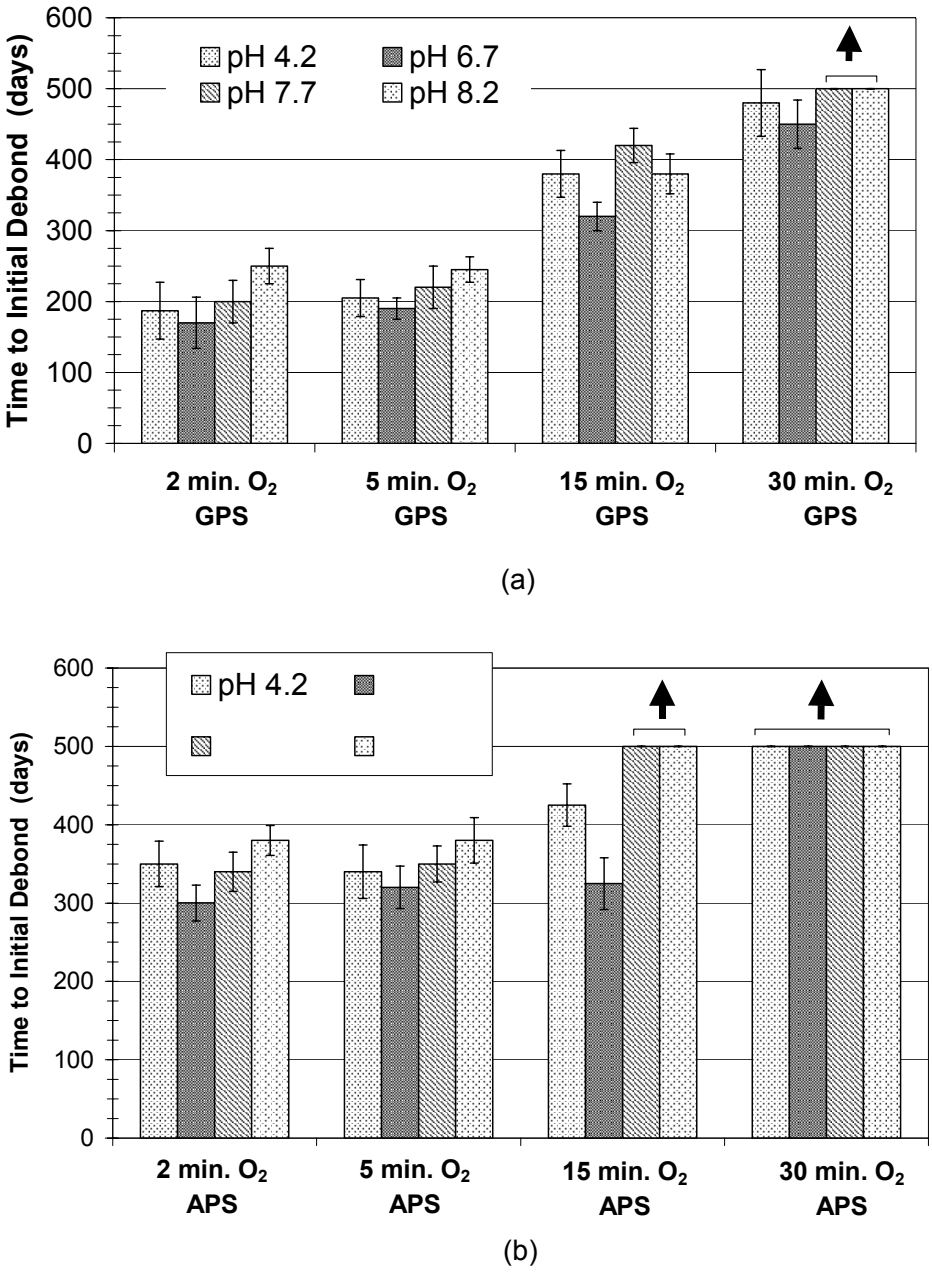

Figure 4.25 Adhesion durability: time to initial debond data for plasma/silane samples tested in various solutions at 60°C: (a) GPS with various O_2 plasma pretreatment times, and (b) APS with various O_2 plasma pretreatment times. Arrows indicate that samples have not yet reached initial failure in 500 days.

As demonstrated by the adhesion results, plasma etching is an extremely effective pretreatment in the silane surface modification process. The notable improvement in adhesion in the epoxy/SiC/Si system may occur for several reasons. The first reason is the cleaning effect of the oxygen plasma. Oxygen plasmas are capable of effectively removing organic contamination from inorganic surfaces.[16] Plasma pretreatments of metals with non-polymerizable gases typically result in clean surfaces that yield stronger bonds than traditionally cleaned surfaces.[17] In this investigation, although XPS data showed that hydrocarbon was still present after plasma treatment, the removal of fluorine contaminants suggests that a cleaning process took place. Surface cleaning with oxygen plasma is believed to contribute to improved bonding; however, improved adhesion in presence of the surface hydrocarbon suggest that this process plays a lesser role as a contributor to increased adhesion. An increase in adhesion is also believed to be due to a plasma-formed oxide. As oxygen plasma etches away the surface and removes carbonaceous contaminants, it also removes weak boundary layers such as the existing oxide and carbide layers and forms a more stable, uniform oxide layer. XPS analysis demonstrated that an increase in etching time resulted in an increase in oxide thickness. Prior to plasma treatment, the native oxide thickness was approximately 7 Å. After oxygen plasma treatment, the oxide layer thickness was in the range 22 Å to 27 Å depending on the treatment time. As plasma time was increased, a thicker and more stable oxide layer was developed, thus replacing a native weak oxide layer. It is also speculated that oxygen containing functionalities, presumably hydroxyl groups, are incorporated onto the surface by the low pressure O_2 plasma. These oxygen-containing functional groups are capable of forming bonds with the organofunctional silanes, resulting in increased silane adsorption. Dilks *et al.*[18] applied O_2 plasma treatment to polyxylylene and found mono-functionalities (such as C-OH) and di-oxygen functionalities (such as O=C-OH) on the plasma-treated surfaces. Grunmeier *et al.*[19] studied the effects of oxygen plasma on steel and observed a thickening of the oxide layer from 30 Å to 60 Å after an O_2 plasma treatment. Iron oxy-hydroxide and iron oxide were detected using FT-IRRA (IR under grazing incidence). The results were assumed to be due to the formation of oxide and hydroxide functionalities resulting from the plasma discharge.

To increase the adsorption of oxygen-containing functionalities to promote siloxane bond formation and adsorption of silane, the utilization of a H_2O/O_2 plasma was investigated. Nuzzo *et al.*[20] used XPS, radioisotope labeling and contact angle measurements in the treatment of

polyethylene with H_2, O_2 and H_2O plasmas. The combination of techniques indicated that the H_2O plasma treatment resulted in the highest concentration of hydroxyl groups on the surface. In theory, the H_2O plasma could be used to obtain a larger concentration of surface hydroxyl groups to react with the hydrolyzed silane molecules in the sol-gel reaction. XPS data, however, indicated that the H_2O/O_2 plasma treated surfaces showed the equivalent surface chemistry and silane adsorption as the O_2 plasma treated surfaces; thus, it was assumed that the H_2O/O_2 plasma surface treatment did not alter the surface significantly compared to the O_2 plasma treatment. From the immersion study (Figure 4.26), the H_2O/O_2 plasma/silane samples showed that adhesion durability was equivalent to the 10min.O_2 plasma/silane samples with initial failure occurring between 200-350 days for 10min.O_2 plasma/GPS samples, and 300-450 days for 10min.O_2/APS samples. Since all of the H_2O/O_2 plasma treated specimens were first exposed to a 10-minute O_2 pretreatment for cleaning purposes then treated with a H_2O/O_2 plasma, the failure results suggest that the improved adhesion performance was a result of the O_2 plasma pretreatment rather than the H_2O/O_2 treatment itself.

Strengthening of the epoxy-SiC interface against degradation for the surfaced treated specimens was also observed in the debonding behavior of the epoxy film when immersed in aqueous solutions at 60°C. For the as-received samples, debonding primarily occurred as lifting of the edges and corners as a result of the ingression of the aqueous solution. Pictures of debond patterns are shown in Figure 4.27. Some blister formation was apparent in the form of small blisters originating at the edges or near the lifting of the film, then growing in size and population inwards toward the rest of the film. This debonding behavior suggests that the ingression of aqueous solution occurred primarily at the interface between the adhesive film and substrate. In the surface modified specimens, initial lifting of the film was not observed. Instead, debonding occurred via random blister formation. Typically, the blisters would grow in size with time, then eventually coalesce with one another and collapse. This type of blistering suggests that the aqueous solution diffusion occurred primarily through the bulk of the epoxy film rather than at the interface.

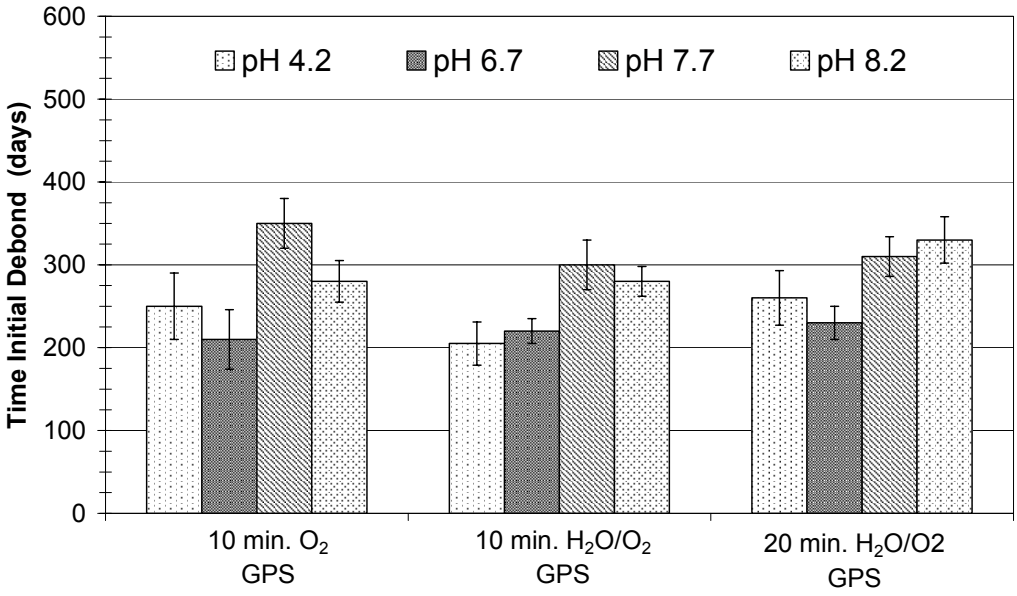

(a)

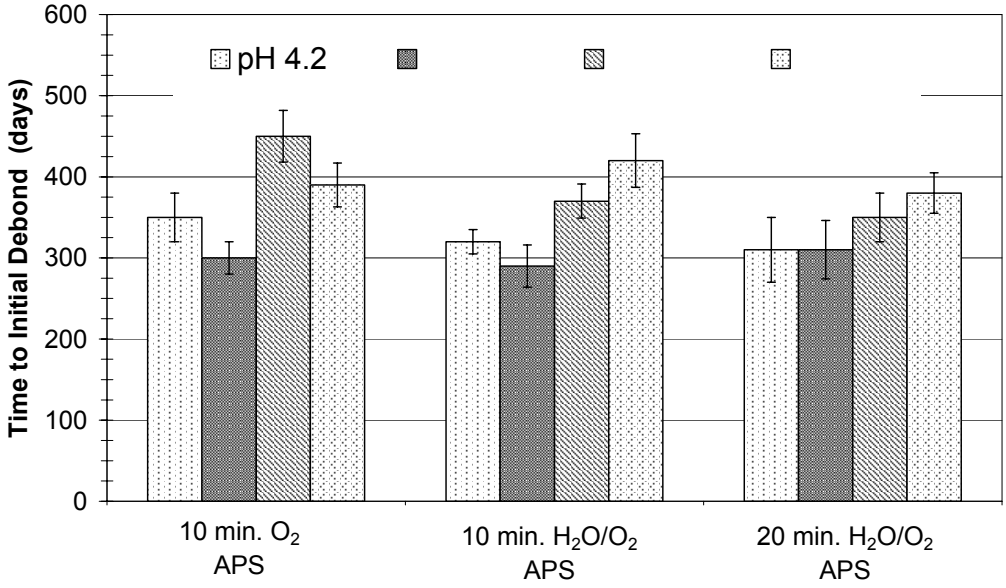

(b)

Figure 4.26 Adhesion durability data for plasma/silane samples tested in various solutions at 60 °C: (a) GPS on O_2- or H_2O- plasma treated surfaces, and (b) APS on O_2- or H_2O- plasma treated surfaces.

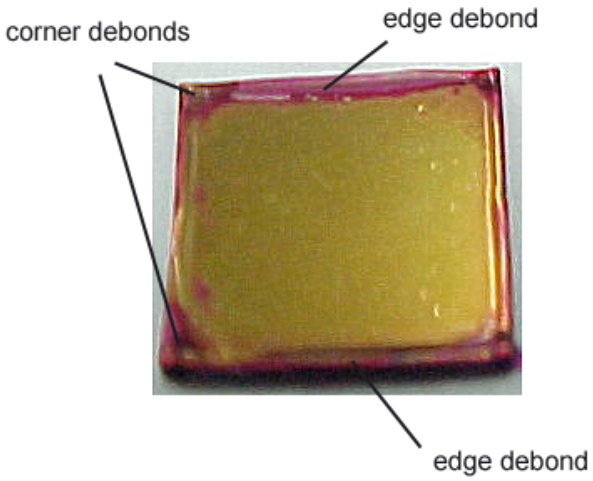

(a)

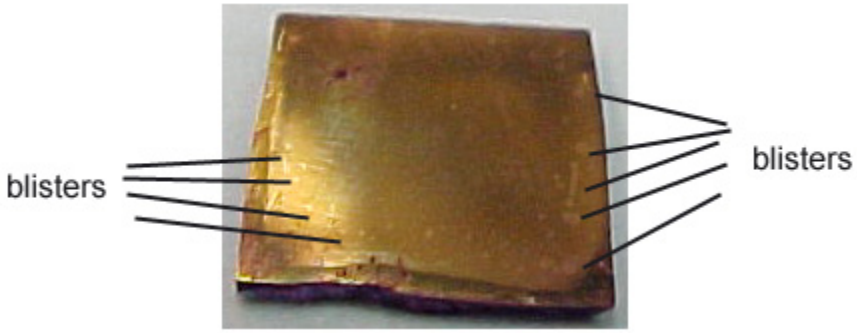

(b)

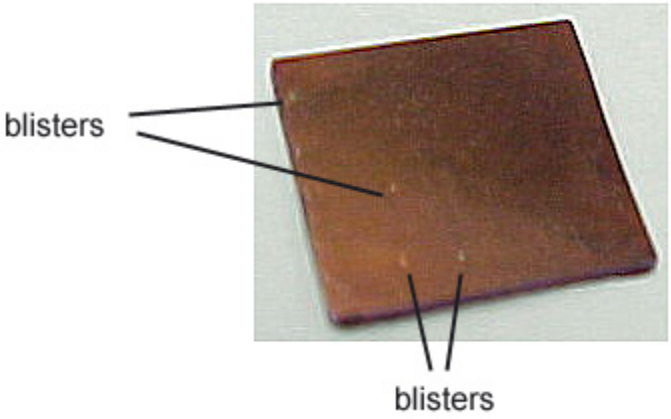

(c)

Figure 4.27 Representations of the various forms of debond behavior: (a) lifting at corners and/or edges, (b) blisters originating at edges, and (c) random blistering.

The time to complete debonding was also affected by the surface treatment. For the as-received system, complete delamination of the epoxy film occurred within 12-15 days after the first appearance of the initial debond. For surface treated samples, complete delamination did not occur before four months after the initial debond. For non-plasma/sol-gel samples, complete lifting of the film occurred approximately 2 months after the initial debond. Complete debonding for some plasma/sol-gel samples occurred at 4+ months; however, many of the plasma/sol-gel samples surpassed four months. Since the test ended at 500 days of immersion, the time to complete failure is not known for plasma/sol gel samples. Nevertheless, as expected, the more effective the surface treatment, the longer the length of time to complete failure.

As for environmental influence, no pattern of debonding or adhesion durability was found among the varying pH solutions

4.6.2 PROBE TEST STUDIES

Figure 4.28 shows the change in the critical strain energy release rate, G_c, for as-received/GPS, as-received/APS, 30min.O_2 plasma/GPS and 30min.O_2 plasma/APS as a function of time in pH 6.7 solution, pH 8.2 solution and deionized water (pH 6.3). With and without immersion, the trend in G_c was O_2 plasma/APS > O_2 plasma/GPS > as-received/APS ≈ as-received/GPS. After four weeks of immersion, an overall decrease in G_c was observed for all specimens. Following 28 days of immersion, APS and GPS had the lowest G_c at ~150 J/m^2 and 30min.O_2 plasma/APS had the greatest G_c at ~350 J/m^2. Table 4.19 lists the average G_c values for specimens without immersion and for those following 28 days of immersion. The adhesion trend is consistent with the immersion test results with the exception of the discrepancy in adhesion durability for as-received/GPS and as-received/APS. In the immersion study, the as-received/APS surface treated samples resulted in better adhesion than the as-received/GPS samples, whereas in the probe test study the two treatments exhibited equivalent adhesion performance. Nevertheless, both studies show that the combination of oxygen plasma treatment and silane treatment resulted in enhanced adhesion performance with 30min.O_2 plasma/APS being the most effective treatment.

In Figure 4.29, the adhesion durability data is shown for H_2O/O_2- vs. O_2- plasma/silane treatments. The G_c curves revealed that O_2 plasma/APS had the best adhesion durability,

H_2O/O_2 plasma/APS and O_2/GPS performed about the same, and H_2O/O_2 plasma/GPS performed the worst. This adhesion trend is consistent with the results from the immersion study.

Table 4.19 Average critical strain energy release rates, G_c, for as-received and surface-treated samples. Values are an average of 3 runs per sample.

Sample	**No Immersion**	**Following 28 Day Immersion**		
	Avg. G_c (J/m^2)	**pH 6.7 Avg. G_c (J/m^2)**	**pH 8.2 Avg. G_c (J/m^2)**	**DI H_2O Avg. G_c (J/m^2)**
as-received	141 ± 29	fail	fail	fail
as-received/ GPS	310 ± 22	112 ± 30	186 ± 35	225 ± 25
as-received/ APS	270 ± 19	89 ± 26	152 ± 21	190 ± 25
10 min H_2O plasma / GPS	372 ± 13	162 ± 13	237 ± 10	252 ± 28
10 min H_2O plasma / APS	423 ± 21	261 ± 14	271 ± 14	326 ± 21
30 min O_2 plasma/ GPS	412 ± 9	230 ± 25	275 ± 16	312 ± 14
30 min O_2 plasma/ APS	488 ± 15	316 ± 25	335 ± 18	389 ± 20

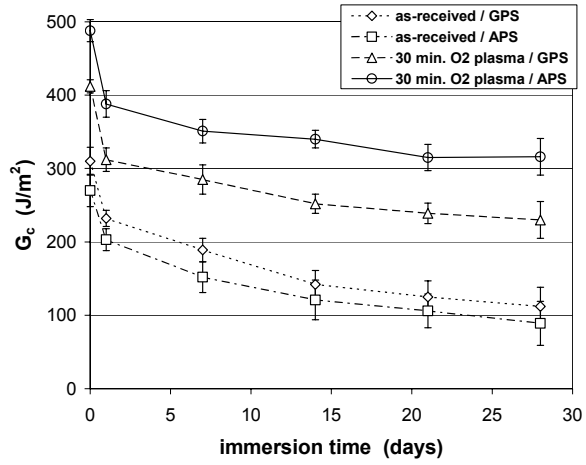

(a)

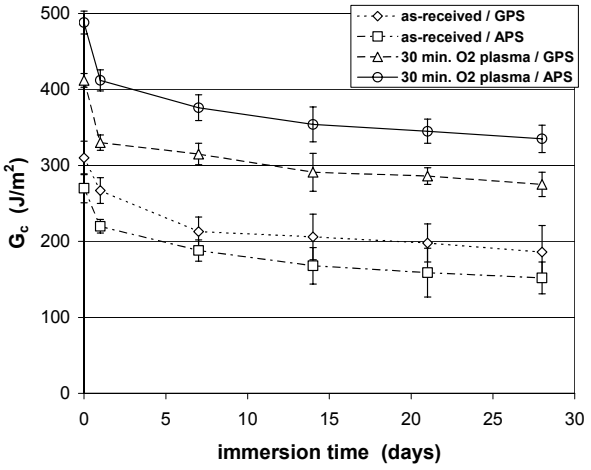

(b)

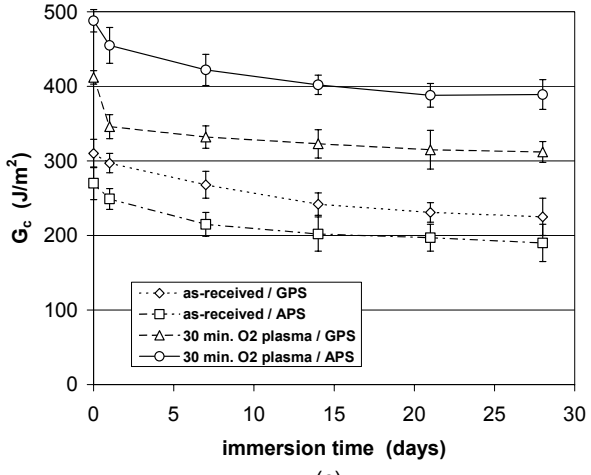

(c)

Figure 4.28 Critical strain energy release rate, G_c, as a function of immersion time for as-received/silane and O_2 plasma/silane samples tested in: (a) pH 6.7 solution, (b) 8.2 solution, and (c) DI H_2O (pH 6.3).

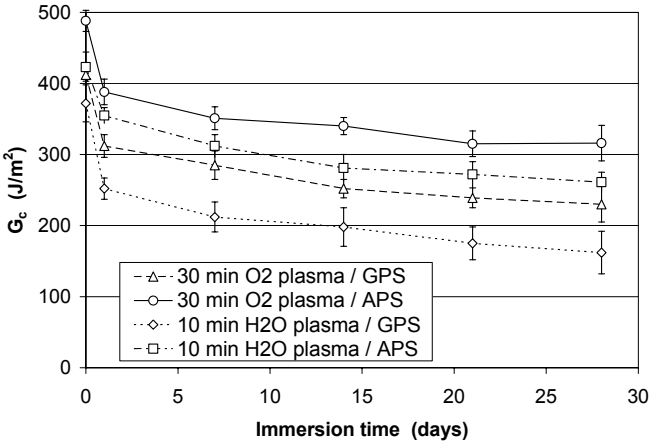

(a)

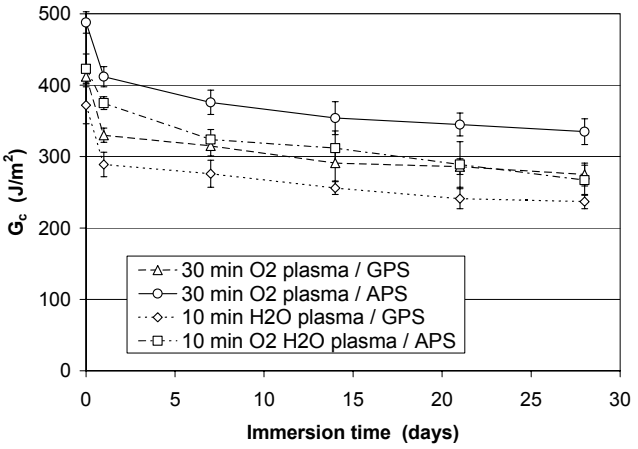

(b)

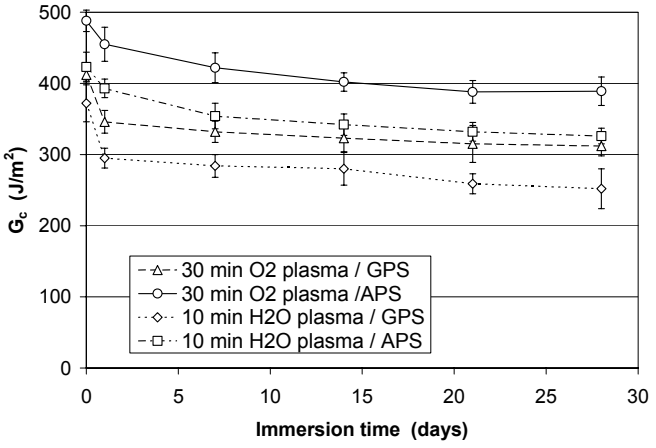

(c)

Figure 4.29 Critical strain energy release rate, G_c, as a function of immersion time for O_2 plasma/silane and H_2O plasma/silane samples tested in: (a) pH 6.7 solution, (b) 8.2 solution, and (c) DI H_2O (pH 6.3).

A comparison of G_c for the non-plasma/silane and plasma/silane treatments is shown in Figure 4.30. The graph shows that the plasma-treated samples (tested in H_2O) exhibited greater adhesion durability over time than the non-plasma treated samples, especially in the case for the APS silane. Probe test data at 4 weeks show that after plasma pretreatment, G_c for GPS increased from ~225 J/m^2 (GPS on as-received) to ~312 J/m^2 (GPS on plasma-modified) and APS increased from ~190 J/m^2 to ~390 J/m^2. This trend was also found for samples tested in pH 6.7- and pH 8.2- solutions. These differences in G_c provide further support that an O_2 plasma surface treatment can notably enhance the effectiveness of a silane as a coupling agent.

As noted above, sample surfaces modified with plasma and APS resulted in better adhesion than for the plasma/GPS samples. It is speculated that improved adhesion for plasma/APS samples may be due to a combination of reasons. One reason may be due to the polarity of the APS silane. In practice, APS treated surfaces were less polar than those treated with GPS when spin coated with epoxy. The critical surface energies for APS and GPS on glass at 20 °C has been reported, 35.0 N/m and 44.6 N/m, respectively[21]. Although the difference in surface energies may be small between APS and GPS, the hydrophobic nature of APS provides a more water-resistant interphase region, thus preventing hydrolysis and aqueous ingression. In addition, XPS spectral analysis suggested that better surface coverage was achieved with APS than GPS. Adequate surface coverage is important to ensure successful interactions between silane/substrate and silane/epoxy interfaces.

The affect of aqueous environment, namely pH, on adhesion behavior was also analyzed as noted in Figures 4.31 and 4.32. The G_c vs. immersion time data were plotted to show adhesion durability of the treated systems as influenced by the different aqueous environments, pH 6.7- and pH 8.2 solutions and DI water (pH 6.3). When the error is taken into consideration, the differences in G_c among the samples tested in varying solutions were small. This observation supports the notion that the decrease in adhesion for the epoxy/SiC/Si bonded system is more a result of the deleterious effects of the aqueous solution rather than the pH of the solution. Recall that in the immersion study, no correlation between solution pH and adhesion durability was observed. In short, little or no adhesion durability differences were found among samples tested in the various solutions.

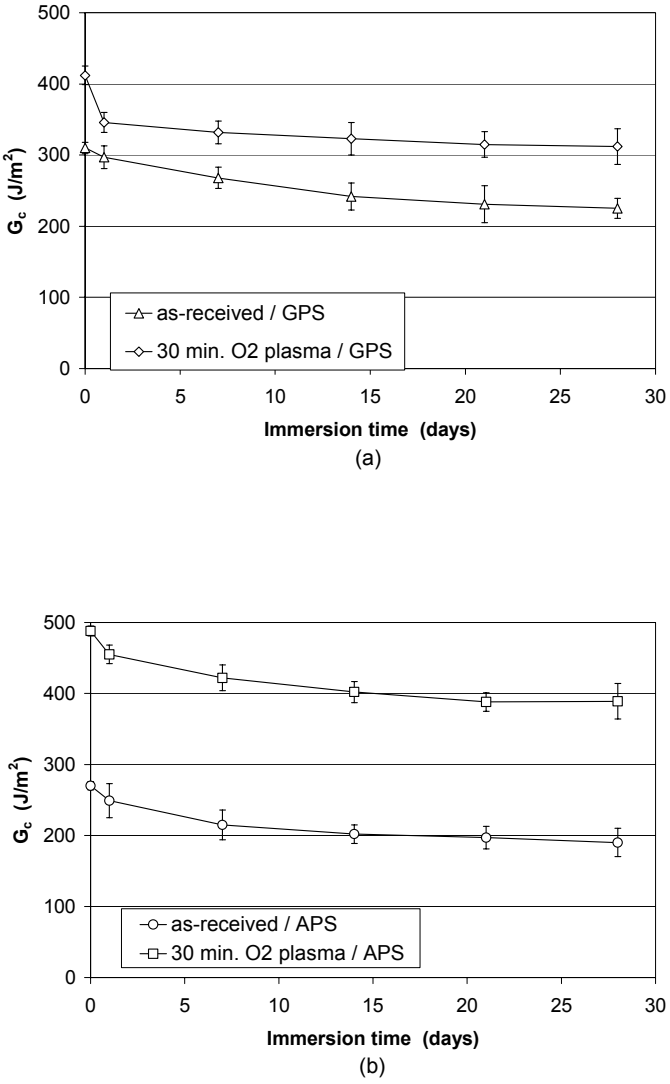

Figure 4.30 G_c vs. immersion time for silane treated samples influenced by O_2 plasma pretreatment: (a) non-plasma/GPS and 30min. O_2 plasma/GPS, and (b) non-plasma/APS and 30min. O_2 plasma/APS. Samples were tested in DI H_2O at 60 °C.

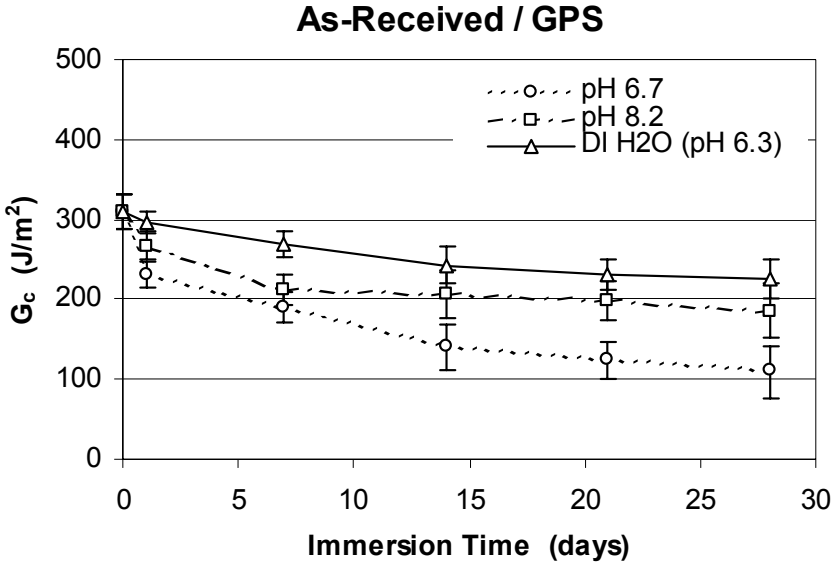

(a)

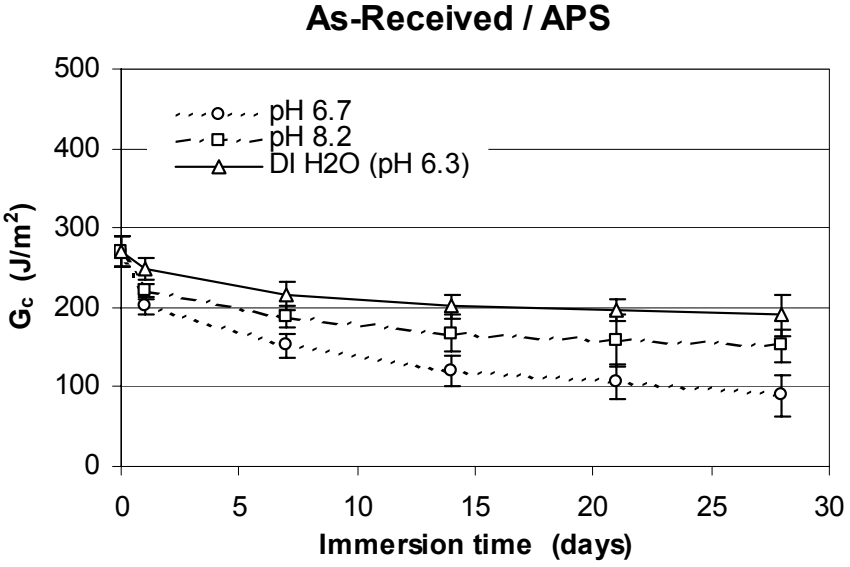

(b)

Figure 4.31 A comparison of G_c vs. immersion time data influenced by testing solutions for: (a) as-received/GPS and (b) as-received/APS.

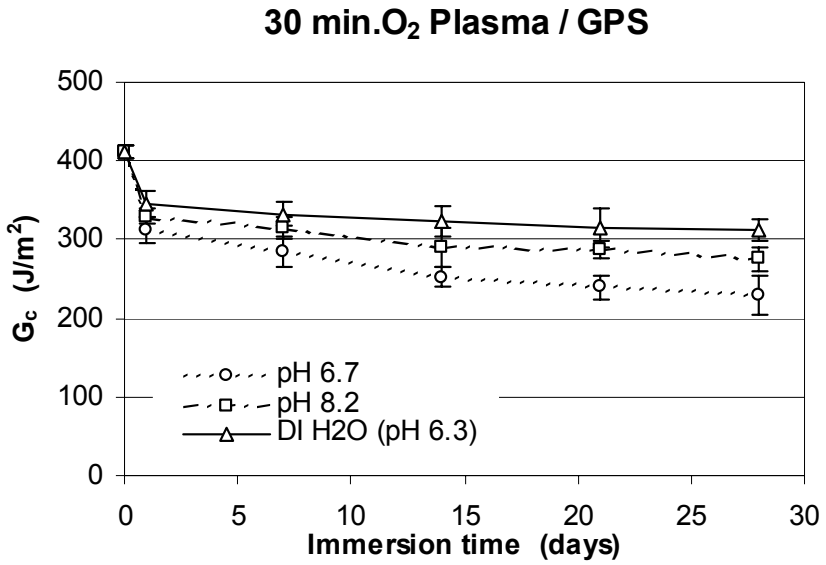

(b)

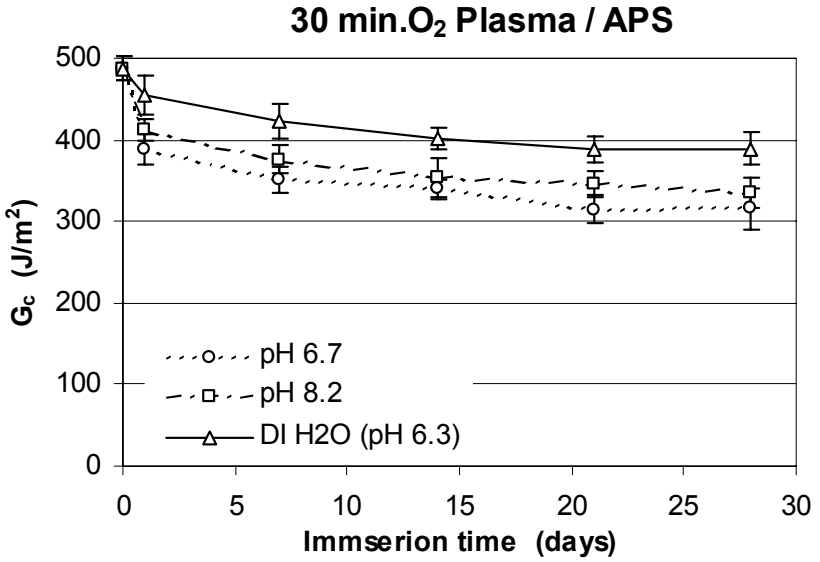

(b)

Figure 4.32 A comparison of G_c vs. immersion time data influenced by testing solutions for: (a) 30min.O_2 plasma/GPS and (b) 30min.O_2 plasma/APS.

4.7 DETERMINATION OF FAILURE MODE FOR THE SURFACE MODIFIED SYSTEMS

Surfaces of failed specimens from the immersion tests were characterized via XPS to determine the failure mode. Detailed XPS analysis showed that all samples, regardless of surface preparation, resulted in failure within the adhesive-silane interfacial region. To illustrate the manner of determining the failure mode, the XPS spectral analysis 5min. O_2/APS and 5min. O_2/GPS samples will be discussed.

The surface compositions of the failed surfaces for 5min.O_2 plasma/APS tested in pH 6.7 solution and for the as-prepared surfaces are shown in Table 4.20. The compositions for the failed SiC surface and for the as-prepared surface (plasma and silane treated) were equivalent: ~36% C, ~40% O, and ~20% Si. Except for the slight decrease in nitrogen content from 3.7% (as-prepared SiC) to 2.2%, the surface chemistry for the two surfaces was similar. For the failed epoxy side, the carbon and oxygen contents were also equivalent (within 2%) to the as prepared epoxy coating.

To further analyze the mode of failure, the C 1s and Si 2p spectral regions of the as prepared SiC surface and as prepared epoxy were compared to the failed substrate and failed adhesive surfaces. The C 1s and Si 2p spectra in Figure 4.33 for the as-prepared and failed surfaces, respectively, are respectively similar. Both C 1s spectra show a prominent C-H/C-C photopeak at 285.0 eV, a C-Si shoulder at 282.8 eV and a very slight C-O shoulder at 286.5 eV. The C 1s spectrum for the failed SiC surface exhibits a small shoulder at ~288.5 eV that is attributed to C=O contamination either from the solution, the atmosphere or oxidation during the test. The Si 2p spectra of both surfaces show a dominant 102.4 eV photopeak assigned to the composite peak (SiO_x) consisting of Si-O_2 and Si-O-Si, and a less prominent photopeak at 99.5 eV that is attributed to silicon in SiC. The intensities for these peaks are equivalent on an absolute basis. For the epoxy failed side and the as-prepared epoxy, the C 1s spectra are equivalent; showing a C-O photopeak at 286.5 eV – 286.7 eV and a C-H/C-C photopeak at 285.0 eV that are characteristic of the epoxy adhesive. The shape and relative intensities of the C-H/C-C, C-Si and C-O photopeaks for the failed and as-prepared epoxy are equivalent to the respective treated and as-cast component surfaces. No silicon was detected on the epoxy failed surface, which indicates that no silane was on the epoxy film. Although it is uncertain whether the low relative

percentage of nitrogen on the epoxy failed surface is attributed to the imidazole curing agent or to the silane coupling agent, all observations indicate that failure occurred within the interfacial region between the epoxy and silane layer.

As a representative of the failed GPS-treated samples, the failure analysis of a 5min.O_2 plasma.GPS sample tested in pH 8.2 solution is discussed. The results in Table 4.21 list the surface compositions of the failed SiC and epoxy sides compared to their prior bonding surface compositions. For the failed SiC surface, XPS results showed that the carbon content slightly increased from 28.7% to 33.7%, oxygen was relatively unchanged at about 45% and silicon decreased from 26.5% to 21.0%. For the epoxy failed side, C, O and Si were detected. The relative percentages of carbon and oxygen for the failed surface are equivalent within 1% of the values for the as-prepared surface. The low concentration of silicon (0.81%) on the failed adhesive side suggests the presence of silane.

XPS spectral data for as-prepared SiC, as-prepared epoxy, failed SiC, and failed epoxy surfaces are shown in Figure 4.34. Compared to the as-prepared surface, the failed SiC surface shows slightly broader C-H/C-C and C-O photopeaks at 285.0 eV and 286.5 eV, respectively. This observation, in addition to the very slight increase in carbon content, suggests that a small amount of epoxy may be present on the substrate. The Si 2p peaks are equivalent to the as-prepared respective photopeaks. This indicates that the silane and oxide layers are still intact on the failed surface, suggesting failure at the epoxy/silane interface. On the epoxy-failed side and as-prepared epoxy surface, the overall shapes of the C-O and C-H/C-C photopeaks are similar and probably equivalent when experimental error is taken into consideration. This finding is consistent with the results that the carbon and oxygen contents were equivalent to those for the as-prepared epoxy. The Si 2p spectrum reveals a photopeak at 102.5 eV that is characteristic of Si-O-Si species. The presence of Si-O-Si is likely due to a small quantity of silane moieties that were detached from the substrate by hydrolysis of the Si-O-Si bond. The overall analysis of the failed surfaces indicates that failure occurred predominantly at the silane-epoxy adhesive interface, with minor failure at the silane-oxide interface.

Table 4.22 summarizes the failure modes, as determined by XPS, for selected samples tested in various solutions. All samples exhibited failure primarily at the silane-epoxy interface. A simplified schematic of the failure mechanism is shown in Figure 4.35. This pattern of failure

indicates that the interactions between the epoxy and silane are more vulnerable to aqueous and chemical attack than those between the silane and SiC/Si substrate. The significant strengthening of the silane/substrate interface indirectly supports the presence of strong primary bond formation between the substrate and silane, presumably by siloxane Si-O-Si linkages. These observations are quite interesting because although siloxane bonds are covalent, it is well known that these bonds are reversible and hydrolyzable by water.[22] Since the silane/substrate interface is highly stable against hydrolysis, it is reasonable to deduce that pH would not play a large role in the adhesion degradation process. The immersion and probe studies support this idea. Regarding the silane/epoxy interface, two ideas are proposed to account for the vulnerability of the interface: 1. inefficient bonding between the silane/epoxy interface, i.e. secondary forces vs. primary forces, and/or 2. stresses across the silane/epoxy interface due to epoxy shrinkage during curing and/or due the epoxy expanding via water absorption from the aqueous solutions. Generally, the adhesion strength and durability for the epoxy bonded to SiC/Si were improved dramatically for surface-modified systems.

Table 4.20 Elemental surface composition for as-prepared (before bonding) and debonded surfaces for 5min.O_2 plasma/APS. The sample was tested in pH 6.7 solution.

Sample	Surface Composition			
	C%	O%	Si%	N%
As-prepared SiC surface	35.7	39.2	21.3	3.7
Model epoxy coating	81.6	18.4	<0.1	<0.1
Failed SiC side	37.3	40.4	20.1	2.2
Failed epoxy side	79.7	17.7	<0.1	2.6

Table 4.21 Elemental surface composition for as-prepared (before bonding) and debonded surfaces for 5min.O_2 plasma/GPS. The sample was tested in pH 8.2 solution.

Sample	Surface Composition			
	C%	O%	Si%	N%
As-prepared SiC surface	28.7	44.8	26.5	<0.1
Model epoxy coating	81.6	18.4	<0.1	<0.1
Failed SiC side	33.7	45.3	21.0	<0.1
Failed epoxy side	80.4	18.8	0.81	<0.1

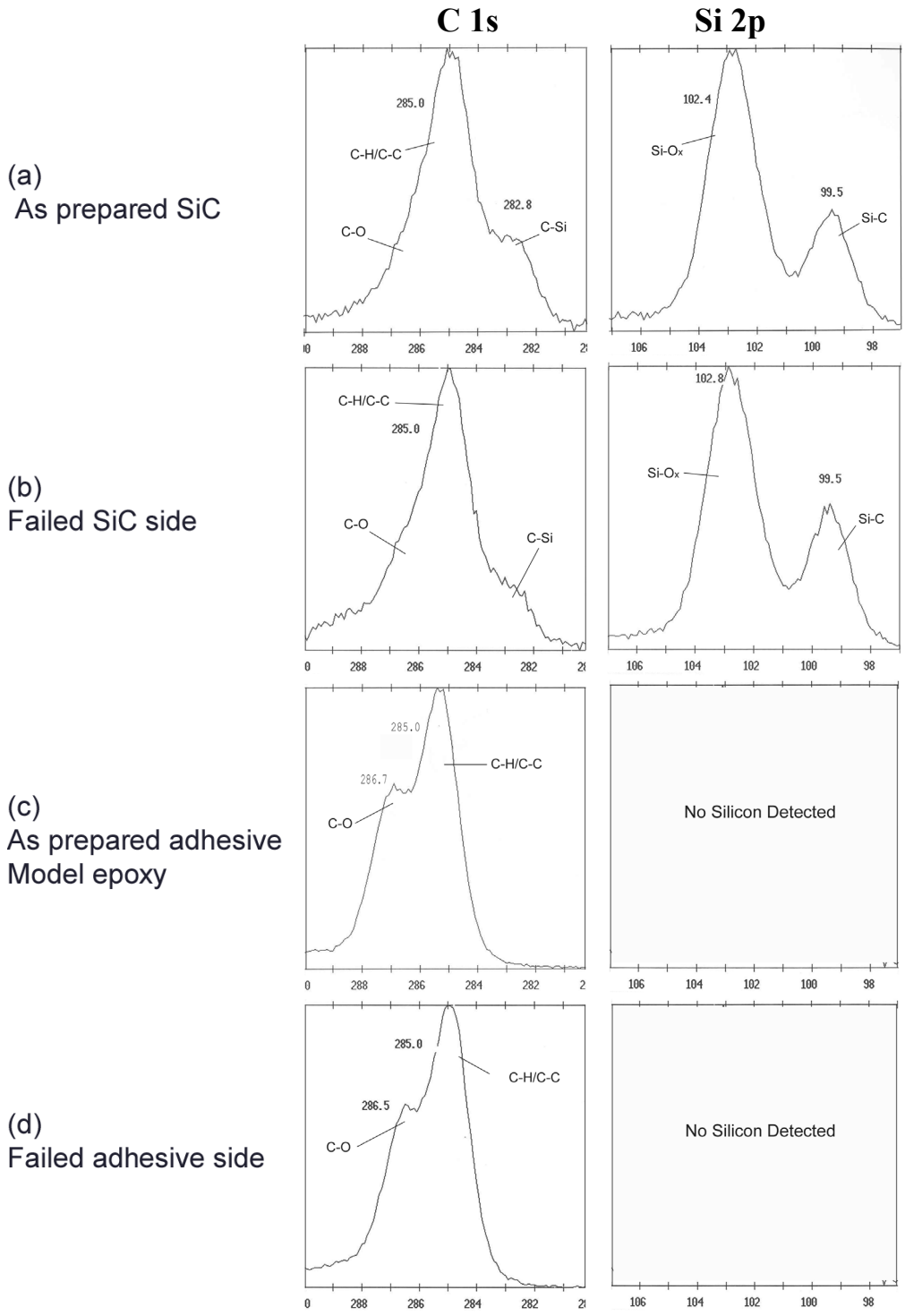

Figure 4.33 C 1s and Si 2p XPS spectral regions of failed surfaces for 5min.O_2 plasma/APS sample tested pH 6.7 solution compared to as-prepared surfaces: (a) as-prepared, 5min.O_2 plasma/APS wafer surface, (b) failed SiC wafer side surface, (c) as-prepared model epoxy coating, and (d) failed epoxy side surface.

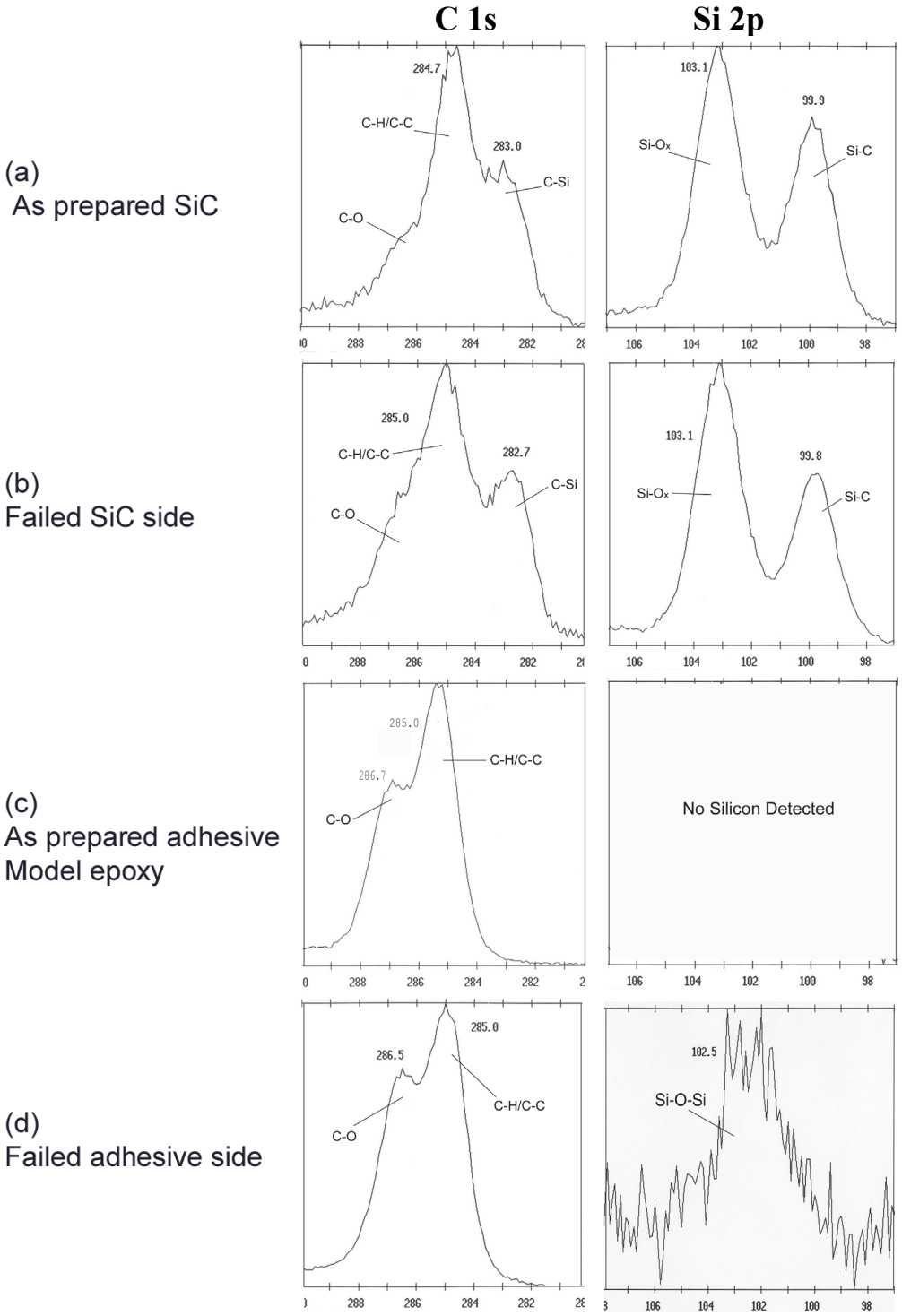

Figure 4.34 C 1s and Si 2p XPS spectral regions of failed surfaces for 5min.O_2 plasma/GPS sample tested pH 8.2 solution compared to as-prepared surfaces: (a) as-prepared, 5min.O_2 plasma/GPS wafer surface, (b) failed SiC wafer side surface, (c) as-prepared model epoxy coating, and (d) failed epoxy side surface.

Table 4.22 Failure modes for epoxy/SiC/Si systems tested in various solutions at 60°C. Interfacial refers to failure in the epoxy-substrate interfacial region. * Samples not fully debonded

Sample	Failure Patterns			
	pH 4.2	**pH 6.7**	**pH 7.7**	**pH 8.2**
as-received / APS	interfacial	interfacial	interfacial	interfacial
as-received / GPS	interfacial	interfacial	interfacial	interfacial
2 min. O_2 plasma / APS	interfacial	n/a	interfacial	n/a
5 min. O_2 plasma / APS	n/a	interfacial	n/a	interfacial
15 min. O_2 plasma / APS	n/a*	interfacial	n/a*	n/a*
30 min. O_2 plasma / APS	n/a*	n/a*	n/a*	n/a*
2 min. O_2 plasma / GPS	interfacial	interfacial	interfacial	interfacial
5 min. O_2 plasma / GPS	n/a	interfacial	n/a	interfacial
15 min. O_2 plasma / GPS	n/a*	n/a*	n/a*	n/a*
30 min. O_2 plasma / GPS	n/a*	n/a*	n/a*	n/a*
10 min. H_2O plasma / APS	n/a	interfacial	n/a	n/a
20 min. H_2O plasma / APS	n/a	n/a	n/a	interfacial
10 min. H_2O plasma / GPS	interfacial	n/a	n/a	n/a
20 min. H_2O plasma / GPS	n/a	n/a	interfacial	n/a

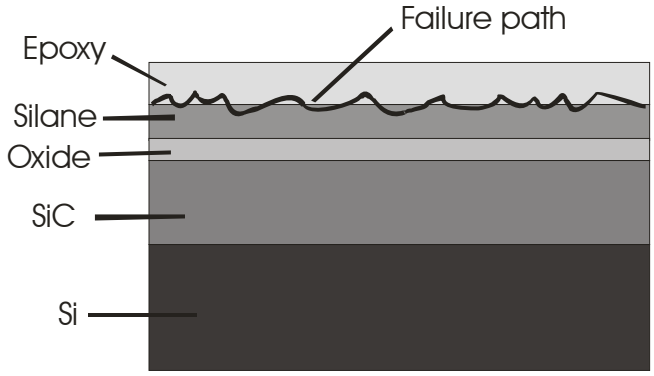

Figure 4.35 Proposed failure mode for surface-modified samples. (not drawn to scale)

[1] R.C. Lee, C.R. Aita and N.C. Tran, *J. Vac. Sci. Technol. A*, **1991**, *9*, 1351.

[2] M.N. Rahaman and L.C. De Longhe, *Am. Ceram. Soc. Bull*., **1987**, *66*, 782.

[3] S. Hoffman, *Practical Surface Analysis by Auger and X-ray Photoelectron Spectroscopy*, D. Briggs and M.P. Seah (Eds.), Wiley: UK, 1983, Chapter 4.

[4] Perkin Elmer ESCA System Model 5400 data bank.

[5] A.J. Kinloch, *Adhesion and Adhesives: Science and Technology*, Chapman and Hall: London, 1987, Chapter 4.

[6] J.E. Ritter, T.J. Lardner, W. Greyeski, G.C. Prakash and J. Lawrence, *J. Adhesion*, **1997**, *63*, 1997.

[7] R. K. Iler, *The Chemistry of Silica*, Wiley: New York, 1975, Chapter 3.

[8] H.J. Kang and F. Blum, *J. Am. Chem. Soc.*, **1991**, *95*, 9391.

[9] H. Ishida and J. Koenig, *J. Colloid Interface Sci.*, **1978**, *64*, 555.

[10] E.T. Vandenberg, L.B. Bertilsson, B.L. Kasjsa Uvdal, R. Erlandsson, H. Elwing and I. Lungstrom, *J. Colloid Interface Sci.*, **1991**, *147*, 103.

[11] C.H. Chiang, N.I. Lui and J.L. Koenig, *J. Colloid Interface Sci.*, **1982**, *86*, 26.

[12] F.J. Boerio, L.H. Schoelein and J.E. Grievenkamp, *J. Appl. Polym. Sci.*, **1978**, *22*, 203.

[13] J.N. Kinkel and K.K. Unger, *J. Chromatogr*., **1984**, *316*, 193.

[14] C.D. Wagner, W.M. Riggs, L.E. Davis, J.F. Moulder and G.E. Muilenburg, *Handbook of X-Ray Photoelectron Spectroscopy,* Perkin Elmer: Eden Prarie, 1979, Appendix 3.

[15] D. Xu and J. Dillard, Unpublished Results, Department of Chemistry, Virginia Tech.

[16] H. Kersten, W.W. Stoffels, M. Otte, C. Csambal, H. Deutsch and R. Hippler, *J. Appl. Phys.*, **2000**, *87*, 3637.

[17] E.M. Liston Paper presented at First International Conference, Namur, Belgium, September 1991; Section IV, p. 429.

[18] A. Dilks and Van Laeken in "The Investigation of the Plasma Oxidation of Pol(p-Xylylene) & its Chloinated Derivatives", *Physio-chemical Aspects of Polymer Surfaces*, K.L Mittal (Ed.), Plenum: New York, 1983, p.749.

[19] G. Grundmeier and M. Stramann, *Mater. Corros*., **1998**, *49*, 150.

[20] R.G. Nuzzo and G. Smolinsky, *Macromol*., **1984**, *17*, 1013.

[21] L.H. Lee, *Adhesion Science and Technology*, Plenum Press: New York, 1975, Vol. 9B, p.647.

[22] E.P. Plueddemann, *Silane Coupling Agents*, Plenum Press: New York, 1982, p. 118.

5 CONCLUSIONS

The effectiveness of three different surface modification treatments of SiC/Si wafers on adhesion durability was studied: 1) silane treatment (APS or GPS), 2) oxygen plasma pretreatment followed by silane treatment, and 3) water/oxygen plasma treatment followed by silane treatment. The effects of surface treatments on surface chemistry were examined using X-ray photoelectron spectroscopy (XPS). Adhesion durability in aqueous solutions (varying pHs) at 60 °C was evaluated qualitatively using an immersion test, and quantitatively by determining the strain energy release rate G_c via a novel probe test.

In the first surface modification treatment, APS and GPS were separately applied to SiC/Si wafers. XPS spectral analyses confirmed that the coupling agents modified on the substrate surface. Immersion study results showed that the adhesion durability of the epoxy to SiC/Si substrate could be improved by approximately five-fold. As-received samples (without modification) resulted in initial failure in 20 days, whereas silane-treated samples yielded initial failure at approximately 100 days.

An O_2 plasma treatment prior to the deposition of silane reagents significantly improved the adhesion durability for the system. In fact, the immersion studies showed that for some plasma/silane samples, no sign of initial failure was evident even at the end of the 500-day immersion test. The effects of varying O_2 plasma treatment time were studied. Observations also showed that an increase in O_2 plasma treatment time yielded an increase in adhesion durability. An approximate determination of oxide thickness from XPS peak intensities for modified surfaces showed that the oxide thickness increased as a function of increased treatment time. In addition, XPS data suggested that an exposure to the O_2 plasma also promoted silane adsorption. The cleaning effect, increase in silane adsorption and stability of the extended plasma-formed oxide layer are believed to account for the significant enhancement in adhesion performance.

To promote silane adsorption by providing more binding sites (i.e. –OH groups) on the substrates, the utilization of a H_2O plasma, with O_2 as a carrier gas, was investigated. The surface chemistry, concentration of silane and adhesion durability were generally equivalent to

that for the O_2 plasma pretreated samples. Since all H_2O/O_2 plasma treated samples were first exposed to an O_2 plasma cleaning process prior to the H_2O/O_2 plasma treatment, these observations suggest that improved adhesion was due to the O_2 plasma cleaning treatment rather than to the H_2O/O_2 plasma treatment.

To test the validity of the immersion study results, a probe test was carried out as a time efficient and informative means to evaluate adhesive strength. This unique approach allows testing of rigid thin-films on rigid substrates by approximating the strain energy release rate, G_c, from the crack profile of the probe-induced semicircular debond. The strain energy release rate as a function of immersion time was determined for as-received and surface-modified samples. The probe test results confirmed that O_2 plasma/silane treated samples exhibited significantly improved adhesion performance compared to samples without plasma treatment. The probe test results exhibited the same adhesion trend as the immersion test results. The 30-minute O_2 plasma/APS treatment, confirmed by both the immersion study and probe test study, exhibited the best adhesion performance.

Adhesion performance of surface modification systems was not influenced by varying the pH of the immersion solutions. Adhesion performance was more influenced by surface treatment than by pH effects. The improvement in adhesion durability is a result of a stable interface, especially at the substrate/silane interface where the rate of hydrolysis of Si-O-Si bonds is dependent on solution pH. These observations are further supported by the failure mode for the surface-modified systems where adhesion failure occurred at the silane/epoxy interfacial region.

This work has shown that a combined surface modification process involving plasma and silane treatments is an effective means for altering the surface chemistry of the epoxy/SiC/Si system to improve adhesive bonding. Since no adhesion study has been published for silicon carbide, this study provides a working foundation for future research in the adhesion of epoxy films in microelectronics technology.

VITA

Elizabeth Minh Huong Vu was born on July 29, 1975 in Hong Kong to Vietnamese refugees, Vu Duc Minh and Le Thi Huong. Raised in San Jose, California, she studied chemistry, emphasizing in biochemistry at Santa Clara University in Santa Clara, CA. After receiving her Bachelor of Science degree in Chemistry in 1997, she became involved in research and development of polymer dispersed liquid crystals for display applications at National Semiconductor Corporation. In 1999, she moved to Blacksburg, Virginia to pursue a graduate education in the field of Materials Science and Engineering (MSE). In the meantime, she became Elizabeth Minh Huong Neyman after her marriage to Patrick J. Neyman, and had a beautiful daughter, Julia Minh Huong Neyman. In the summer of 2003, she received her Masters of Science degree in MSE, and plans to continue her education in a pursuit of a Masters of Business Administration.